NTNU – Trondheim
Norwegian University of
Science and Technology

Power Converters as smart instruments and actuators in a smarter grid

Berhane Dimd

Master of Science in Electric Power Engineering
Submission date: June 2015
Supervisor: Ole-Morten Midtgård, ELKRAFT

Norwegian University of Science and Technology
Department of Electric Power Engineering

Abstract

Climate change is one of the biggest challenges facing the world. One of the biggest issues to address is energy. At the moment we get most of our energy from fossil fuels, like oil, coal and gas, but these release greenhouse gases that trap heat in the earth's atmosphere. To avoid dangerous levels of global warming and give a more secure future, we need to switch to clean, green renewable energy.

With the increasing penetration of renewable energies as distributed generation (DG) in smart grid scheme, technical problems arise in both distribution and transmission system level. Today's storage technologies are becoming more efficient and higher performing.

Power electronics based loads such as adjustable speed drives, rectifiers, power supplies, domestic appliances, and the like offer highly non-linear characteristics. These non-linear loads draw distorted currents from the grid and cause reactive power burden and excessive neutral current.

The purpose of this thesis is to study and analyze the potential of smart power converters and batteries at telecom sites, to aid the grid in power quality improvement. Power converters can provide more information about the grid quality and also contribute to grid quality. When connected to energy storage and renewable energy, the power conversion system represents an additional flexibility. Converter-battery combination is studied in SAF (Shunt active filter) configuration to compensate harmonic and reactive currents.

A control strategy based on *p-q* theory is used for extracting the three-phase reference currents for SAF , and performance evaluation is carried out with *dq-PI* and adaptive HCC controllers in Matlab/Simulink 2015a environment.

When used in three-phase, three-wire configurations, the two controllers give a relatively similar compensation characteristics. The THD (Total harmonic distortion) in the source current reduced from 28.08% to 2.24% with *dq-PI* and to 3.10% using adaptive HCC control for distorted source and unbalanced load conditions. However, under three-phase, four-wire systems, they give significantly different results. The THD in the source current reduced from 28.17% to 7.23% with *dq-PI* control and to 0.51% with adaptive HCC control for the same source and load conditions.

These results point that, *dq-PI* control is not able to give the required compensation characteristics in a highly distorted and complex systems. Except for *dq-PI* control in three-phase, four-wire systems under distorted source and unbalanced load conditions, the THD in the source current is within the limits defined in IEEE-519. The over all obtained results have demonstrated the effectiveness of using telecom sites to aid in the improvement of grid power quality.

Acknowledgment

It would not have been possible to do this thesis without the help and support of kind people around me, only to some of whom is possible to give particular mention here.

I would like to thank my supervisor Professor Ole-Morten Midtgård at the Department of Electric Power Engineering, NTNU, for his valuable guidance, support, and motivation throughout this study. My gratitude also goes to my co-supervisors Iromi Kurume (PhD. student) and Dr. Ole Jacob Sørdalen from Eltek AS for their support.

I want to thank my good friend Ashenafi Lulseged Yifru for proof reading this thesis, his input was invaluable. I must also thank my friends and family for being there and support me with everything.

Finally, and above all, I would like to express my deepest gratitude to my loving wife Beza Assefa Akalewold for her unceasing support, encouragement and for being my inspiration.

Berhane Darsene Dimd
Trondheim, June 2015

Contents

List of Figures

List of Tables

Acronyms

AC	Alternating Current
DC	Direct Current
DER	Distributed Energy Resource
DG	Distributed Generation
FACTS	Flexible Alternating Current Transmission System
HCC	Hysteresis Current Control
ICT	Information Communication Technology
LV	Low Voltage
MOSFET	Metal Oxide Semiconductor Field Effect Transistor
PCC	Point of Common Coupling
PMU	Phasor Measurement Unit
PWM	Pulse Width Modulation
RES	Renewable Energy Source
SAF	Shunt Active Filter
SMPS	Switch Mode Power Supply
STATCOM	STAtic COMpensator
SVC	Static VAr Compensator
T&D	Transmission and Distribution
TCR	Thyristor Controlled Reactor
TSC	Thyristor Switched Capacitor
UPFC	Universal Power Flow Controller
UPS	Uninterrupted Power Supply
VSC	Voltage Source Converter

Chapter 1

Introduction

This chapter introduces the problem addressed by this thesis and the motivations for solving it; and consequently state the project objectives, scopes and limitations. And at last, the structure of the report is outlined.

1.1 Motivation

In order to stop the global climate change and its quiet obvious consequences, it is urgently necessary to further develop distributed energy production based on the renewable energy sources. Current irreversible destruction processes should not be allowed to continue, and much more intensive growth of energy efficiency and renewable energy source (RES) utilization should be implemented [2].

More efforts are being made all over the world towards the promotion of clean energy for environmental protection and scheduling energy consumption pattern to meet its increasing demand. The grid is to be modified or upgraded to promote clean energy, control the energy consumption pattern and bring security to grid. The smart grid will fulfill these requirements. The developments in information and communication technology (ICT) together with efficient power electronic converters support the smart grid vision. However there are many challenges and issues in the implementation of smart grid [3].

With the increasing penetration of renewable energies as distributed generation (DG) in smart grid scheme, technical problems arise in both distribution and transmission system level. Today's storage technologies are becoming more efficient and higher performing and they are looked as an enabling technology necessary in a smart grid environment. The converter systems associated with energy storage devices can also provide power quality benefits by acting like a system filter and eliminating unwanted variations in frequency and voltage.

Extensive use of power electronic converters, however, add disturbances to the grid by drawing harmonic and reactive currents. A number of mitigation techniques are implemented to avoid these power quality issues.

The power converters in telecom sites are primarily used to charge the battery banks which supply dc telecom loads. Since these power converters are bi-directional, the combined rectifier and inverter modules can perform full four quadrant operation. Additional features that help improve the grid power quality can be added to these converters. The cost effectiveness of this arrangement is open to research study but it would be an interesting alternative to the growing power quality problem and in support with "Towards Smart grid" movement.

In this thesis, battery banks from different telecom sites together with their associated power converters are used in shunt active filter configuration to mitigate harmonic components and to provide reactive power support to the grid.

1.2 Objectives of the Study

The main objectives of this study are:

- Smart grid overview and challenges, identifying power quality issues in smart grids and reviewing the different methods to mitigate the issues
- Understanding the roles of smart power electronic converters and battery storage systems to improve power quality issues
- Design of active filter controller based on instantaneous power theory (p-q Theory)
- Analyzing Battery-Power converter combination in telecom sites as shunt active filter to mitigate harmonics and compensate reactive power using Matlab/Simulink R2015a.

1.3 Scope of Work

The following scope of work is based on the objectives described:

- The ICT portion of smart grid technology is not the area of interest here
- Only two of the main grid power quality issues, harmonic current pollution and reactive power consumption are analyzed in detail
- Instantaneous power theory (p-q Theory) is used in the design of all active filter controllers

1.4 Structure of the Thesis

Chapter 2 starts with smart grid overview and follows with the different challenges and technologies involved in the implementation of smart grid. And it gives an overview of the different smart grid power quality issues together with their effect on the system and the different methods to mitigate the issues.

Chapter 3 discuses the different electric power definitions and presents the details of instantaneous power theory (p-q theory) which will be used in the design of shunt active filter.

Chapter 4 presents the details of shunt active filters in both three-phase, three-wire systems and three-phase, four-wire systems.

Chapter 5 gives the detail system model to be analyzed using Matlab/Simulink. It presents the control techniques used to force the converter synthesize the required compensating currents for harmonics and reactive power compensation.

Chapter 6 presents and discuses the different simulation results that are simulated on Matlab/Simulink.

Chapter 7 concludes the main findings in the study and gives recommendations for further work.

Chapter 2

Smart Grid and Power Quality Issues

2.1 Smart Grid Overview

A smart grid is a new approach to the integration of power generation, transmission systems, distribution networks, and consumption. Over the last few years, electrical energy consumption has continuously grown and, at the same time, investment in the transmission and distribution infrastructure has correspondingly declined. Traditional solutions for upgrading the electrical system infrastructure have been primarily in the form of new power plants, new transmission lines, substations, and associated equipments. However, as experience has proven, the process of authorizing, locating, and constructing new transmission lines has become difficult, expensive and time-consuming. As a result, the power grid is under stress, resulting in compromised reliability and higher energy costs [4].

Despite the above problems, system reliability is vital and cannot be compromised. To overcome this, grid operators are moving away from radial systems towards networked, however, this degrades controllability of the network because current flows along particular lines which cannot easily be controlled. The situation is even worse if an incident such as loss of a line results in overload, increasing the possibility of a blackout [5].

The answer seems to lie in transforming the current electric power system into Smart electric grid. Future smart grids will be strong, more flexible, reliable, self-healing, fully controllable, and asset efficient [6].

2.1.1 Smart Grid Definition

It is a difficult task to find a particular definition for Smart grid; every author, energy organization and government defines it in their own ways.

According to the author of [7], "*A smart grid is the use of sensors, communications, computational ability and control in some form to enhance the overall functionality of the electric power delivery system.*"

According to [8], "*A Smart Grid is an electricity network that can intelligently integrate the actions of all users connected to it; generators, consumers and those that do both; in order to efficiently deliver sustainable, economic and secure electricity supply.*"

2.1.2 Smart Grid Challenges

Key benefits of smart grid are uninterrupted power supply, reduced transmission and distribution loss, high penetration of renewable energy sources, cyber secured electrical grid, large scale energy storage, and flexibility to consumers to interact with electricity market, and market based electricity pricing. Despite all the above benefits, it brings also challenges and issues which have to be addressed [9, 10]. Some of these are:

- Self-Healing Actions

  A smart grid has to be able to self-heal itself; meaning it should be able to take action in order to continue to deliver power after a contingency occurs. To do so, a micro-controller has to be associated to all and every asset of the grid while tied through a reliable communication system linked to a central command center. The challenges facing this configuration are security and reliability of the grid.

- Renewable Energy Integration with the Grid

  Renewable energy such as wind or solar-based generation systems when integrated with the electric grid faces a series of challenges such as wind forecast, wind generation dispatch, power flow optimization, power system optimization and power system stability.

- Energy Storage Systems

  When relying on more renewable energy generation system, it is essential to integrate more energy storage systems. The challenges with energy storage systems are cost, complexity and non-flexibility.

- Consumer's Motivation

A key function of a smart grid is to motivate consumer to actively participate in the energy management of the grid. This function encounters challenges like privacy, security and consumer education.

- Reliability

  Smart grid is expected to deliver reliable power to customers. Power grid reliability is assessed by the frequency and duration of outages. Smart grid is required to reduce both numbers in order to improve the system reliability.

- Power Quality

  Smart grid is required to provide power with a high quality level to consumers through features like:

  – Disturbance Identification

    Smart grid has to find the proper cause of distortion in the grid to determine if the disturbance is from the generation side or the load side.

  – Harmonic Compensation

    In order to provide high quality power, harmonic mitigation techniques need to be developed such that harmonics are suppressed and any other power quality events such as sag, swell, spikes, over-voltage, under-voltage, voltage flicker, frequency deviations and voltage unbalance should be avoided.

The main issues to be studied and analyzed in this thesis are power quality and energy storage systems. The other issues of smart grid are not in the scope of the study.

2.1.3 Smart Grid Technologies

Advanced information, telecommunication and control technologies play a critical role in making a grid 'smart'. The smart grid technologies and their applications could be considered in three dimensions,

1. Functional characteristics such as integrated communication, protection and control infrastructure
2. Device technologies such as meters and phasor measure units (PMU) and
3. Application use cases such as customer engagement, demand response incentive and dynamic pricing.

All the three mentioned areas of smart grid technologies are not in the scope of this study. Their detail description can be found in [11]. The main interest of smart grid technologies in this study are, FACTS (Flexible Alternating Current Transmission System) devices, Voltage Control and VAr Support Devices, Unified Power Flow

Controller and Energy storage. The details of these devices will be discussed in the next section.

2.2 Smart Grid Power Quality Issues

With the increasing penetration of renewable energies as distributed generation (DG) in smart grid scheme, technical problems arise in both distribution and transmission system level. Undesirable voltage is the main problem for connection of DGs in distribution systems while excessive reactive power demand from transmission system is the major concern for Transmission System Operators.

The low power generation capacity of DER (Distributed Energy Resources) has motivated the need for integration of different types of DERs and loads in the form of micro-grid to enhance the power generation capacity, reliability and marketability of dispersed type of micro-sources [12, 13]. Current harmonics and Reactive power consumption are the two power quality issues that are addressed in this thesis.

2.2.1 Current Harmonics

Power system harmonics are sinusoidal voltages and currents at frequencies that are integer multiples of the main generated (or fundamental) frequency. They constitute the major distorting components of the main voltage and load current waveforms.

Most countries have in the past developed their own harmonic standards or recommendations, to suit local conditions. However, with the growth of global trade, the need for equipment manufactured in one country to comply with standards in another, has prompted concerted effort in formulating international standards on harmonics and inter-harmonics [14].

In the view of the proliferation of the power electronic equipment connected to the utility system, various national and international agencies have been considering limits of harmonic current injection to maintain good power quality. As a consequence, various standards and guidelines have been established that specify limits on the magnitudes of harmonic currents and harmonic voltage distortion at various harmonic frequencies [15] . IEEE-519, which is used as a standard in this study can be found in Appendix A.

According to the French mathematician Jean Baptiste Joseph, any periodic waveform can be deconstructed into a sinusoid at the fundamental frequency and with a number of sinusoids at harmonic frequencies . This is shown in Equation 2.1:

$$f(x) = \frac{a_0}{2} + \sum_{n=1}^{\infty} a_n \cos nx + \sum_{n=1}^{\infty} a_n \sin nx \tag{2.1}$$

where $f(x)$ is a generic periodic waveform, a_0 is the dc component, calculated as in Equation 2.2, a_n and b_n are the coefficients of the series, calculated as in Equation 2.3 , n is an integer between 1 and infinity, and $T = 2\pi$, is the period.

$$a_0 = \frac{1}{\pi}\int_0^{2\pi} f(x)dx \tag{2.2}$$

$$a_n = \frac{1}{\pi}\int_0^{2\pi} f(x)\cos(nx)dx \quad \text{and} \quad b_n = \frac{1}{\pi}\int_0^{2\pi} f(x)\sin(nx)dx \tag{2.3}$$

Any harmonic component can be represented as a percentage of the fundamental (%f) or a percentage of the rms(root mean square) value (%r) of the total current , with the following formula [16]

$$I_h = 100\%\frac{I_n}{I_1} \tag{2.4}$$

where I_n is the amplitude of current harmonic n and I_1 is the amplitude of fundamental current (or the r.m.s. value of the total current).

The ratio of the rms value of the sum of all the harmonic components up to a specified order to the rms value of the fundamental component is called total harmonic distortion (THD) and it can be represented as

$$THD = 100\%\sqrt{\sum_{n=2}^{\infty} {I_h}^2} = 100\%\sqrt{\sum_{n=2}^{\infty}\left(\frac{I_n}{I_1}\right)^2} \tag{2.5}$$

In the simulation of the system under study, a FFT analysis is used from Simulink to obtain the different harmonic spectrum of the source current.

2.2.1.1 Cause and Effect of Harmonics

Power electronic devices, together with operation of non-linear appliances, inject harmonics into the grid which may potentially create voltage distortion problem. Operating harmonics need to be minimized to keep the total harmonic distortion within acceptable limits.

Non-linear loads, unlike linear loads, draw non-sinusoidal current from a sinusoidal voltage supply. The distortion to the normal incoming sinusoidal current wave can be considered to result from the load emitting harmonic currents. These emitted harmonic currents, like any generated current, will circulate via available paths and return to the other pole of the non-linear load. In doing so, they cause harmonic voltage drops in all the impedances through which they pass. The aim must therefore be to shunt the emitted harmonic currents into low impedance paths as close to the

non-linear load as possible. This is to minimize the resulting voltage distortion, as the voltage distortion will cause harmonic currents to flow in other linear and non-linear connected loads [17, 18].

Harmonic currents generated by non-linear loads such as SMPS (Switch Mode Power Supply), variable speed motors, drive computers, power electronic inverters are applicable for micro grids. Most power systems accommodate harmonic current up to a certain level but when it becomes significant, it will cause communication errors, overheating, excessive line losses, spurious tripping of circuit breaker [12, 19, 20].

Some of the main causes of harmonic pollution are [21]:

- Switch mode power supplies
- Televisions and Computers
- Fluorescent lamps with electronic ballasts
- Variable speed drives
- Thyristor controls for heating and ovens and Welding equipment
- Rectifiers and Light dimmers
- Uninterruptible power supplies

The main effects of harmonic pollution are:

- Heating Effects of Harmonics

  Harmonic currents flowing in rotating machines cause heating effects both in the conductors and in the iron circuit. In particular, eddy current losses are proportional to the square of the frequency. Further, some harmonics are negative-phase sequence in nature and these give rise to additional losses by inducing higher frequency currents and negative torques in machine rotors [17, 22, 23].

- Harmonic Over voltages

  Harmonic voltages, generated by harmonic currents flowing against impedance to the harmonic, can lead to significant over voltages. Such effects are known to cause equipment failures, and capacitors are particularly susceptible [15, 17].

- Resonances

  Any inductive-capacitive-resistive (LCR) circuit, such as a power system, will exhibit a resonant response to one or more frequencies. Such natural system resonances are not, by themselves, necessarily causes for concern. It is only when such system responses, coupled with significant harmonic current inputs from non-linear loads, lead to excessive harmonic voltages [17].

Other adverse effects of harmonics include [17, 21]:

- Over-stressing and heating of insulation
- Machine vibration and Malfunctioning of electronic devices
- Over stressing of power factor correction capacitors
- Nuisance tripping of protective devices
- Interference

2.2.1.2 Harmonics Mitigation Methods

Different types of filters are used to mitigate harmonic distortion. According to the IEEE-519 standard, harmonics in the power system should be limited for both the harmonic current that a user can inject into the network at the PCC, and the harmonic voltage that the utility can supply to any customer at the PCC [24, 25]. The two common passive methods of harmonics mitigation are briefly discussed as follows.

1. Harmonic Filters

   Harmonic filters are series or parallel resonant circuits designed to shunt or block harmonic currents. They reduce the harmonic currents flowing in the power system from the source and thereby reduce the harmonic voltage distortion in the system. Such devices are expensive and should only be used after other methods have been assessed [15, 17].

2. Capacitor Detuning

   It is possible for power factor correction capacitors, particularly on thyristor controlled drives, to form a low impedance path for harmonics or to inadvertently resonate with one of the harmonics produced by the non-linear load. A solution is to detune the capacitors from high harmonics by the insertion of a series reactor forming a tuned circuit with the resonant frequency typically around the fourth harmonic. The capacitor circuit then will look inductive to all harmonics above the fourth harmonic and resonance will be quenched [17].

Passive methods of harmonic mitigation are not implemented in the newer technologies. By using power electronic converters, shunt active filters can make the current drawn by non-linear loads sinusoidal and in phase with the input voltage [15]. The focus of this thesis is also in shunt active filters for harmonics mitigation and reactive power compensation.

Other methods of preventing harmonics pollution are [21],

- Delta/star isolation transformers
- Equipment with built-in power factor correction

- Avoidance of long cable runs to suspect equipment

2.2.2 Reactive Power Consumption

The consumption of reactive power by an induction generator is a common problem which affects the grid power quality. An induction generator requires an increasing amount of reactive power as the amount of power generated increases, and it is essential to provide reactive power locally as close as possible to the demand levels.

The reactive power management in distribution network with large penetration of distributed energy resources is also an important task in future power systems. The control of reactive power allows the inclusion of more distributed resources and a more efficient operation of distributed network [26].

2.2.2.1 Cause and Effect of Reactive Power Consumption

The main causes of reactive power consumption are:

- Induction motors and generators
- Large penetration of DER
- Transformers, Transmission lines and cables
- Power electronic converters and reactive loads

An increase in reactive power demand at PCC would affect the system power factor at PCC. As a result, voltage stability tends to become a binding technical criterion [27]. In particular, reactive power demand of smart grids is changing with growing installation of renewable energy sources [28].

2.2.2.2 Reactive Power Compensation

Reactive power compensation is typically implemented by using a fixed capacitor, a switched capacitor or a static compensator. Precise reactive power compensation considering proper size and proper control can remove voltage collapse and instability of the power system [24]. Two categories of reactive power compensation are discussed here [5, 15].

1. Power Injection Using Static Compensators

   Power electronic switching devices are used to control the connection of either fixed units or switchable units of reactors and capacitors to the transmission lines.

i. Thyristor Switched Capacitor (TSC)

TSC configuration is shown in Figure 2.1(a). The switching device in TSC is used only to switch ON or OFF the capacitor banks, and no phase angle control is used. The switching of the capacitor units is used when load demands capacitive support. In general, series reactor is connected in series with capacitor bank to limit the inrush current while switching.

ii. Thyristor Controlled Reactor (TCR)

TCR acts like a variable susceptance and is dependent on thyristor switching control. By phase angle control of the switch from 90^0 to 180^0, the flow of current through the reactor is varied. The fundamental inductor current is, therefore, a function of the branch susceptance that is dependent on the firing delay angle α. TCR configuration is shown in Figure 2.1(b).

iii. Thyristor-Switched Capacitor and Thyristor-Controlled Reactor (TSC-TCR)

TSC-TCR combines the functionality of thyristor switched capacitor and thyristor controlled reactor. The circuit arrangement for this configuration is shown in Figure 2.1(c).

The details of these devices including other configurations can be found in [5, 15].

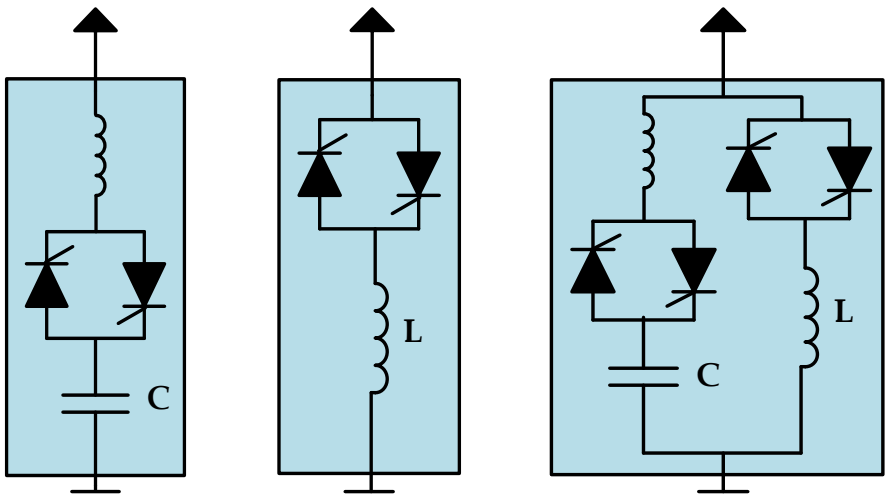

(a) TSC (b) TCR (c) TSC-TCR

Figure 2.1: Thyristor Switched Capacitor, Thyristor Controlled Reactor and TSC-TCR combined configurations

2. Power Injection Using Advanced Static Devices

Passive and switchable compensators generate low frequency harmonics while providing the required VAr supplement. By using advanced fast switching devices, reduced reflected harmonics are achieved with low cost high pass filter units. The advantages of using forced commutated switching devices that control compensation capacitors and reactors, give the compensation system the ability to control both active and reactive power. The following devices are included in this category [5].

A. Static Synchronous Compensator (STATCOM)

STATCOM is a highly recommended compensation unit for flicker mitigation as well as injecting reactive power components to distribution system. It is made of six power electronics forced commutating switching devices in a three-phase full bridge configuration. The bridge is controlled to supply current to a large DC capacitor. The switching devices are controlled by a PWM switching logic driver circuit. They generate harmonics at the switching frequency and its multiples, but these high frequency harmonic components can easily be filtered using high frequency tuned passive elements. STATCOM is connected in shunt to the distribution network through a limiting reactor or coupling transformer [5, 15].

B. Unified Power Flow Controller (UPFC)

UPFC basically consists of two fully controlled converters sharing a common DC link. The converters are controlled to compensate for the voltage as well as the power of the coupled transmission lines. One converter performs the main function of the UPFC, which is injecting an AC voltage with controllable magnitude and phase angle in series with the transmission line. The other converter, on the other hand, supplies or absorbs the active power demanded by the first converter. Both converters can be controlled to generate or absorb controllable reactive power or provide independent shunt reactive compensation for the line. In principle, a UPFC can perform voltage support, power flow control and dynamic stability improvement at the same time [5].

Harmonic current mitigation and reactive power compensation in this thesis are realized through converters and batteries in different telecom sites and using them in shunt active filter configuration.

2.2.3 Other Power Quality Issues

1. Voltage Disturbance

Voltage fluctuation or instability as well as voltage sags/dips, noise, surges and power outages are the common problems encountered during integration of large-scale DER into the grid. Variability of wind speed with time is not the

only reason for these problems; grid connection issues, faults during operations and starting of large motors, etc., are also responsible [24].

Effects on loads are usually noticed when the voltage fluctuates more than 10% above or below the nominal voltage, and the severity of the effects depend upon the duration of the change. Extended under voltage causes 'brownouts' which is characterized by dimming of lights and inability to power some equipment such as fridge compressors. Extended over voltage decreases the life of most equipments and can damage sensitive electronic equipments [13].

The main mitigations for voltage disturbance include energy storage, balancing, Static VAr Compensators (SVCs) and the STATCOM [15, 17].

2. Frequency Fluctuation

Frequency is one of the most important factor in power quality. The frequency is controlled by maintaining balance between connected loads and generation. It is controlled within a small deviation.

DG inverters are able to help with frequency control. Inverters can provide frequency control in milliseconds, which is significantly faster than conventional generation. Of course, grid-connected inverters would only be able to control frequency to the extent that, changes in their real power output actually influence the overall supply–demand balance. Generally they will not be able to change the frequency unless they represent a significant amount of generation; such as in relatively small grids. In addition, special control algorithms would need to be developed to take advantage of the fast response time and at present DG is unproven in this application [29, 13].

The advancement of electrical device technologies can be used to balance the frequency of the system by adjusting power consumption. However, this can only be achieved by having good data communication management [30].

2.3 Active Filters

Figure 2.2 shows a one-line diagram of how an active filter functions. The current drawn by non-linear loads consists of a fundamental frequency component, i_{L1} and a distortion component, $i_{L,dist}$. Under a current mode control, a switched mode converter is operated to deliver the current $i_{L,dist}$ to the grid. Therefore, in an ideal case, the harmonics in the grid are eliminated. On the dc side of the converter, only a capacitor with a minimum energy storage is needed [15] . This is the type of active filtering configuration that would be used and studied in this thesis.

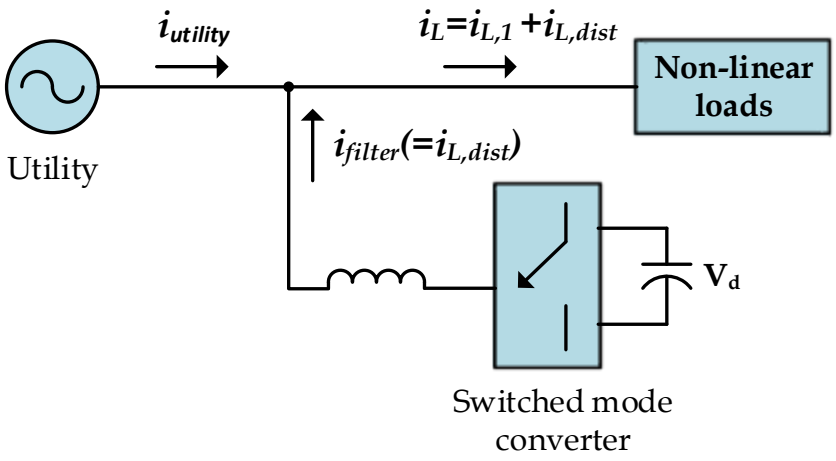

Figure 2.2: One-line diagram of an active filter

Chapter 3

Electric Power Definitions and Instantaneous Power Theory

3.1 Electric Power Definitions

The concepts and definitions of electric power for sinusoidal ac systems are well established and accepted worldwide. However, under non-sinusoidal conditions, several different power definitions are still in use. For instance, the conventional concepts of reactive and apparent power lose their usefulness in non-sinusoidal cases [31]. At early times, two important approaches to power definitions under non-sinusoidal conditions were introduced by Budeanu [32] in 1927, and by Fryze [33] in 1932. Budeanu's power definition was in the frequency domain, where as Fryze defined power in the time domain.

The problems related to non-linear loads became increasingly significant at the beginning of advances in power electronics devices. These modern devices behave as non-linear loads and most of them draw a significant amount of harmonic current from the power system. Hence, this required a consistent set of power definitions that are valid also under transient and non-sinusoidal conditions.

3.1.1 Power Definitions Under Sinusoidal Balanced Conditions

Here electric power definitions for sinusoidal voltages and currents are described for single-phase and three-phase systems.

(a) Single-Phase System

Consider an ideal single-phase system with a sinusoidal voltage and an inductive R-L load. The voltage and current equations are given by

$$v(t) = \sqrt{2}V \sin(\omega t) \quad \text{and} \quad i(t) = \sqrt{2}I \sin(\omega t - \phi) \tag{3.1}$$

where V and I represent rms values of the voltage and current, respectively, and ω is the angular line frequency. The instantaneous power is given by the product of the instantaneous voltage and current.

$$p(t) = v(t)i(t) = 2VI \sin(\omega t) \sin(\omega t - \phi) \tag{3.2}$$

$$p(t) = VI \cos\phi - VI \cos(2\omega t - \phi) \tag{3.3}$$

Equation 3.3 shows that the instantaneous power of a single-phase system is not constant. It has an oscillating component at twice the line frequency added to an average value. Decomposing the oscillating component and rearranging Equation 3.3 give

$$p(t) = \underbrace{VI \cos\phi[1 - \cos 2\omega t]}_{I} - \underbrace{VI \sin\phi \sin 2\omega t}_{II} \tag{3.4}$$

Equation 3.4 shows that instantaneous power in single-phase system has two parts that can be interpreted as:

1. The first part has an average value equal to $VI\cos\phi$ and has an oscillating component on it, pulsing at twice the line frequency. It represents a unidirectional power flow from the source to the load.
2. The other has a pure oscillating component at the double frequency (2ω), and has a peak value equal to $VI\sin\phi$. Clearly, it has a zero average value.

Active power, P is defined as the average value of part one of Equation 3.4 and is given by

$$P = VI\cos\phi \tag{3.5}$$

Reactive power, Q is defined as the peak value of part two of Equation 3.4 and is given by

$$Q = VI\sin\phi \tag{3.6}$$

Apparent power, S is defined as the maximum reachable active power at unity power factor

$$S = PI \tag{3.7}$$

Another quantity called the power factor is defined as a measure of how effectively the load draws the real power [15], and it is given by

$$Power factor = \frac{P}{S} = \frac{P}{VI} = \cos\phi \tag{3.8}$$

Ideally, the power factor should be 1.0 to draw power with a minimum current magnitude and hence minimize losses in the system.

(b) Three-Phase System

Consider three-phase voltages and line currents that contain only positive-sequence fundamental component (sinusoidal and balanced system)

$$\begin{aligned} v_a(t) &= \sqrt{2}V \sin(\omega t + \phi_v) \\ v_b(t) &= \sqrt{2}V \sin(\omega t + \phi_v - 2\pi/3) \\ v_c(t) &= \sqrt{2}V \sin(\omega t + \phi_v + 2\pi/3) \end{aligned} \tag{3.9}$$

and

$$\begin{aligned} i_a(t) &= \sqrt{2}I \sin(\omega t + \phi_i) \\ i_b(t) &= \sqrt{2}I \sin(\omega t + \phi_i - 2\pi/3) \\ i_c(t) &= \sqrt{2}I \sin(\omega t + \phi_i + 2\pi/3) \end{aligned} \tag{3.10}$$

For a three-phase system with or without a neutral conductor, three-phase instantaneous active power, $p_{3\phi}(t)$ describes the total instantaneous energy flow per time unit being transferred between two subsystems [31], and it is given by

$$p_{3\phi}(t) = v_a(t)i_a(t) + v_b(t)i_b(t) + v_c(t)i_c(t) \tag{3.11}$$

Substituting Equation 3.9 and Equation 3.10 in to Equation 3.11 results in,

$$p_{3\phi}(t) = 3VI\cos(\phi_v - \phi_i) = 3P \tag{3.12}$$

The instantaneous active three-phase power is constant as shown in Equation 3.12, that, it is time-independent in contrast to the single-phase power.

The three-phase active (average) power, $P_{3\phi}$ is given by

$$P_{3\phi} = 3VI\cos(\phi_v - \phi_i) = 3P \tag{3.13}$$

The three-phase apparent power, $S_{3\phi}$ is given by

$$S_{3\phi} = 3S = 3VI \tag{3.14}$$

Three-phase reactive power, $Q_{3\phi}$ is given by

$$Q_{3\phi} = 3Q = 3VI\sin(\phi_v - \phi_i) \tag{3.15}$$

The reactive power, $Q_{3\phi}$ in Equation 3.15 is just a mathematical definition without any precise physical meaning [31]. In other words, the three-phase circuit includes no oscillating power components in the three-phase instantaneous active power, in contrast to the single-phase instantaneous active power.

3.1.2 Power Definitions Under Non-Sinusoidal Conditions

The concepts of power under non-sinusoidal conditions are not unique; they are divergent and lead to different results in some aspects [31].

(a) Single-Phase System

Two distinct sets of power definitions are commonly used; one is established in the frequency domain and the other in time domain. They are briefly discussed below.

Power Definition by Budeanu - If a single-phase ac circuit with a generic load and source is in steady state, its voltage and current waveforms can be decomposed in Fourier series. Then, the corresponding phasor for each harmonic component can be determined, and the following definitions of powers can be derived.

Apparent power, S

$$S = VI \tag{3.16}$$

where V and I are the rms values of generic, periodic voltage and current waveforms, which are calculated as

$$V = \sqrt{\frac{1}{T}\int_0^T v^2(t)dt} = \sqrt{\sum_{n=1}^{\infty} V_n^2} \tag{3.17}$$

and

$$I = \sqrt{\frac{1}{T}\int_0^T i^2(t)dt} = \sqrt{\sum_{n=1}^{\infty} I_n^2} \tag{3.18}$$

Here, V_n and I_n correspond to the rms value of the n^{th} order harmonic components of the Fourier series, and T is the period of the fundamental component.

Active power, P

$$P = \sum_{n=1}^{\infty} P_n = \sum_{n=1}^{\infty} V_n I_n \cos\phi_n \tag{3.19}$$

Reactive power, Q

$$Q = \sum_{n=1}^{\infty} Q_n = \sum_{n=1}^{\infty} V_n I_n \sin\phi_n \tag{3.20}$$

where ϕ_n represents the displacement angle of each pair of the n^{th} order harmonic voltage and current components.

However, under non-sinusoidal conditions, both reactive power and apparent power can not characterize satisfactorily the issues of power quality. The details of Budeanu power definitions can be found in [32].

Power Definition by Fryze - In the early 1930s, Fryze proposed a set of power definitions based on rms values of voltage and current. The basic equations according to the Fryze's approach are given below.

Active power, P_w

$$P_w = \frac{1}{T}\int_0^T p(t)dt = \frac{1}{T}\int_0^T v(t)i(t)dt = V_w I = V I_w \tag{3.21}$$

where V and I are the voltage and current rms values and V_w and I_w are the active voltage and active current defined below.

Apparent power, P_s

$$P_s = VI \tag{3.22}$$

Active power factor, λ

$$\lambda = \frac{P_w}{P_s} = \frac{P_w}{VI} \tag{3.23}$$

Reactive power, P_q

$$P_q = \sqrt{P_s^2 - P_w^2} = V_q I = V I_q \tag{3.24}$$

where V_q and I_q are the reactive voltage and current as defined below.

Reactive power factor, λ_q

$$\lambda_q = \sqrt{1 - \lambda^2} \tag{3.25}$$

Active voltage, V_w and Active current, I_w

$$V_w = \lambda V \qquad and \qquad I_w = \lambda I \tag{3.26}$$

Reactive voltage V_q and Reactive current I_q:

$$V_q = \lambda_q V \qquad and \qquad I_q = \lambda_q I \tag{3.27}$$

The details of Fryze power definitions can be found in [33].

(b) Three-Phase Systems

Three-phase systems are commonly used in generation, transmission and distribution of electric power. Power in a three-phase system is constant.

Three-Phase systems can be classified as, Three-Phase, Three-Wire System (if the system has no ground or there is only one grounded node in the whole sub-network) and Three-Phase, Four-Wire System (if the system is grounded at more than one point under normal operation, and the ground can provide additional path for current circulation or it can have a fourth conductor).

Three-Phase systems can also be classified as, Three-Phase Balanced System (Sinusoidal condition where the amplitude of the three phases are equal and are $2\pi/3$ degree out of phase to each other), Three-Phase Unbalanced System (Sinusoidal condition where the amplitude of the three phases are not equal or/and they are

not $2\pi/3$ degree out of phase to each other) and Three-Phase Distorted System (Non-sinusoidal condition, it contains both harmonics and unbalance).

Symmetrical components are most commonly used for analysis of three-phase electrical power systems under unbalanced and distorted conditions. If the phase quantities are expressed in phasor notation using complex numbers, a vector can be formed for the three phase quantities. For example, a vector for three phase voltages could be written as [34]

$$V_{abc} = \begin{bmatrix} V_a \\ V_b \\ V_c \end{bmatrix} = \begin{bmatrix} V_{a,0} \\ V_{b,0} \\ V_{c,0} \end{bmatrix} + \begin{bmatrix} V_{a,1} \\ V_{b,1} \\ V_{c,1} \end{bmatrix} + \begin{bmatrix} V_{a,2} \\ V_{b,2} \\ V_{c,2} \end{bmatrix} \tag{3.28}$$

where the subscripts $0, 1$, and 2 refer to the zero, positive, and negative sequence components respectively. The sequence components differ only by their phase angles, $2/3\pi$ radians. The sequence components are calculated using

$$V_{012} = \begin{bmatrix} V_0 \\ V_1 \\ V_2 \end{bmatrix} = \frac{1}{3} \begin{bmatrix} 1 & 1 & 1 \\ 1 & \alpha & \alpha^2 \\ 1 & \alpha^2 & \alpha \end{bmatrix} \begin{bmatrix} V_a \\ V_b \\ V_c \end{bmatrix} \tag{3.29}$$

where the constant α is a complex number that acts as a 120^0 phase shift operator, and it is given by

$$\alpha = e^{j(2\pi/3)} = -\frac{1}{2} + j\frac{\sqrt{3}}{2} \tag{3.30}$$

Similar transformations can also be made for the current phasors. After the decomposition is made for the voltages and currents, power calculation can be made on the respective components. Details of symmetrical component power calculation can be found in [34].

The degree of unbalance is usually expressed as the ratio of the negative and zero sequence components to the positive sequence component. Imbalances at the fundamental frequency can be caused by negative-sequence or zero-sequence components. However, it is important to note that only an imbalance from a negative-sequence component can appear in a three-phase grounded or ungrounded system. Imbalance from zero-sequence component only appears in a three-phase, four-wire (grounded) system, which induces the current flowing through the neutral wire.

The traditional concepts of apparent power and reactive power are in contradiction if applied to unbalanced and/or distorted three-phase systems. Therefore, the instantaneous power theory is chosen in the next section as the fundamental equation for power definitions in three-phase systems and in the design active filter controllers.

3.2 Instantaneous Power Theory (*p-q* Theory)

The development of power electronic devices and their associated converters have brought new boundary conditions to the energy flow problem. This is not exactly because the problem is new, but because these converters behave as non-linear loads and represent a significant amount of power compared with other traditional linear loads. The speed response of these converters and the way they generate reactive power and harmonic components have made it clear that conventional approaches to the analysis of power are not sufficient in terms of taking average or rms values of variables. Therefore, time-domain analysis has evolved as a new manner to analyze and understand the physical nature of the energy flow in a non-linear circuit [31].

The *p-q* Theory is based on a set of instantaneous powers defined in the time domain. No restrictions are imposed on the voltage or current waveforms, and it can be applied to three-phase systems with or without a neutral wire for three-phase generic voltage and current waveforms. Thus, it is valid not only in the steady state, but also in the transient state.

The *p-q* Theory first transforms voltages and currents from *abc* coordinates to $\alpha\beta 0$, and then defines instantaneous power on these coordinates.

3.2.1 The Clarke Transformation

The *p-q* theory implements a transformation from a stationary reference system in *abc* coordinates to a system with coordinates $\alpha\beta 0$. It corresponds to an algebraic transformation known as Clarke transformation [35], which also produces a stationary reference system. The coordinates $\alpha\beta$ are orthogonal to each other, and coordinate 0 corresponds to the zero-sequence component.

The voltages and currents in $\alpha\beta 0$ coordinates are calculated using

$$\begin{bmatrix} v_0 \\ v_\alpha \\ v_\beta \end{bmatrix} = T \begin{bmatrix} v_a \\ v_b \\ v_c \end{bmatrix} \quad \text{and} \quad \begin{bmatrix} i_0 \\ i_\alpha \\ i_\beta \end{bmatrix} = T \begin{bmatrix} i_a \\ i_b \\ i_c \end{bmatrix} \tag{3.31}$$

where T is a transformation matrix and it is given by

$$T = \sqrt{\frac{2}{3}} \begin{bmatrix} \frac{1}{\sqrt{2}} & \frac{1}{\sqrt{2}} & \frac{1}{\sqrt{2}} \\ 1 & -\frac{1}{2} & -\frac{1}{2} \\ 0 & \frac{\sqrt{3}}{2} & -\frac{\sqrt{3}}{2} \end{bmatrix} \tag{3.32}$$

The inverse transformation is given by

$$\begin{bmatrix} v_a \\ v_b \\ v_c \end{bmatrix} = T^* \begin{bmatrix} v_0 \\ v_\alpha \\ v_\beta \end{bmatrix} \quad \text{and} \quad \begin{bmatrix} i_a \\ i_b \\ i_c \end{bmatrix} = T^* \begin{bmatrix} i_0 \\ i_\alpha \\ i_\beta \end{bmatrix} \tag{3.33}$$

where T^* is the inverse transformation matrix given by

$$T^* = \sqrt{\frac{2}{3}} \begin{bmatrix} \frac{1}{\sqrt{2}} & 1 & 0 \\ \frac{1}{\sqrt{2}} & -\frac{1}{2} & \frac{\sqrt{3}}{2} \\ \frac{1}{\sqrt{2}} & -\frac{1}{2} & -\frac{\sqrt{3}}{2} \end{bmatrix} \tag{3.34}$$

One advantage of applying the $\alpha\beta 0$ transformation is to separate zero-sequence components from the *abc* phase components. The α and β axes make no contribution to zero-sequence components.

If v_0 can be eliminated (for balanced three-phase voltage) from the transformation matrix, the Clarke transformation and its inverse transformation will reduce to

$$\begin{bmatrix} v_\alpha \\ v_\beta \end{bmatrix} = \sqrt{\frac{2}{3}} \begin{bmatrix} 1 & -\frac{1}{2} & -\frac{1}{2} \\ 0 & \frac{\sqrt{3}}{2} & -\frac{\sqrt{3}}{2} \end{bmatrix} \begin{bmatrix} v_a \\ v_b \\ v_c \end{bmatrix} \tag{3.35}$$

and

$$\begin{bmatrix} v_a \\ v_b \\ v_c \end{bmatrix} = \sqrt{\frac{2}{3}} \begin{bmatrix} 1 & 0 \\ -\frac{1}{2} & \frac{\sqrt{3}}{2} \\ -\frac{1}{2} & -\frac{\sqrt{3}}{2} \end{bmatrix} \begin{bmatrix} v_\alpha \\ v_\beta \end{bmatrix} \tag{3.36}$$

Similarly, if i_0 can be eliminated (for three-phase, three-wire system), Equation 3.35 and Equation 3.36 also applies for the current waveforms.

3.2.2 Instantaneous Powers based on *p-q* Theory

For a three-phase system with or without a neutral conductor in the steady state or during transients, the three-phase instantaneous active power, $p_{3\phi}$ describes the total instantaneous energy flow per second between two subsystems [31].

The three-phase instantaneous active power can be calculated in terms of the $\alpha\beta 0$ as

$$p_{3\phi} = v_a i_a + v_b i_b + v_c i_c \Leftrightarrow p_{3\phi} = v_\alpha i_\alpha + v_\beta i_\beta + v_0 i_0 \tag{3.37}$$

Three instantaneous powers, the instantaneous zero-sequence power p_0, the instantaneous real power p, and the instantaneous imaginary power q are defined from the instantaneous phase voltages and line currents on the $\alpha\beta 0$ axes as

$$\begin{bmatrix} p_0 \\ p \\ q \end{bmatrix} = \begin{bmatrix} v_0 & 0 & 0 \\ 0 & v_\alpha & v_\beta \\ 0 & v_\beta & -v_\alpha \end{bmatrix} \begin{bmatrix} i_0 \\ i_\alpha \\ i_\beta \end{bmatrix} \tag{3.38}$$

Each power component can be separated into its mean and alternating parts[1].

1. Instantaneous Zero-Sequence Power (p_0)

$$p_0 = \bar{p_0} + \widetilde{p_0} \tag{3.39}$$

$\bar{p_0}$: Mean value of the instantaneous zero-sequence power which corresponds to the energy per unit time that is transferred from the power source to the load through the zero-sequence components of voltage and current.

$\widetilde{p_0}$: Alternating value of the instantaneous zero-sequence power which corresponds to the energy per unit time that is exchanged between the power source and the load through the zero-sequence components of voltage and current.

2. Instantaneous Real Power (p)

$$p = \bar{p} + \tilde{p} \tag{3.40}$$

The real power p represents the total energy flow per time unity in the circuit.

$\bar{p}$: Mean value of the instantaneous real power that corresponds to the energy per time unity that is transferred from the power source to the load, in a balanced way.

$\tilde{p}$: Alternating value of the instantaneous real power that represents the oscillating energy flow per time unity, which naturally produces a zero average value, representing an amount of additional power flow in the system without effective contribution to the energy transfer from the source to the load or from the load to the source.

3. Instantaneous Imaginary Power (q)

$$q = \bar{q} + \tilde{q} \tag{3.41}$$

The instantaneous imaginary power has to do with power (corresponding to undesirable currents) that is exchanged between the system phases, and which does not imply any transfer or exchange of energy between the power source and the load.

$\bar{q}$: This corresponds to the conventional three-phase reactive power and does not contribute to energy transfer.

$\tilde{q}$: This also corresponds to a power that is being exchanged among the three phases, without transferring any energy between source and load.

Figure 3.1 summarizes the above power definitions about real, imaginary, and zero-sequence powers.

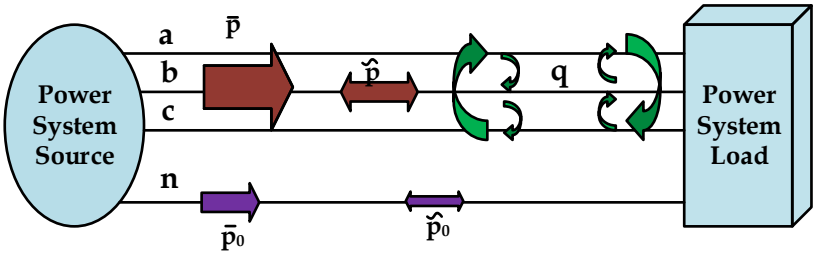

Figure 3.1: Physical meaning of instantaneous powers defined on $\alpha\beta 0$ reference frame [1]

3.2.3 The *p-q* Theory in Three-Phase, Three-Wire Systems

If v_0 can be neglected, an instantaneous voltage vector can be defined from instantaneous α and β voltage components, that is

$$e = v_\alpha + jv_\beta \tag{3.42}$$

And similarly, if i_0 can be neglected (no neutral current in three-phase, three-wire system), the instantaneous current vector is defined as

$$i = i_\alpha + ji_\beta \tag{3.43}$$

The instantaneous complex power, s is defined as the product of the voltage vector, e and the conjugate of the current vector, i^*, and it is given in the form of complex numbers by

$$s = ei^* = (v_\alpha + jv_\beta)(i_\alpha - ji_\beta) = \underbrace{(v_\alpha i_\alpha + v_\beta i_\beta)}_{p} + j\underbrace{(v_\beta i_\alpha - v_\alpha i_\beta)}_{q} \tag{3.44}$$

or in matrix form

$$\begin{bmatrix} p \\ q \end{bmatrix} = \begin{bmatrix} v_\alpha & v_\beta \\ v_\beta & -v_\alpha \end{bmatrix} \begin{bmatrix} i_\alpha \\ i_\beta \end{bmatrix} \tag{3.45}$$

The two powers have a constant value and an oscillating component as explained earlier. The $\alpha\beta$ currents can be calculated as functions of voltages and the real and imaginary powers p and q using Equation 3.46.

$$\begin{bmatrix} i_\alpha \\ i_\beta \end{bmatrix} = \frac{1}{v_\alpha^2 + v_\beta^2} \begin{bmatrix} v_\alpha & v_\beta \\ v_\beta & -v_\alpha \end{bmatrix} \begin{bmatrix} p \\ q \end{bmatrix} \tag{3.46}$$

The *p-q* Theory has the prominent merit of allowing complete analysis and real-time calculation of various powers and respective currents involved in a three-phase circuit. Knowing in real time the values of undesirable currents in a circuit allow us to eliminate them [31]. This is one of the basic ideas of active filtering that will be presented in detail in Chapter 4.

3.2.4 The *p-q* Theory in Three-Phase, Four-Wire Systems

The presence of a fourth conductor, a neutral conductor, is very common in low-voltage distribution systems, in addition to the cases of grounded transmission systems. The reduced transformation and equations used in the previous section are not applicable here [31].

Three-phase, four-wire systems can include both zero-sequence voltage and current. Therefore, to represent the system correctly, the instantaneous zero-sequence power, p_0 has to be introduced as the third instantaneous power in addition to the instantaneous real power, p and the instantaneous imaginary power, q.

$$\begin{bmatrix} p_0 \\ p \\ q \end{bmatrix} = \begin{bmatrix} v_0 & 0 & 0 \\ 0 & v_\alpha & v_\beta \\ 0 & v_\beta & -v_\alpha \end{bmatrix} \begin{bmatrix} i_0 \\ i_\alpha \\ i_\beta \end{bmatrix} \tag{3.47}$$

The three-phase instantaneous active power, $p_{3\phi}$ is equal to the sum of the real power, p and the zero-sequence power, p_0. In the case of a three-phase, three-wire circuit, the power, p_0 does not exist, and so $p_{3\phi}$ is equal to p.

$$p_{3\phi} = v_a i_a + v_b i_b + v_c i_c = v_\alpha i_\alpha + v_\beta i_\beta + v_0 i_0 = p + p_0 \tag{3.48}$$

Zero-sequence power has the same characteristics as the instantaneous power in a single-phase circuit. It has an average value and an oscillating component at twice the line frequency. The average value, $\bar{p_0}$ represents a unidirectional energy flow. It has the same characteristics as the conventional (average) active power. The oscillating component, $\tilde{p_0}$ also transfers energy instantaneously. However, it has an average value equal to zero. Ideally, the average value of the zero-sequence power helps to increase the total energy transfer, and in this sense, it can be considered as a positive point. However, even for the simplest case of a zero-sequence component in the voltage and current, the zero-sequence power, p_0 cannot produce constant power, $\bar{p_0}$ alone. In other words, p_0 always consists of $\bar{p_0}$ together with $\tilde{p_0}$. The elimination of $\tilde{p_0}$ is accompanied by the elimination of $\bar{p_0}$ [31].

3.2.5 Application of *p-q* theory for Shunt Current Compensation

Figure 3.2 illustrates the basic idea of shunt current compensation. It shows a source supplying a non-linear load that is being compensated by a shunt compensator. The shunt compensator behaves as a three-phase, controlled current source that can supply any set of calculated current references i^*_{Ca}, i^*_{Cb} and i^*_{Cc} [31].

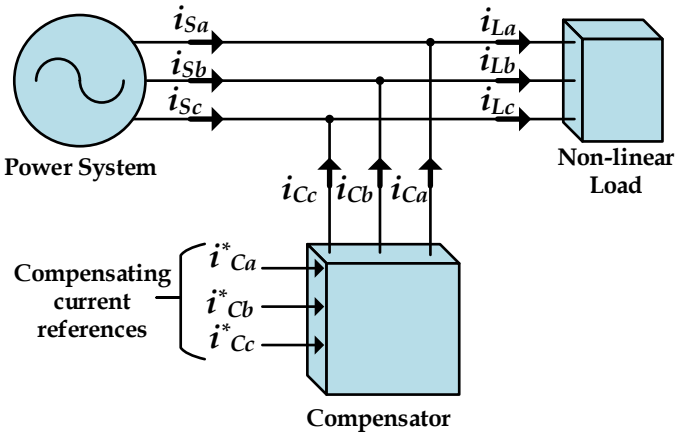

Figure 3.2: Basic principle of shunt current compensation

Figure 3.3 shows a general control method implemented in the controller of a shunt compensator using p-q theory. The calculated real power, p of the load can be separated into its average ($\bar{p}$) and oscillating ($\tilde{p}$) parts. Likewise, the load imaginary power, q can be separated into its average ($\bar{q}$) and oscillating ($\tilde{q}$) parts. Then, undesired portions of the real and imaginary powers of the load that should be compensated are selected. Then, the inverse transformation from $\alpha\beta$ to abc is applied to calculate the instantaneous values of the three-phase compensating current references, i^*_{Ca}, i^*_{Cb} and i^*_{Cc} [31].

Table 3.1 presents the various possible compensation objectives that can be achieved by implementing the control algorithm in Figure 3.3 with the active shunt filter shown in Figure 3.2, considering the same system conditions in all cases.

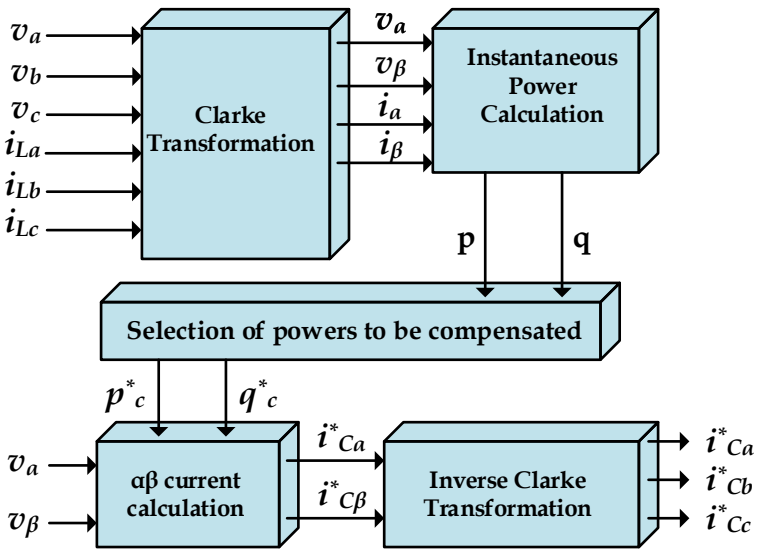

Figure 3.3: Control method for shunt current compensation based on p-q theory

Table 3.1: Various possible compensation results based on Figure 3.2

Case	Compensated Parameters	Comments
1	Average load imaginary power($\bar{q}$)	Source imaginary power will have only oscillating part
2	Load imaginary power(q)	Source imaginary power will be zero, it's fully compensated
3	Oscillating load active power($\tilde{p}$)	The source will supply a constant active power
4	Oscillating load active power and Oscillating load imaginary power($\tilde{p}$ and $\tilde{q}$)	The source will supply constant active and imaginary power
5	Oscillating load active power and load imaginary power($\tilde{p}$ and q)	All undesirable current components are eliminated. Source current is sinusoidal and produce constant active power and no imaginary power

Case 5 in Table 3.1 is what will be studied in this thesis to obtain a sinusoidal source current and to fully compensate reactive power of the load, and it will be discussed in detail in the coming chapters.

Chapter 4

Shunt Active Filter based on *p-q* Theory

Nowadays, the use of electric and electronic equipments (rectifiers, variable speed drives, computers and industrial installations) containing power semiconductors such as Thyristor converters, are in considerable progress. The non-linear behavior of these equipments generate harmonics that affect the distribution utility operation directly[36, 37]. The main power quality issues to be focused here are harmonic pollution and reactive power consumption.

In order to overcome these problems and ensure the electrical sources safety, several solutions have been investigated.

One of the most popular solution to reduce harmonic pollution is the use of passive filters. However, the use of these filters is not suitable when the impedance of the power network varies. In addition, they may cause series or parallel resonances which will result in amplification of harmonic currents in the power network [38].

To overcome the problems of passive filters, shunt active filtering concept was first introduced by Gyugyi and Strycula in 1976 [39]. The associated controllers with these shunt active filters can determine in real time the compensating current reference, and force a power converter to synthesize it accurately. In this way, the active filtering can be selective and adaptive [31]. The shunt active filter considered in this thesis has controller based on the instantaneous active and reactive power theory (*p-q* Theory) presented in Chapter 3.

4.1 Overview of Shunt Active Filters

Shunt active filters generally consist of two distinct main blocks: The PWM converter (power processing) and the active filter controller (signal processing).

The PWM converter is responsible for power processing in synthesizing the compensating current that should be drawn from the power system. The active filter controller is responsible for signal processing in determining in real time the instantaneous compensating current references, which are continuously passed to the PWM converter.

Figure 4.1 shows the basic configuration of a shunt active filter for harmonic current compensation of a specific load [31]. It consists of a voltage source converter with a PWM current controller and an active filter controller that results in an almost instantaneous control algorithm. The shunt active filter controller works in a closed-loop manner, continuously sensing the load current i_L, and calculating the instantaneous values of the compensating current reference, i_C^* for the PWM converter. In an ideal case, the PWM converter may be considered as a linear power amplifier, where the compensating current, i_C tracks correctly its reference, i_C^*.

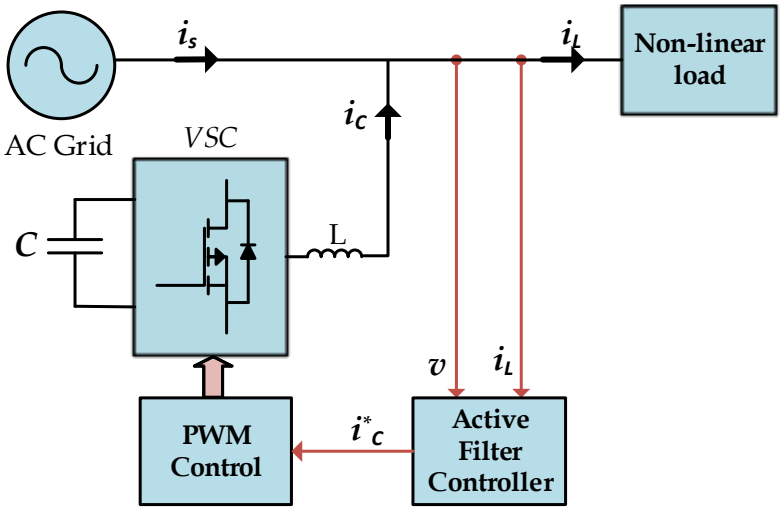

Figure 4.1: Basic configuration of a shunt active filter

4.1.1 Converters for Shunt Active Filters

Figure 4.2 and Figure 4.3 show three-phase power converters for implementing shunt active filters. Figure 4.2 is a voltage-source converter (VSC) and Figure 4.3 is a current source converter (CSC).

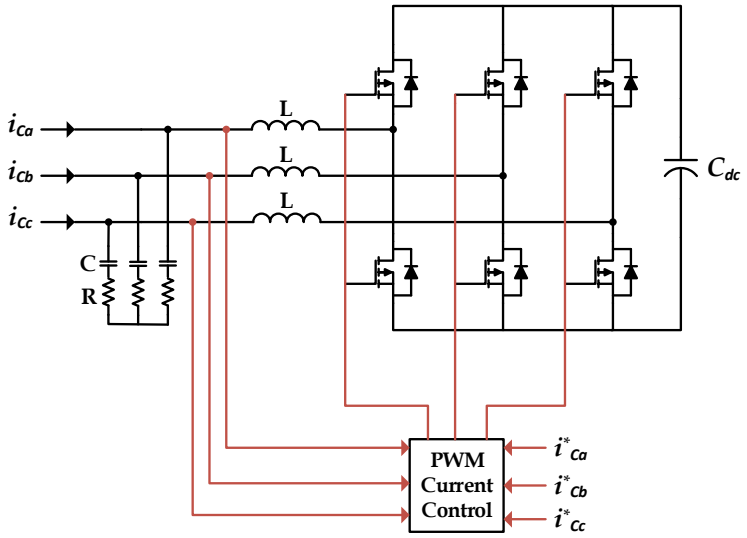

Figure 4.2: Voltage source converter

These PWM controllers have the same functionality which is to force the converter to behave as a controlled current source. It should be noted that no power supply, only an energy storage element (capacitor for the VSC and inductor for the CSC) is connected on the DC side of the converters. The reason is that the principal function of a shunt active filter is to behave as a compensator.

Nowadays, almost all shunt active filters in commercial operation use voltage source converters. A performance comparison between voltage source converter and voltage source converter is given in Table 4.1 [40].

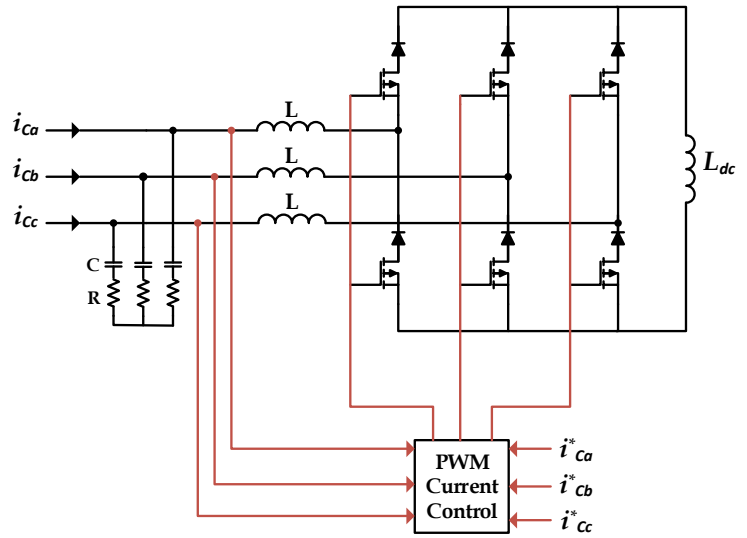

Figure 4.3: Current source converter

Table 4.1: Comparison between VSC and CSC

	VSC	CSC
Pros	Effective in filtering of harmonics	Effective in filtering of harmonics
	High efficiency at normal operating point	Simple open-loop current control
	More flexible	Robust
	Small size	Simple current protection
Cons	Switching ripple in the output	Bulky and heavy dc inductor
	Low efficiency with low power loads	High dc link losses
	Limited life time of the dc link capacitor	Over-voltage protection is needed

PWM converters generate undesirable current harmonics around the switching frequency and its multiples. If the switching frequency of the PWM converter is sufficiently high, these undesirable current harmonics can be easily filtered out by using small, passive high-pass filters represented by R and C in Figure 4.2 and Figure 4.3.

4.1.2 Active Filter Controllers

The control algorithm implemented in the controller of the shunt active filter determines the compensation characteristics of the shunt active filter. There are many ways to design a control algorithm for active filtering. Certainly, the *p-q* Theory forms a very efficient basis for designing active filter controllers [31].

There are three optimal compensation characteristics in the design of active filter controller,

(a) Draw a constant instantaneous active power from a source

(b) Draw a sinusoidal current from a source

(c) Draw the minimum rms value of a source current

Only under three-phase sinusoidal and balanced systems, it is possible to satisfy simultaneously all the three optimal compensation characteristics given above. Otherwise a choice must be made between the three before designing a controller for shunt active filter. This is the reason why one need to derive three different control strategies [31].

1. Constant instantaneous power control strategy

   This control strategy guarantees that only average power is drawn from a source. According to the *p-q* theory, to draw constant instantaneous active power from the source means that the shunt active filter must compensate for

the oscillating real power ($\tilde{p}$). Additionally, the rms value of the compensated current is minimized by the compensation of the total imaginary power(q) of the load. This control strategy is interesting if no real-power oscillation between the source and the load is desired.

2. Sinusoidal current control strategy

   This control strategy is applied if the shunt active filter must compensate the load current to guarantee balanced, sinusoidal current drawn from the power system. Additionally, the active filter is compensating reactive power so that the compensated current is in phase with the fundamental positive-sequence component of the voltage. However, this current does not produce constant real power as long as the system voltage is non-sinusoidal and unbalanced.

3. Generalized Fryze current control strategy

   This control strategy minimizes the compensated current, and gives the minimum rms value of current that can transfer the same amount of energy as the uncompensated current. Hence, this minimum rms current produces minimum ohmic losses in the transmission line. It cannot guarantee any sinusoidal compensated current or constant instantaneous active power drawn from the power system.

In this thesis, sinusoidal current control strategy is used to minimize harmonics and compensate reactive power in a distorted power system with non-linear loads.

4.2 Three-Phase, Three-Wire Shunt Active Filter

A particular characteristic of three-phase, three-wire systems is the absence of the neutral conductor and, consequently, the absence of zero-sequence current components. Thus, the zero-sequence power is always zero in these systems [31].

Figure 4.4 shows the most important parts of a three-phase, three-wire shunt active filter for current compensation. The active filter controller consist three main functional control blocks:

1. Instantaneous power calculation

   This block calculates the instantaneous powers of the non-linear load. According to the p-q theory, only the real and imaginary powers exist, because the zero-sequence power is always zero. The instantaneous real and imaginary powers are given by Equation 4.1.

$$\begin{bmatrix} p \\ q \end{bmatrix} = \begin{bmatrix} v_\alpha & v_\beta \\ v_\beta & \text{-}v_\alpha \end{bmatrix} \begin{bmatrix} i_\alpha \\ i_\beta \end{bmatrix} \tag{4.1}$$

2. Power compensation selection

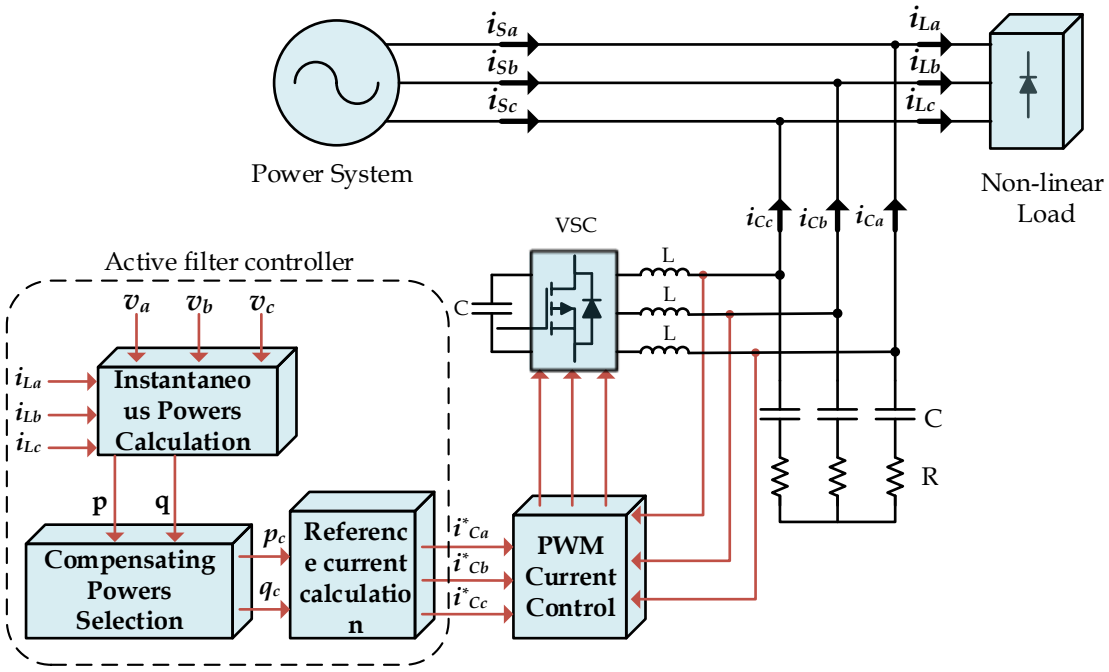

Figure 4.4: Three-phase, three-wire shunt active filter

This block determines the behavior of the shunt active filter. In other words, it selects the parts of the real and imaginary powers of the non-linear load that should be compensated by the shunt active filter.

The instantaneous real power of the non-linear load should be continuously measured, and separated into its average and oscillating parts. In a real implementation, the separation of $\bar{p}$ and $\tilde{p}$ from p is realized through a low-pass filter. Unfortunately, the unavoidable time delay introduced by the low-pass filter may degenerate the entire performance of the shunt active filter during transients. In the simulation, a fifth-order Butterworth low-pass filter with a cutoff frequency, 50 Hz is used to separate $\bar{p}$ from p.

3. Current reference calculation

The compensating real power p_C, which, together with the compensating imaginary power q_C, are passed to the current-reference calculation block. It determines the instantaneous compensating current references from the compensating powers and voltages. The instantaneous compensating reference currents are calculated using Equation 4.2.

$$\begin{bmatrix} i_\alpha \\ i_\beta \end{bmatrix} = \frac{1}{(v_\alpha)^2 + (v_\beta)^2} \begin{bmatrix} v_\alpha & v_\beta \\ v_\beta & -v_\alpha \end{bmatrix} \begin{bmatrix} p_c \\ q_c \end{bmatrix} \tag{4.2}$$

The power circuit of the shunt active filter consists of a three-phase voltage source converter made up of MOSFETs and anti-parallel diodes. The PWM current control forces the VSC to behave as a controlled current source. In order to avoid high di/dt,

the coupling of a VSC to the power system must be made through a series inductor, commonly known as a coupling inductor.

4.2.1 Sinusoidal Current Control Strategy in Three-phase, Three-wire Systems

Sinusoidal current control strategy is a compensation method that makes the active filter compensate the current of a non-linear load to force the compensated source current to become sinusoidal and balanced.

In order to make the compensated current sinusoidal and balanced, the shunt active filter should compensate all harmonic components as well as the fundamental components that differ from the fundamental positive-sequence current, I_1. Only this component is left to be supplied by the source. In order to determine the fundamental positive-sequence component of the load current, a positive-sequence detector is needed in the active filter controller. The control block diagram for three-phase, three-wire sinusoidal current control strategy is shown in Figure 4.5 [41].

The positive-sequence detector block extracts instantaneously the fundamental positive-sequence voltages v'_a, v'_b and v'_c that correspond to the phasor V_1(positive-sequence phasor) of the system voltage $v_a, v_b$and v_c.

The instantaneous phase voltages v'_a, v'_b and v'_c that correspond to the phasor V_1 of the fundamental positive-sequence voltage are transformed into the $\alpha\beta$ coordinates by means of the Clark transformation block. Then, they are used in both instanta-

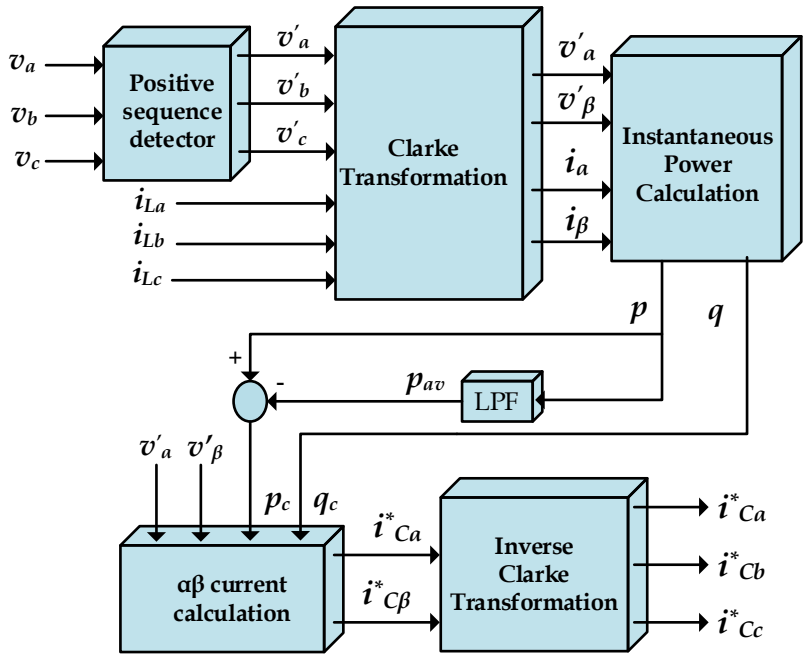

Figure 4.5: The control block diagram for the sinusoidal current control strategy

neous powers calculation block and in $\alpha\beta$ currents calculation block. Together with the power being compensated, that is, $\tilde{p}$ and q, the $\alpha\beta$ currents calculation block determines exactly all the required current components.

Positive-Sequence Detector The detection of the fundamental positive-sequence component of v_a, v_b and v_c is necessary in the sinusoidal current control strategy. This control strategy makes the shunt active filter to compensate load currents. Thus, only the active portion of the fundamental positive-sequence component, which produces average real power, $\bar{p}$ only is supplied by the source.

Figure 4.6 shows the complete functional control block diagram of the fundamental positive-sequence voltage detector [31]. An important part of the positive-sequence detector is the phase-locked-loop (PLL) circuit. The voltages v_a, v_b, and v_c are transformed into the $\alpha\beta$ axes to determine v_α and v_β. They are used together with auxiliary currents i'_α and i'_β, produced in the PLL circuit, to calculate the auxiliary powers p' and q'. The auxiliary currents i'_α and i'_β with any magnitude are derived only from an auxiliary positive-sequence current, I_1 at the fundamental frequency, detected by the PLL circuit.

Only the fundamental positive-sequence voltage component, V_1 contributes to the average value of the auxiliary powers, p' and q', represented by p_{av} and q_{av} in Figure 4.6 . The influence of the fundamental negative-sequence, V_2 and other voltage harmonics will appear only in the oscillating components $\tilde{p}'$ and $\tilde{q}'$ of the auxiliary powers, which are being excluded from the inverse voltage calculation. Two fifth order Butterworth low-pass filters with cutoff frequency of 50 Hz are used for obtaining the average powers $\bar{p}'$ and $\bar{q}'$.

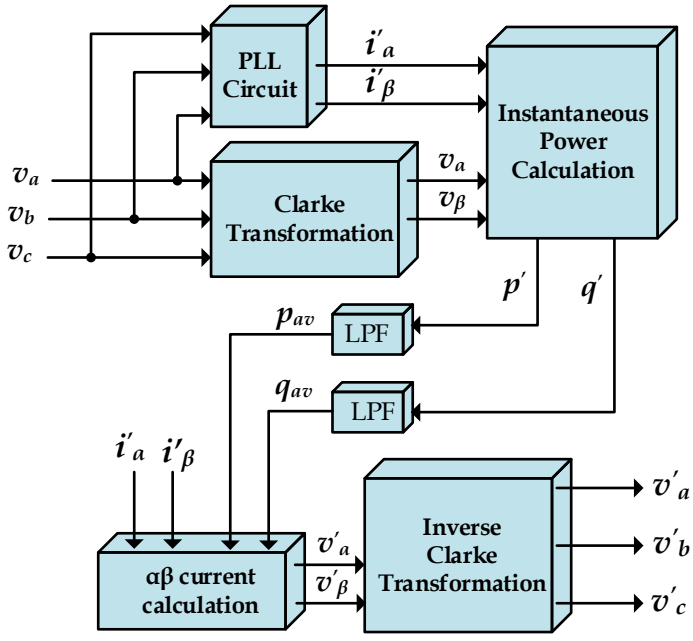

Figure 4.6: Fundamental positive-sequence detector

The $\alpha\beta$ voltage calculation block calculates the instantaneous voltages v'_α and v'_β, which correspond to time functions of the fundamental positive-sequence phasor, V_1 of the system voltage,

$$\begin{bmatrix} v'_\alpha \\ v'_\beta \end{bmatrix} = \frac{1}{(i'_\alpha)^2 + (i'_\beta)^2} \begin{bmatrix} i'_\alpha & -i'_\beta \\ i'_\beta & i'_\alpha \end{bmatrix} \begin{bmatrix} p_{av} \\ q_{av} \end{bmatrix} \tag{4.3}$$

The instantaneous abc fundamental phase voltages v'_a, v'_b and v'_c can be calculated by applying the inverse Clarke transformation,

$$\begin{bmatrix} v'_a \\ v'_b \\ v'_c \end{bmatrix} = \sqrt{\frac{2}{3}} \begin{bmatrix} 1 & 0 \\ -\frac{1}{2} & \frac{\sqrt{3}}{2} \\ -\frac{1}{2} & -\frac{\sqrt{3}}{2} \end{bmatrix} \begin{bmatrix} v'_\alpha \\ v'_\beta \end{bmatrix} \tag{4.4}$$

The PLL circuit must provide accurately the auxiliary currents i'_α and i'_β, corresponding to sinusoidal functions at the fundamental frequency. Author of [31] gives a detailed analysis of positive-sequence detector and PLL circuit.

Phase-Locked-Loop Circuit The PLL circuit continuously tracks the fundamental frequency of the measured system voltages. The appropriate design of the PLL allows proper operation under distorted and unbalanced voltage waveforms. The PLL circuit determines automatically the system frequency and the phase angle of the fundamental positive-sequence component of a three-phase generic input signal. Figure 4.7 illustrates its functional block diagram [31].

The algorithm is based on a fictitious instantaneous active power expression given in Equation 4.5. This power, $p'_{3\phi}$, is not related to any instantaneous active power of the power system.

$$p'_{3\phi} = v_a i'_a + v_b i'_b + v_c i'_c = v_{ab} i'_a + v_{cb} i'_c \tag{4.5}$$

The PLL can reach a stable point of operation only if the input $p'_{3\phi}$ of the PI controller has, in the steady state, a zero average value, that is, $\bar{p}'_{3\phi}$. Moreover, the

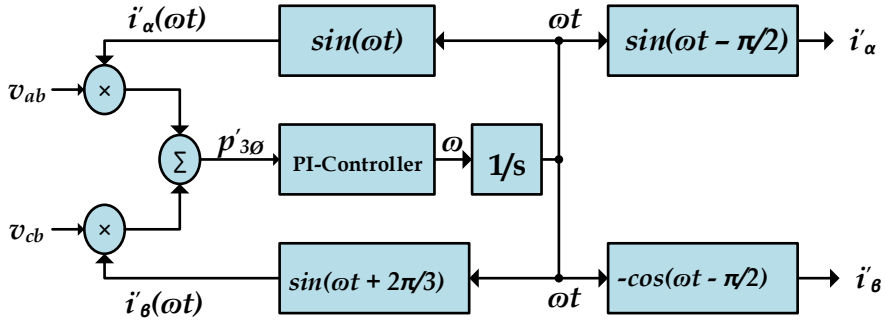

Figure 4.7: Functional block diagram of the PLL circuit

control circuit should minimize oscillations in $p'_{3\phi}$ at low frequencies. The oscillating portion $\tilde{p}'_{3\phi}$, where $p'_{3\phi} = \bar{p}'_{3\phi} + \tilde{p}'_{3\phi}$, at low frequencies is not well attenuated by the PI controller and may bring instability to the PLL control circuit. The above constraints are found only if ω equals the system frequency, and the current $i'_a(\omega t)$ becomes orthogonal to the fundamental positive-sequence component of the measured three-phase voltages v_a, v_b, and v_c. The PLL has only one stable point of operation, that is, $i'_a(\omega t)$ leading by 90^0 the phase voltage v_a.

In the simulation model, $K_p = 3$ and $K_i = 100$ are used in the PI-controller block. The tuning is made manually by hit and try method, thus it does not work as per the requirement for highly distorted system. The 'Sequence Analyzer' block from Simulink is used instead to extract the fundamental positive-sequence components.

4.3 Three-Phase, Four-Wire Shunt Active Filter

Three-phase, Four-wire shunt active filters are intended for grounded three-phase systems or three-phase systems with neutral conductors. These active filters are specially designed for compensating neutral currents (zero-sequence current components) and also have all those compensation characteristics discussed in the previous section for three-phase, three-wire systems.

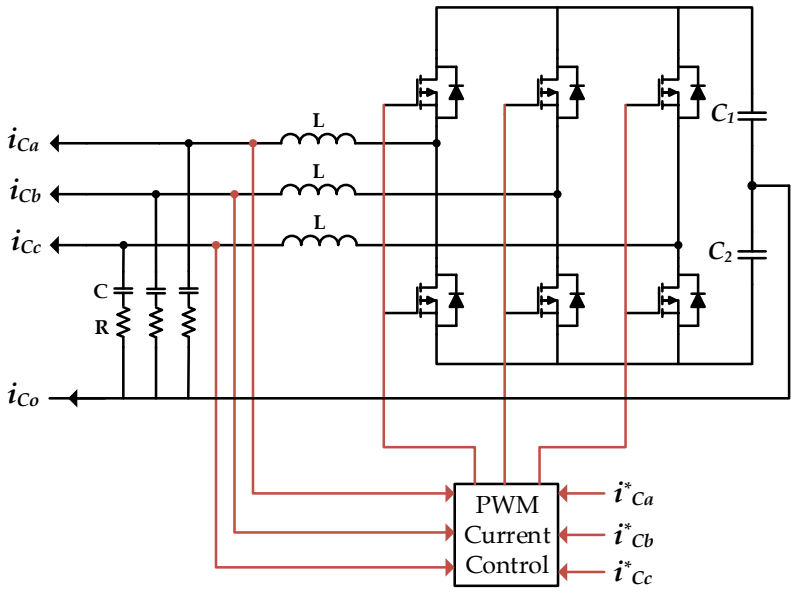

Figure 4.8: Three-leg "split-capacitor" converter topology

4.3.1 Converter Topologies

To employ SAF in three-phase, four-wire systems, two types of converter configurations are possible; one is a three-leg structure with the neutral conductor being

connected to midpoint of dc-link capacitor (Figure 4.8); and the other is a four-leg structure, where the fourth leg is provided exclusively for neutral current compensation [42] (Figure 4.9).

A performance comparison between the two converter topologies is given in Table 4.2 [43, 44]. In this thesis, the conventional three-phase "split capacitor" topology is used in the simulations, and it is preferred for its less number of power semiconductor switches.

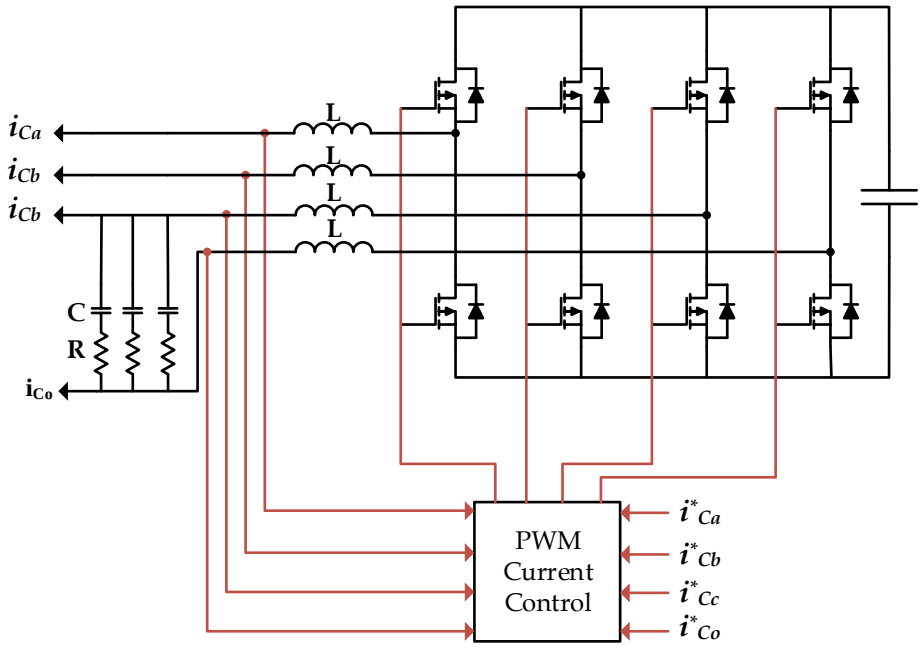

Figure 4.9: Four-leg converter topology

Table 4.2: Comparison between three-leg and four-leg converter topologies

	Three-leg converter	Four-leg converter
Pros	Small number of power switches	Easy control circuit
	Lower switching loss for the same rating	Requires smaller dc-link capacitor
	Lower cost	No need of balancing the dc voltage
Cons	Complex control circuit	High switching loss and high cost
	High dc-link capacitor required	More number of power switches

Figure 4.10 shows a three-phase, four-wire shunt active filter implemented with the "split-capacitor" converter topology. The active filter controller realizes sinusoidal current control strategy, and additionally compensates the load neutral current. Ideally, $i_{C0} = -i_{L0}$, and the neutral current to the source (i_{S0}) is zero.

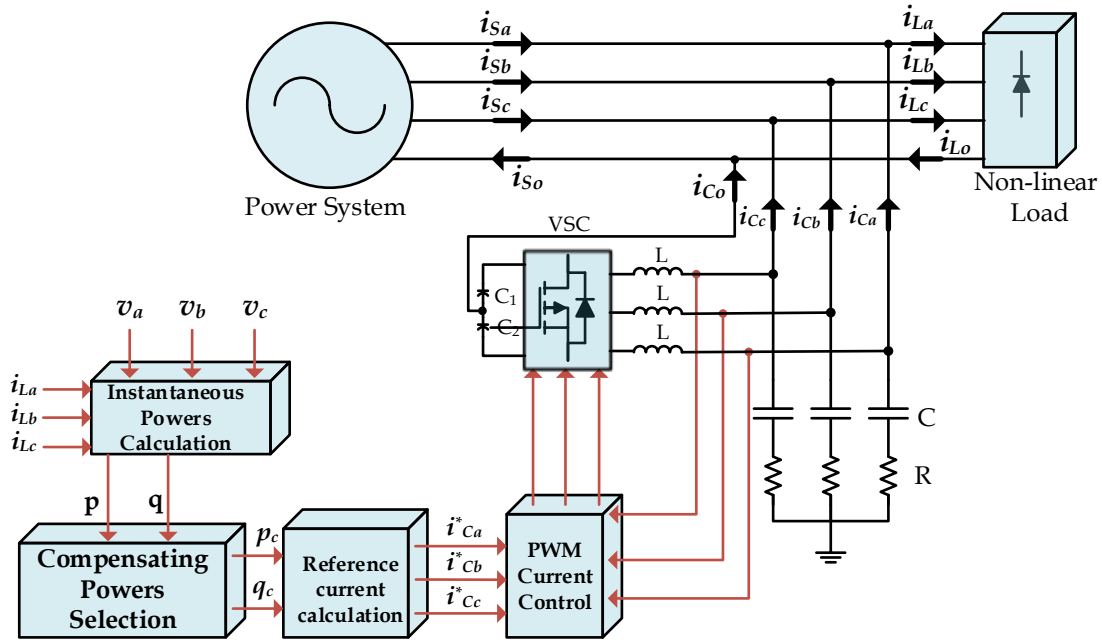

Figure 4.10: Three-phase, four-wire shunt active filter using three-leg converter

4.3.2 Sinusoidal Current Control Strategy in Three-phase, Four-wire Systems

The sinusoidal current control strategy makes the active filter to compensate the current of a non-linear load to guarantee balanced, sinusoidal current drawn from the network, even under an unbalanced and/or distorted system voltage. It compensates also the neutral current of the load, in addition to all the compensation features presented for active filters in three-phase, three-wire systems.

The phase angle and frequency of the fundamental positive-sequence voltage, corresponding to the phasor V_1, must be accurately determined by the positive-sequence detector. Otherwise, the active filter controller cannot exactly determine the fundamental reactive power of the load included in $\bar{q}$, which in turn cannot produce AC currents I_1 orthogonal to the AC voltages V_1 to produce only $\bar{p}$ [31].

A similar functional block diagram that results in sinusoidal current, as Figure 4.5 for three-phase, three-wire systems, is shown in Appendix A for three-phase, four-wire systems. This control block guarantees sinusoidal and balanced compensated currents drawn from the network. Additionally, the shunt active filter can supply non-zero average negative-sequence and zero-sequence powers.

Chapter 5

Network Modeling

Simulation is a very important and powerful method that helps to reduce development time and to study the dynamics of different systems. In this thesis, Matlab/Simulink 2015a is used as a simulation tool to implement shunt active filtering.

5.1 System Layout

Telecom sites are equipped with battery banks to supply DC loads planted at different sites for telecommunication purpose. The batteries are charged from the grid through a bi-directional voltage source converter. In addition to supplying power to the DC loads, the battery banks can be used to support the low voltage ac grid with power quality improvement

The block diagram representation of the system to be studied in this thesis is shown in Figure 5.1. The main components in the system are Supply system (LV AC Grid), Telecom sites with their batteries, loads and converters, and Linear and non-linear loads connected at PCC. A brief description of each component and their model is discussed as follows.

5.1.1 Supply System Modeling

Different telecom sites are connected to a three-phase low voltage ac grid. Three different cases of system supply voltages are considered in the simulation, a balanced three-phase voltage, unbalanced three-phase voltage and unbalanced-distorted three-phase voltage source. Parameters of an ideal three-phase voltage are given in Table 5.1.

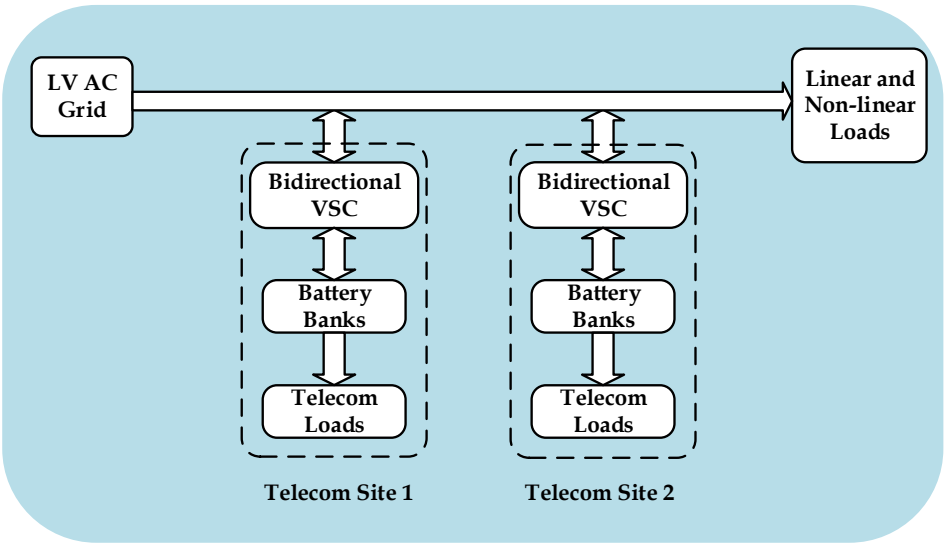

Figure 5.1: Telecom sites and loads connected to a LV grid

Table 5.1: Parameters of an ideal three-phase voltage

Parameter	Value
Voltage,v_s	$\sqrt{3} \times 230$ $[V_{LL,\ rms}]$
Frequency,f	50 [Hz]
Source resistance,R_S	0.01 $[m\Omega]$
Source inductance,L_s	0.01 $[mH]$

The supply voltage in an ideal case is given by the expression in Equation 5.1,

$$\begin{bmatrix} v_a \\ v_b \\ v_c \end{bmatrix} = \sqrt{2} \times 230 \begin{bmatrix} \sin(\omega t) \\ \sin(\omega t - 120^0) \\ \sin(\omega t + 120^0) \end{bmatrix} \tag{5.1}$$

An unbalance in the system voltage is created by introducing an unbalance of 30% fundamental negative-sequence component. The phase angle of the fundamental positive-sequence component is set to zero and the other components are made orthogonal to it. The system voltage in this case is given by

$$\begin{bmatrix} v_a \\ v_b \\ v_c \end{bmatrix} = \sqrt{2} \times 230 \left\{ \begin{bmatrix} \sin(\omega t) \\ \sin(\omega t - 120^0) \\ \sin(\omega t + 120^0) \end{bmatrix} + 0.3 \begin{bmatrix} \sin(\omega t + 90^0) \\ \sin(\omega t + 90^0 + 120^0) \\ \sin(\omega t + 90^0 - 120^0) \end{bmatrix} \right\} \tag{5.2}$$

The Matlab/Simulink model for a-phase voltage given in Equation 5.2 is shown in Figure 5.2. Similar models can be made for b-phase and c-phase voltages.

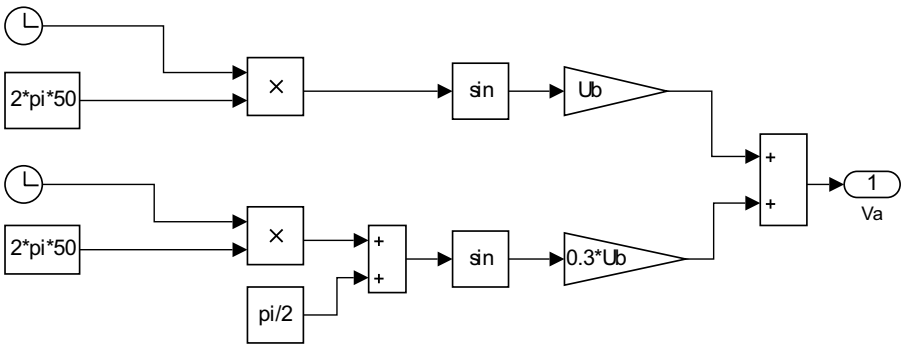

Figure 5.2: Simulink model for phase-a voltage

For the third case, the system voltage is made both unbalanced and distorted. A distortion of 15.5% third harmonic, 11.5% fifth harmonic and 7.7% seventh harmonic is introduced. The harmonic components are made purely from the negative-sequence component. The time function corresponding to this voltage is given by Equation 5.3.

$$\begin{bmatrix} v_a \\ v_b \\ v_c \end{bmatrix} = \sqrt{2} \times 230 \left\{ \begin{bmatrix} \sin(\omega t) \\ \sin(\omega t - 120^0) \\ \sin(\omega t + 120^0) \end{bmatrix} + 0.3 \begin{bmatrix} \sin(\omega t) \\ \sin(\omega t + 120^0) \\ \sin(\omega t - 120^0) \end{bmatrix} + 0.2 \begin{bmatrix} \sin(3\omega t) \\ \sin(3\omega t + 120^0) \\ \sin(3\omega t - 120^0) \end{bmatrix} + 0.15 \begin{bmatrix} \sin(5\omega t) \\ \sin(5\omega t + 120^0) \\ \sin(5\omega t - 120^0) \end{bmatrix} + 0.1 \begin{bmatrix} \sin(7\omega t) \\ \sin(7\omega t + 120^0) \\ \sin(7\omega t - 120^0) \end{bmatrix} \right\} \tag{5.3}$$

5.1.2 Load Modeling

Both linear (passive) and non-linear loads are connected to the LV ac grid under study. Passive loads are added primarily for the purpose of studying reactive power compensation. An *R-L* passive load in wye-grounded configuration (Figure 5.3)is considered in the model. This load draws linear but reactive current from the grid.

The different parameters of this load are given in Table 5.2.

Table 5.2: Parameters of passive *R-L* load

Parameter	Value
Voltage,v_s	$\sqrt{3} \times 230$ $[V_{LL,rms}]$
Frequency,f	50 [Hz]
Active power,P	1500 $[W]$
Inductive power,Q_L	250 $[VAr]$

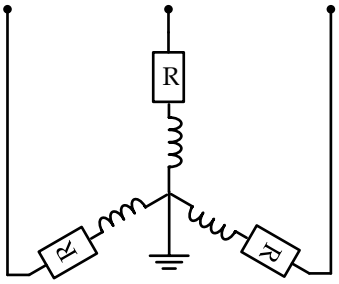

Figure 5.3: R-L load in wye-grounded configuration

In the system model, non-linear loads are used in order to introduce harmonic currents in to the system and also draw reactive power from the grid. A three-phase, six-pulse, full-bridge diode rectifier shown in Figure 5.4 is used which is a commonly used circuit arrangement [15]. The different parameters of this load are given in Table 5.3.

Table 5.3: Parameters of diode bridge *R-L* load

Parameter	Value
Voltage,v_s	$\sqrt{3} \times 230$ $[V_{LL,\ rms}]$
Frequency,f	50 [Hz]
Commutation inductance, L_d	3 $[mH]$
Resistive load,R_{load}	50 $[\Omega]$
Inductive load,L_{load}	50 $[mH]$
Snubber resistance, R_{sn}	1 $[k\Omega]$
Snubber capacitance, C_{sn}	0.1 $[\mu F]$
Internal resistance, R_{on}	1 $[m\Omega]$

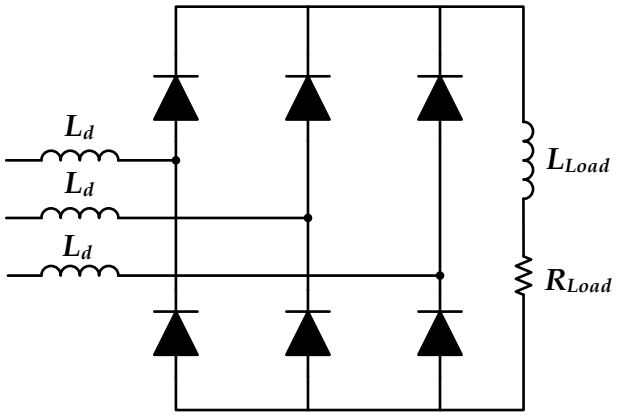

Figure 5.4: R-L load in diode bridge rectifier configuration

5.1.3 Telecom Sites

Telecom sites are equipped with battery banks with power electronic converter as an interface with the grid. High efficiency converters are being demanded in different application areas, especially in telecom sector. Several dc loads in telecom sites are fed by power electronic converters. These converters are used to charge a number of batteries which serve as a backup power source in case of power outage. Most of the time, the energy stored in the batteries is not utilized due to uninterrupted power from the ac grid. By using bi-directional converter between the grid and the batteries, the reserve energy in the batteries can be used to aid the grid power quality.

Figure 5.5: Power converter and battery for telecom application

The advancement in the network technology and the increase in power demand lifted the battery market to new height. Nickel cadmium (Ni-Cad), lead acid and lithium-ion batteries can be used for telecom applications. In the simulation model, lithium ion battery of 5.6 $[kWh]$ capacity supplying a dc load of 3 $[kW]$ and with a nominal voltage of 700 $[V]$ is used.

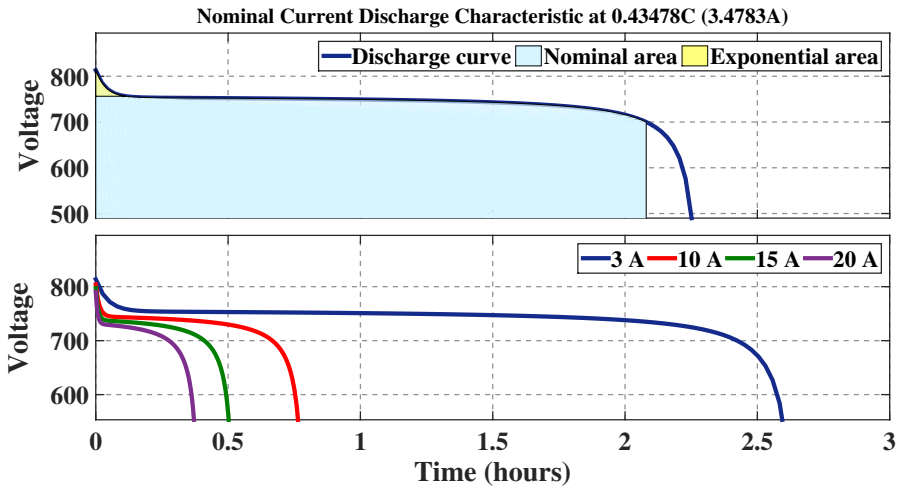

Figure 5.6: Li-ion battery discharge characteristic

The batteries are continuously charged from the grid and discharged when supplying power to the DC loads. If power balance is managed properly and fed back to the grid, it can be used to aid grid power quality and other ancillary services. Figure 5.6 shows discharge characteristics of the Li-ion battery used in the simulation model at different discharge currents. These batteries with their converter will be used as a SAF in addition to their primary purpose.

5.2 Bi-Directional Voltage Source Converter

Power processing is to convert a power source into a voltage or current supply that is suitable for the load. It involves the integration of power electronic devices and a controller [45].

In this thesis, a bi-directional AC-DC converter capable of transferring power in both directions; from the grid to the battery banks and back to the grid is studied. This nature of the converter and proper implementation of a control algorithm enables improving power quality of the grid. The focus in this study will be on harmonic elimination and reactive power compensation.

Figure 5.7 shows a VSC used in the simulation model as an interface between the battery banks and the grid. It has two modes of operation. In the rectifier mode, it charges the battery banks from the grid and in the inverter mode, power flows from the battery banks to the grid. The combined Rectifier and Inverter modules can perform full 4 quadrant control (Active and Reactive Power import/export). It consists of six power switches (MOSFETs) connected to anti-parallel diodes. MOSFET switches are used in the simulation for the following reasons [15],

- MOSFET turn on and off very rapidly because it is a majority carrier device and there is no stored charge that must be injected in to or removed from it
- MOSFET has relatively “small” on state losses for LV applications
- MOSFET has a positive temperature coefficient, which makes it easy to parallel MOSFETs for increased current handling capability if required
- It has a large SOA (Safe Operating Area) for switch mode applications, which means that in most situations, snubber circuits are not needed.

The main limitation of VSC is the switching frequency of the switches. The switching frequency is limited by the switching losses of the MOSFET. It causes a time delay from the measurement of signals until the output voltage is updated. This time delay will limit the bandwidth of any controller.

A related limitation of the converter is the requirement for a low-pass filter to smoothen the voltage output. The ripple current induced by the switching output voltage and the bandwidth of the controller dictate the minimum size of these filter components [46].

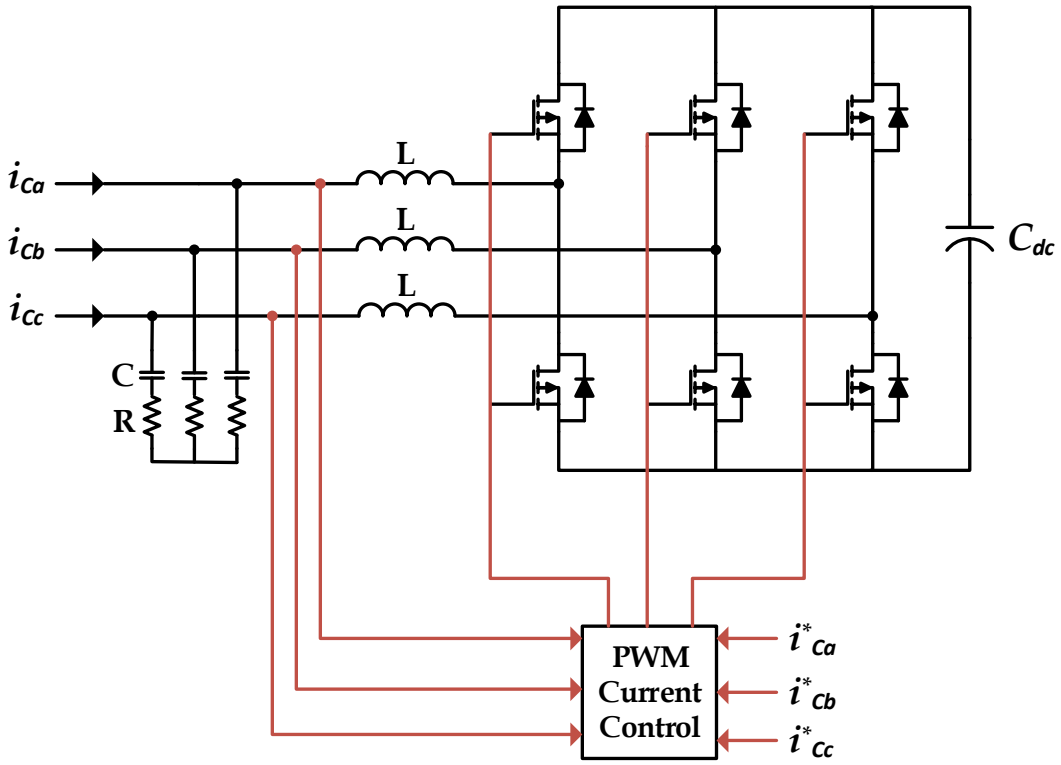

Figure 5.7: Bi-directional voltage source converter

For low power application, like telecom sites considered in this thesis, simple L-filter is used to meet harmonics standards [47]. A filter of 4 [mH] is used in the simulations.

The performance of the active filter heavily depends on the way the required compensating current components are generated and the method implemented to produce the gating signals to force the VSC reproduce these compensating currents.

In this thesis, the *pq*-theory is used as a control algorithm to generate the required reference currents and two type of modulation techniques are implemented to produce the gating signals: *dq-PI* control and Adaptive hysteresis current control.

Both control systems have the same functionality, which is to force the converter to behave as a controlled current source. Active and reactive power will be controlled independent of each other. Both control techniques are discussed in the next section.

5.2.1 *dq-PI* Control

Figure 5.8 shows a one-line diagram of the system model for analyzing *dq-PI* modulation technique. Three-phase VSC is connected to the utility grid through a series line reactor filter. The filter is modeled by an inductor,L_f and a resistor,R_f [48].

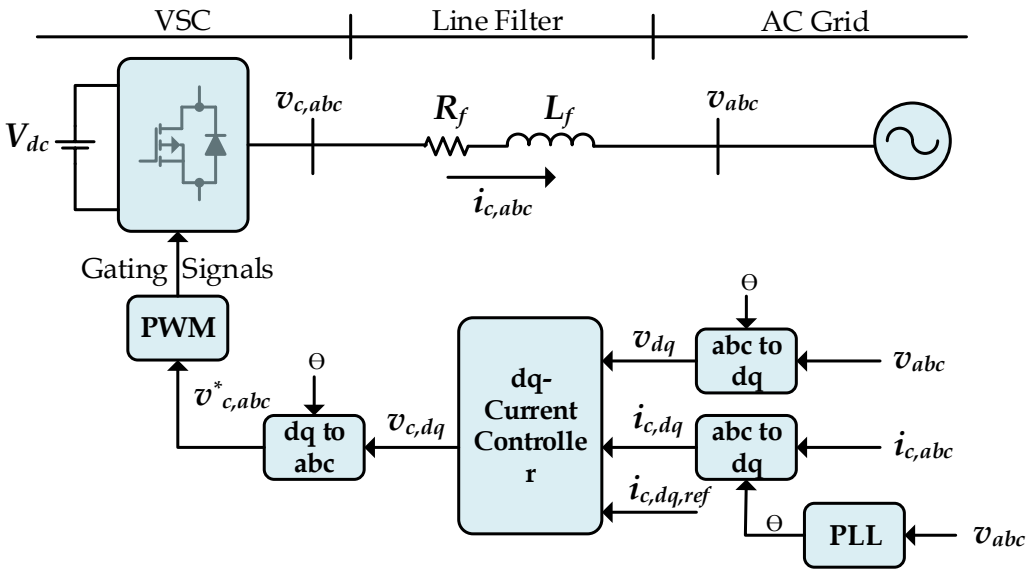

Figure 5.8: One line diagram for *dq-PI* control

Table 5.4 presents the parameters of the system. Note that the dynamics of the VSC DC-side are neglected because of the available battery banks, the voltage is maintained at constant value. Thus, DC voltage regulation is not included in this study.

Table 5.4: Parameters of the system in Figure 5.8

Parameter	Value
VSC rated power	20 [kVA]
Voltage,v_s	$\sqrt{3} \times 230$ $[V_{LL,\ rms}]$
Frequency,f	50 [Hz]
Switching frequency,f_{sw}	20 $[kHz]$
Filter inductance, L_f	4 $[mH]$
Filter resistance,R_f	0.1 $[m\Omega]$
DC bus voltage, V_{dc}	700 [V]

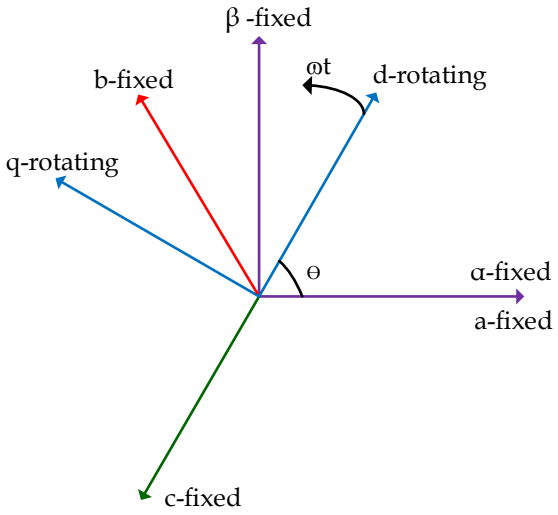

Figure 5.9: Park and Clarke transformation reference frames with respect to *abc* frame

The behavior of three-phase systems is usually described by their voltage and current equations. The coefficients of the differential equations that describe their behavior are time dependent. The mathematical modeling of such a system tends to be complex. For such a complex system analysis, mathematical transformations are often used to decouple variables and to solve equations involving time varying quantities by referring all variables to a common frame of reference.

Park and Clarke Transformations are used in this control method. Clark transformation convert the phase values of voltage and current into stationary $\alpha\beta$ reference frame and Park transformation convert the stationary $\alpha\beta$ reference frame into synchronously rotating *d-q* reference frame. Park and Clarke transformations are given by the expressions in Equation 5.4 and Equation 5.5 respectively.

$$\begin{bmatrix} v_\alpha \\ v_\beta \end{bmatrix} = \sqrt{\frac{2}{3}} \begin{bmatrix} 1 & -\frac{1}{2} & \frac{1}{2} \\ 0 & \frac{\sqrt{3}}{2} & -\frac{\sqrt{3}}{2} \end{bmatrix} \begin{bmatrix} v_a \\ v_b \\ v_c \end{bmatrix} \tag{5.4}$$

$$\begin{bmatrix} v_d \\ v_q \end{bmatrix} = \begin{bmatrix} \cos\theta & \sin\theta \\ -\sin\theta & \cos\theta \end{bmatrix} \begin{bmatrix} v_\alpha \\ v_\beta \end{bmatrix} \tag{5.5}$$

The *d-q* reference frame is rotating at speed ω with respect to the stationary $\alpha\beta$-reference frame. The position of d-axis at any instant of time is given by Equation 5.6 with respect to α-axis.

$$\theta = \omega * t \tag{5.6}$$

The value of θ (theta) is computed using PLL circuit. The three coordinate systems are shown in Figure 5.9. The details of these mathematical transformations can be found in [35].

The dynamics of the VSC ac-side variables of Figure 5.8 can be described in an *abc*-frame as [48, 49]

$$v_{c,abc} = R_f i_{c,abc} + L_f \frac{di_{c,abc}}{dt} + v_{abc} \tag{5.7}$$

where v_{abc} and $v_{c,abc}$ are the grid voltages and the VSC terminal voltages respectively and $i_{c,abc}$ represents the converter currents. By applying Park transformation to the voltages and currents in Equation 5.7

$$v_{c,dq} = R_f i_{c,dq} + L_f \frac{di_{c,dq}}{dt} + j\omega L_f i_{c,dq} + v_{dq} \tag{5.8}$$

where ω is the nominal angular frequency. Separating the real and imaginary terms, the dynamics of the d- and q-axes are as follows

$$R_f i_{c,d} + L_f \frac{di_{c,d}}{dt} = v_{c,d} + \omega L_f i_{c,q} - v_d \tag{5.9}$$

and

$$R_f i_{c,q} + L_f \frac{di_{c,q}}{dt} = v_{c,q} - \omega L_f i_{c,d} - v_q \tag{5.10}$$

Equation 5.9 and Equation 5.10 represent the relationship between the control signals and the current of each axis along with the mutual coupling effect of the axes. Applying Laplace transformation to Equation 5.9 and Equation 5.10, the structural diagram of the system in the rotating reference frame can be achieved, as shown in Figure 5.10, which contains the coupling terms.

However, by designing proper controllers, the closed-loop system can be decoupled. In the following section, inner current control is implemented to control the currents in dq-axis.

5.2.1.1 Inner Current Controller

The inner current control loop can be implemented in the dq-frame, based on the basic relationship of the system model. The control loop consists of PI controllers, decoupling factors and feed-forward terms. This current control is represented by the general block diagram as in Figure 5.11.

Inside the current control block, there are two PI regulators, for d- and q-axis current control. They transform the error between d- and q- components of currents into voltage values.

PI-Controller - The PI-Controller is represented in s-domain as

$$C(s) = K_p + \frac{K_i}{s} = K_p \left(\frac{1 + T_i s}{T_i s} \right) \tag{5.11}$$

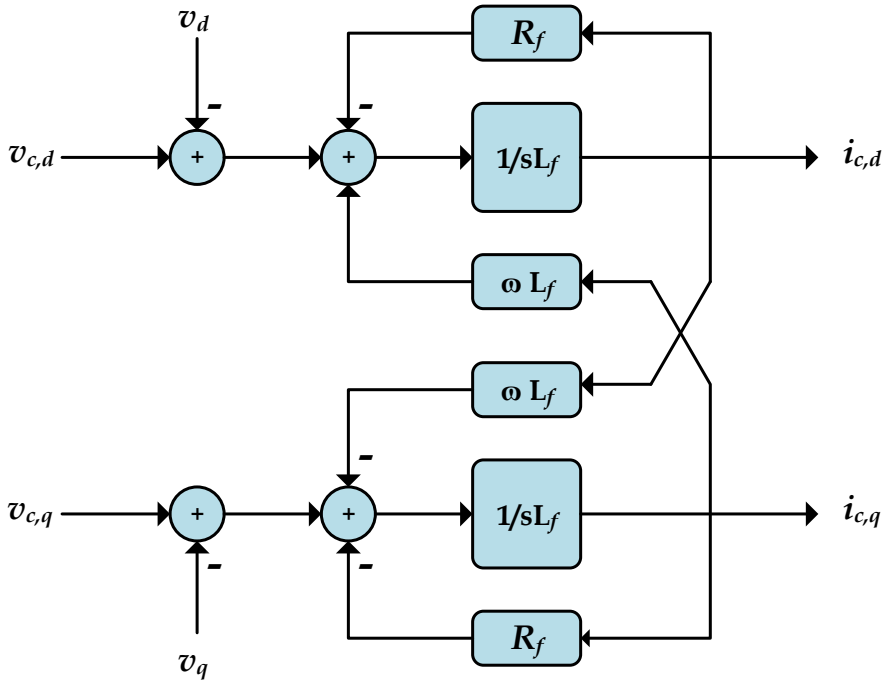

Figure 5.10: Structural diagram of the system in Figure 5.8 in dq-frame

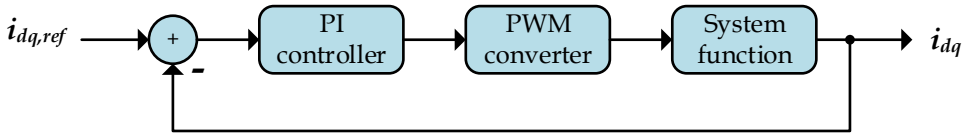

Figure 5.11: Inner current controller design

Where K_p is the proportional gain, K_i is the integral gain and T_i is the integral time constant ($T_i = K_p/K_i$). This block performs

$$\{I_{dq,ref} - I_{dq}\}K_p\left(\frac{1+T_i s}{T_i s}\right) = V_c^* \tag{5.12}$$

PWM Converter - From the control point of view, the PWM is considered as an ideal power transformer with a time delay. The output voltage of the converter is assumed to follow a voltage reference signal with an average time delay equals half of a switching cycle, due to VSC switches. Hence the general expression is

$$P(s) = \frac{1}{1+T_a s} \tag{5.13}$$

where $T_a = T_{sw}/2$. Thus it performs

$$V_c^* \frac{1}{1+T_a s} = V_c \tag{5.14}$$

System - The system behavior is governed by Equation 5.9 and Equation 5.10. As seen from these equations, the model of the VSC in the synchronous reference frame is a multiple-input multiple-output, strongly coupled non-linear system. And it is difficult to realize the exact decoupled control with general linear control strategies.

The transformed voltage equations of each axis have speed/frequency induced term ($\omega L i_d$ and $\omega L i_q$) that gives cross-coupling between the two axes. For each axis, the cross-coupling term can be considered as disturbance from control point of view. Thus, a dual-close-loop direct current controller with decoupled current compensation and voltage feed-forward compensation is required to obtain a good control. The system equations can be re-written as

$$\begin{aligned} v_d - v_{d,c} &= L_f \frac{di_d}{dt} + R_f i_d - \omega L_f i_q \\ v_q - v_{q,c} &= L_f \frac{di_q}{dt} + R_f i_q + \omega L_f i_d \end{aligned} \tag{5.15}$$

Using separate inner loop current controllers for i_d and i_q, give the output of voltage reference for the two axes, which will be fed to the converter.

$$\begin{aligned} V_{d,c} &= \{I_{d,ref} - I_d\} K_p \left(\frac{1 + T_i s}{T_i s}\right) \left(\frac{1}{1 + T_a s}\right) \\ V_{q,c} &= \{I_{q,ref} - I_q\} K_p \left(\frac{1 + T_i s}{T_i s}\right) \left(\frac{1}{1 + T_a s}\right) \end{aligned} \tag{5.16}$$

As seen from Equation 5.15, the d and q components of the converter voltages are cross coupled. Hence, the reference used as input to system can be split in two components, one of which is obtained from converter whereas the other is a feed-forward term to eliminate the cross-coupling. With the compensation terms used for decoupling, the system input from converter will be

$$\begin{aligned} V^*_{d,c} &= -(i_{d,ref} - i_d) K_p \left(\frac{1 + T_i s}{T_i s}\right) + \omega L_f i_q + v_d \\ V^*_{q,c} &= -(i_{q,ref} - i_q) K_p \left(\frac{1 + T_i s}{T_i s}\right) - \omega L_f i_d + v_q \end{aligned} \tag{5.17}$$

By substituting Equation 5.17 into Equation 5.14 and equating it with Equation 5.15 gives

$$\begin{aligned} L_f \frac{di_d}{dt} + R_f i_d &= v_{d,c} \\ L_f \frac{di_q}{dt} + R_f i_q &= v_{q,c} \end{aligned} \tag{5.18}$$

As we can see from Equation 5.18, the cross coupling terms are canceled out and independent control in d and q axes is achieved, which is one of the important features of *dq-PI* control using vector analysis. Thus, current controllers of each axis operate independently.

The system can finally be represented by a transfer function given as

$$G(s) = \frac{1}{R_f}\frac{1}{1+\tau s} \tag{5.19}$$

where the line time constant is given by $\tau = L_f/R_f$

5.2.1.2 Tuning of PI controller

The per-unit system simplifies the analysis of complex power systems by choosing a common set of base parameters. It is also ideal for computer simulations and design of controllers. The per-unit system is based on nameplate rated values for power, phase current and voltage [50]. The calculation of any quantity in the per-unit system is given by

$$Quantity\ (per\ unit) = \frac{Quantity\ (normal\ unit)}{Basevalue\ (normal\ unit)} \tag{5.20}$$

The base quantities used in this thesis are:

$$\begin{aligned} S_b &= \frac{2}{3}S_n = \frac{2}{3} \times 2 \times 10^4 = 1.33 \times 10^4\ [VA] \\ V_{d,b} = V_{q,b} &= \sqrt{\frac{2}{3}}V_n = \sqrt{\frac{2}{3}} \times 400 = 326\ [V] \\ I_{d,b} = I_{q,b} &= \frac{S_b}{V_b} = 41\ [A] \\ Z_{d,b} = Z_{q,b} &= \frac{V_b}{I_b} = 7.9\ [\Omega] \end{aligned} \tag{5.21}$$

where $V_{d,b}$ and $V_{q,b}$ are the base voltages in the dq coordinates, $I_{d,b}$ and $I_{q,b}$ are base currents in the dq coordinates, $Z_{d,b}$ and $Z_{q,b}$ are base impedances in dq frame and V_n and S_n are rated voltage and rated apparent power respectively.

In order to achieve satisfactory performance, the PI controllers must be properly tuned. The fundamental objectives of PI tuning are,

- Fast response of the system by increasing the cut-off frequency as high as possible
- Small overshoot and good damping of oscillations

To optimize the speed of response and system stability, Modulus Optimum and Symmetrical Optimum techniques are applied depending on the form of the open loop transfer function of the control loop [51]. In this study, Modulus Optimum is used to tune the PI controllers.

The objective is to make the cut-off frequency as high as possible. Hence, when there is one dominant and another minor pole in the transfer function, the integral time constant of the PI controller is chosen to cancel out the dominant pole.

The over all open loop transfer function of the system (Figure 5.11) is given by:

$$G_{OL} = K_p \left(\frac{1+T_i s}{T_i s}\right)\left(\frac{1}{1+T_a s}\right)\frac{1}{r}\left(\frac{1}{1+\tau s}\right) \tag{5.22}$$

Using Modulus Optimum criterion

$$T_i = \tau = \frac{L_f}{R_f} \tag{5.23}$$

The chosen crossover frequency ω_c is one or two orders of magnitude smaller than f_{sw} in order to avoid interference from the switching frequency components. Following the requirement of unity gain at ω_c

$$|G_{OL}| = \left|\left(\frac{K_p}{T_i s}\right)\left(\frac{1}{1+T_a s}\right)\frac{1}{r}\right| = 1 \tag{5.24}$$

Reorganizing Equation 5.24 , the proportional gain of the PI controller is calculated as

$$K_p = \omega_c T_i r\sqrt{1+\omega_c {T_a}^2} \tag{5.25}$$

The detail of Modulus Optimum design can be found in [52]. The values of K_p and K_i that are used in the simulations are 122 and 3.04 respectively. But these values does not represent the exact calculated values; they are tuned manually to match the desired characteristics.

5.2.2 Adaptive Hysteresis Control

The effectiveness of active power filter depends on the design and characteristics of the current controller. There are various PWM current control strategies proposed for SAF applications. But in terms of quick current controllability and easy implementation, HCC has highest rating among other methods [53, 54]. This section describes adaptive HCC for shunt active filter.

Hysteresis-based current control is a common PWM (pulse width modulation) control used in voltage-fed converters to force them behave as a controlled ac current source to the power system. The scheme of this control strategy used to control the shunt active filter is shown in Figure 5.12 [55, 56].

This hysteresis current controller is developed to generate the switching pulses to control VSC switches by comparing the real measured currents to the reference currents. The control scheme gives the switching pattern for the active filter switches in order to maintain the real injected current within a desired hysteresis band (HB) as illustrated in Figure 5.12 [55, 56, 57].

The switching logic of Figure 5.12, for a-phase current is given as:

- If $i_{ca} < (i^*_{ca} - HB_a)$, the upper switch of leg-a is OFF and the lower switch is ON

- If $i_{ca} > (i^*_{ca} + HB_a)$, the upper switch is ON and the lower switch is OFF

The switching pattern for phase-b and phase-c are determined in the same manner, using their corresponding reference and measured currents and their hysteresis bandwidth (HB).

The bandwidth of the hysteresis current controller determines the allowable current shaping error. By changing the bandwidth, the average switching frequency of the active power filter can be controlled. In principle, increasing the converter operating frequency helps to get a better compensating current waveform. However, there are device limitations and increasing the switching frequency causes increased switching losses, and EMI related problems. The range of switching frequencies used is based on a compromise between these factors.

The adaptive hysteresis band current controller changes the hysteresis bandwidth according to instantaneous compensation current variation (di^*_c/dt) and V_{dc} voltage to minimize the influence of current distortion on modulated waveform. In this study, the adaptive hysteresis band current controller, proposed by Bose [58] for electrical machine drives is used.

Figure 5.13 shows current and voltage waves of the PWM-voltage source converter for phase-a. The current i_a tends to cross the lower hysteresis band at point 1, where the switch T_1 is switched ON. The linearly rising current (i^+_a), then, touches the upper band at point 2 where the transistor T_4 is switched ON. The linearly falling current (i^-_a), then, touches the lower band at point 3. The following equations can be written in the switching intervals t_1 and t_2 [58, 59].

$$\frac{di^+_a}{dt} = \frac{1}{L_f}(0.5V_{dc} - v_s) \tag{5.26}$$

$$\frac{di^-_a}{dt} = -\frac{1}{L_f}(0.5V_{dc} + v_s) \tag{5.27}$$

where L_f is the per phase coupling inductance and i^+_a and i^-_a are the respective rising

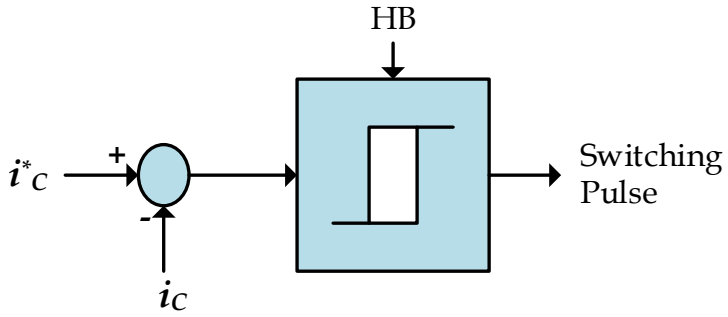

Figure 5.12: Hysteresis current control

and falling current segments. From the geometry of Figure 5.13, we can write

$$\frac{di_a^+}{dt}t_1 - \frac{di_a^*}{dt}t_1 = 2HB \tag{5.28}$$

$$\frac{di_a^-}{dt}t_2 - \frac{di_a^*}{dt}t_2 = -2HB \tag{5.29}$$

$$t_1 + t_2 = T = 1/f_{sw} \tag{5.30}$$

where t_1 and t_2 are the respective switching intervals, and f_{sw} is the switching frequency. Adding Equation 5.28 and Equation 5.29 and substituting in to Equation 5.30 we can write

$$\frac{di_a^+}{dt}t_1 + \frac{di_a^-}{dt}t_2 - \frac{1}{f_{sw}}\frac{di_a^*}{dt} = 0 \tag{5.31}$$

Subtracting Equation 5.29 from Equation 5.28, we get

$$\frac{di_a^+}{dt}t_1 - \frac{di_a^-}{dt}t_2 - (t_1 - t_2)\frac{di_a^*}{dt} = 4HB \tag{5.32}$$

Substituting Equation 5.31 in to Equation 5.32, we get

$$\frac{di_a^+}{dt}(t_1 + t_2) - (t_1 - t_2)\frac{di_a^*}{dt} = 4HB \tag{5.33}$$

Substituting Equation 5.27 into Equation 5.31, we get

$$(t_1 - t_2) = \frac{di_a^*/dt}{f_{sw}(di_a^+/dt)} \tag{5.34}$$

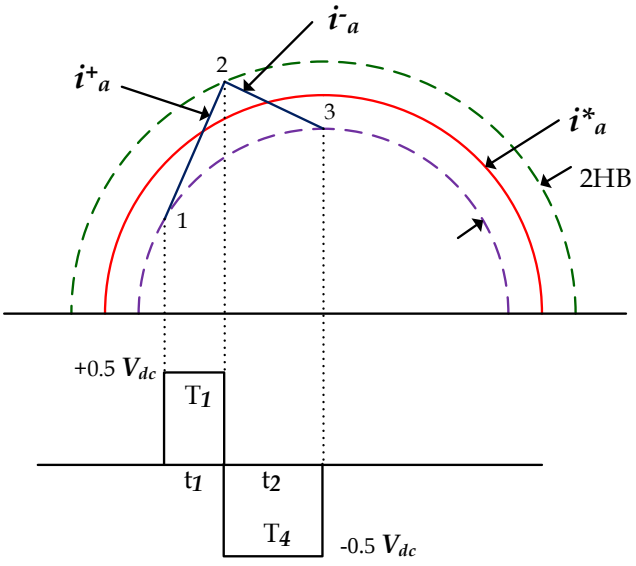

Figure 5.13: Current and voltage waveform of leg-a of VSC

Finally, substituting Equation 5.34 into Equation 5.33, we get the expression for hysteresis band calculation as

$$HB = \left\{ \frac{0.125 V_{dc}}{f_{sw} L_f} \left[1 - \frac{4L_f^2}{V_{dc}^2} \left(\frac{v_s}{L_f} + m \right)^2 \right] \right\} \tag{5.35}$$

where, $m = di^*{}_a/dt$ is the slope of reference current signal. The hysteresis band HB will then be applied to the variable HCC. The Simulink model for obtaining hysteresis band (HB) is shown in Appendix A.

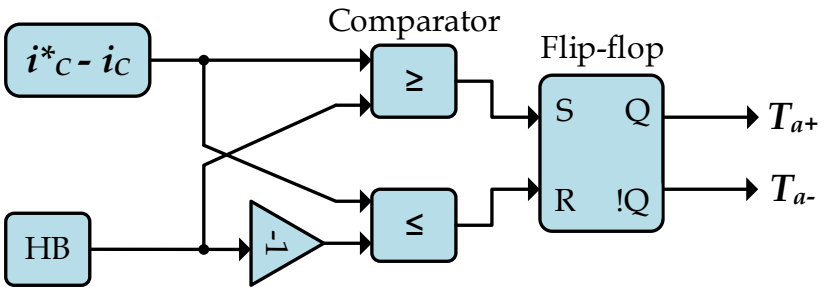

Figure 5.14: Simplified model of hysteresis band control

Figure 5.14 shows a two-level hysteresis current control method implementation using S-R flip-flop circuits for a three-phase converter. The comparator outputs go into the flip-flop and the positive inner band limit output goes to set input(S) while the negative inner band limit output goes to reset input(R) of the flip-flop. The output of the flip-flop is used to gate the power switches; Q gates the upper switch and !Q gates the lower switch. The details of this circuit arrangement can be found in [60, 61].

Chapter 6

Simulation Results and Discussion

Non-linear and passive loads connected to the grid draw harmonic current and consume reactive power which cause voltage distortion and harmonic pollution to the other loads connected at PCC.

Telecom sites (VSC together with batteries) can be used to improve grid power quality. The system model given in Figure 4.1 is analyzed in Matlab/Simulink for different system conditions. Simulations are carried out for both three-phase, three-wire systems and three-phase, four-wire systems.

6.1 Harmonic Elimination and Reactive Power Compensation in Three-Phase, Three-Wire System

In this section, simulation results for harmonic elimination and reactive power compensation in three-phase three-wire systems are presented and discussed. In these configurations, since there is no neutral conductor, the zero-sequence current is always zero, thus there will be no zero-sequence power compensation ($p_0 = 0$). The oscillating portion of the real power and all of the imaginary power are to be compensated.

Six different cases for both *dq-PI* control and adaptive HCC control are simulated. The different cases are identified based on whether the source is balanced or unbalanced or distorted and if the connected loads are balanced or unbalanced.

6.1.1 Case 1: Balanced Source with Balanced Load

In this case, a balanced three phase supply voltage is considered with a source impedance of $R_s = 10\ [\mu\Omega]h$ and $L_s = 1\ [\mu H]$. Two three-phase R-L diode bridge loads and one three phase sinusoidal R-L laod are connected at PCC. The Simulink model of the system can be found in Appendix B. The SAF is connected at 0.2 sec and the total simulation time is 0.4 sec. The supply voltage is given by the following expression,

$$\begin{bmatrix} v_a \\ v_b \\ v_c \end{bmatrix} = \sqrt{2} \times 230 \begin{bmatrix} \sin \omega t \\ \sin(\omega t - 120°) \\ \sin(\omega t + 120°) \end{bmatrix} \tag{6.1}$$

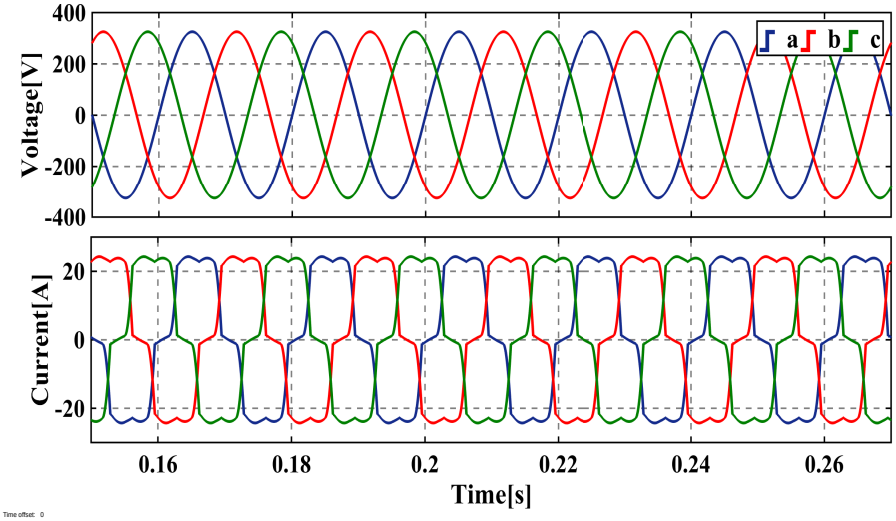

Figure 6.1: Three-phase source voltage and load current(case:1)

Figure 6.1 shows the supply three-phase voltage and the current drawn by the non-linear load. It can be seen that the load draws highly distorted harmonic current.

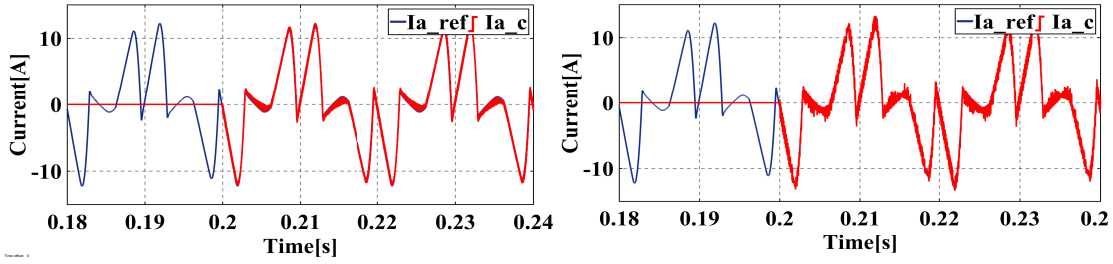

(a) *dq-PI* (b) adaptive HCC

Figure 6.2: Reference current and converter current comparison(case:1)

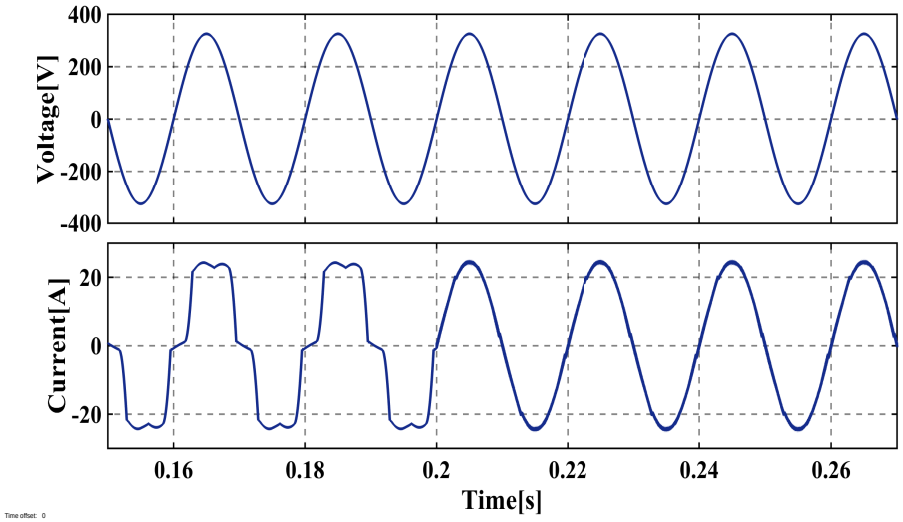

Figure 6.3: Phase-a current and voltage for *dq-PI* control(Case:1)

Figure 6.2 shows phase-a reference harmonic current generated applying the *pq-theory* and the corresponding harmonic current supplied by the converter with *dq-PI* control (Figure 6.2(a)) and with adaptive HCC control (Figure 6.2(b)). We can see that in both cases, the converter is able to follow the reference current satisfactorily.

From Figure 6.3, we can see that as soon as the SAF starts supplying compensating currents at 0.2 sec, the distorted source current become sinusoidal in less than one power cycle. As a result the THD in the source current changes from 20.29% to 1.37% for *dq-PI* control. For adaptive HCC control (Figure 6.4), the THD in the source current changes to 1.22%.

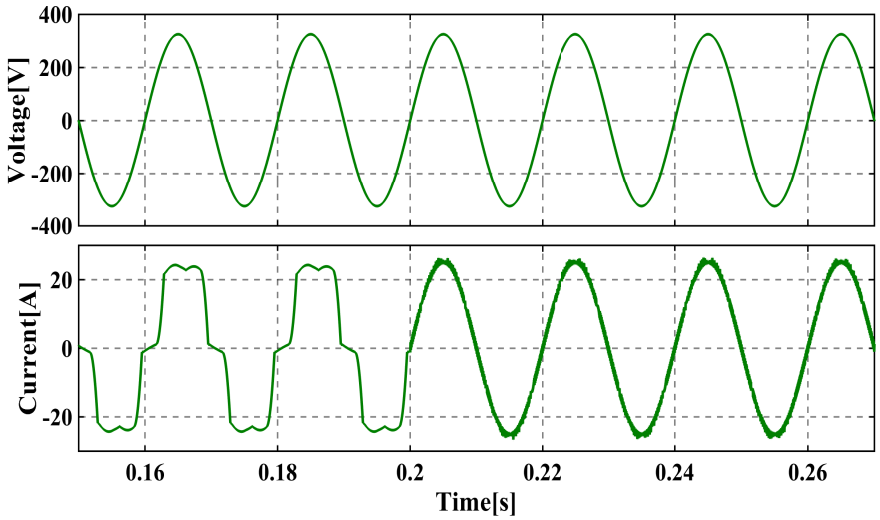

Figure 6.4: Phase-a current and voltage for HCC control(Case:1)

Table 6.1 shows the percentage of different harmonic contents in the source current before and after the connection of SAF relative to the fundamental 50 Hz component. These new improved percentages of harmonics are well within the permissible limits defined in IEEE-519.

Table 6.1: Harmonics spectra of the source current(%) (case:1)

Harmonic Order	1	5	7	11	13	17	19	**THD**
Without Compensation	100	17.14	8.89	4.74	3.23	1.58	1.16	20.29
Compensation with dq-PI	100	0.97	0.38	0.56	0.36	0.30	0.19	1.37
Compensation with HCC	100	0.59	0.10	0.34	0.12	0.11	0.03	1.22

From Figure 6.3 and Figure 6.4, we can also see that phase-a voltage is in-phase with the phase-a source current. This shows that the SAF resulted in a unity power factor operation.

The SAF also successfully compensated the reactive power in the system. Figure 6.5 shows the instantaneous active and reactive power drawn from the source before and after the connection of SAF. After the connection of the SAF at 0.2 sec, the load only draws the average power required from the source and the oscillating portion will be compensated by the converter. The load draws no reactive power from the source since all of the reactive power is being compensated. The converter supplies all the reactive power required in the system. This is also evident from unity power factor operation.

Although the main target is obtaining a sinusoidal source current, since we are considering a balanced three phase system, we can simultaneously achieve all the three basic control objectives described in chapter 3. Since the SAF is compensating

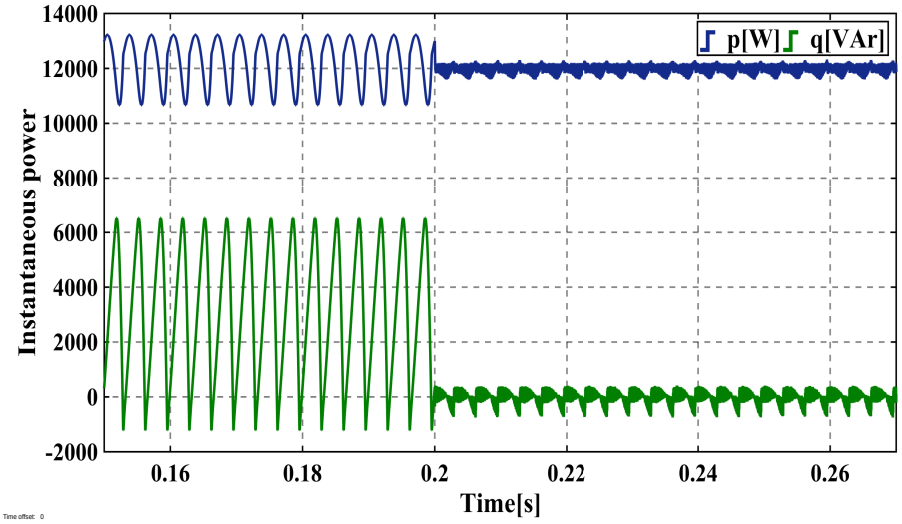

Figure 6.5: Instantaneous three-phase active and reactive power(case:1)

all of the imaginary power and the oscillating portion of real power, the required rms current from the source is smaller now (1.07[A] less) after the connection of the SAF (Generalized Fryze current control strategy). The loads only draw constant instantaneous active power from the source ensuring, Constant instantaneous power control strategy.

6.1.2 Case 2: Balanced Source with Unbalanced Load

The supply voltage in this case is the same as the case considered above(Equation 6.1) but unbalance is introduced in the load. The main system parameters that are used for this simulation are summarized in Table 6.2.

Table 6.2: Main parameters of the simulated system (case:2)

Parameter	Description
Source impedance	$R_s = 10\ [\mu\Omega],\ L_s = 1\ [\mu H]$
Converter filter	$R_f = 100\ [\mu\Omega],\ L_f = 4\ [mH]$
Load	One three-phase $R-L$ load, $P = 1.5\ [kW], Q = 250\ [VAr]$ One single-phase diode rectifier connected between the a-phase and the ground with commutation inductance, $L_d = 3\ [mH]$ One single-phase diode rectifier connected between the b-phase and the ground with commutation inductance, $L_d = 3\ [mH]$

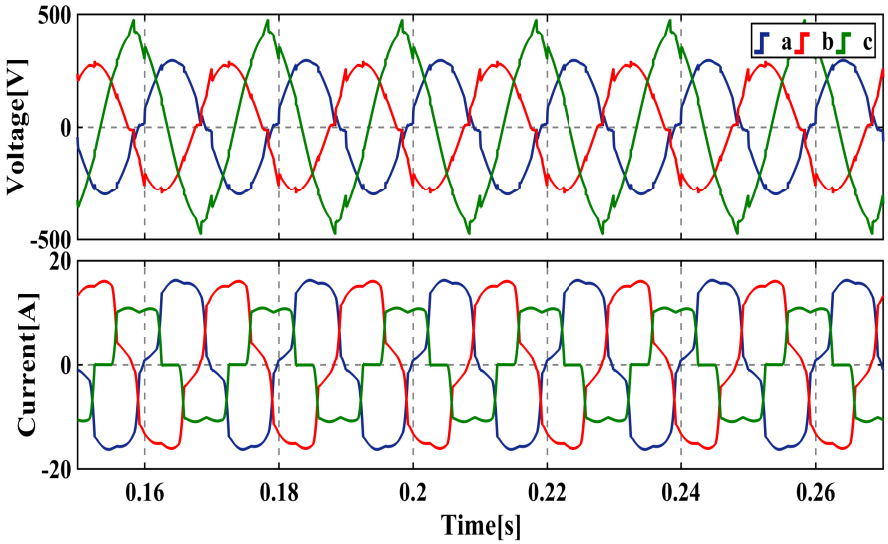

Figure 6.6: Three-phase source voltage and load current(case:2)

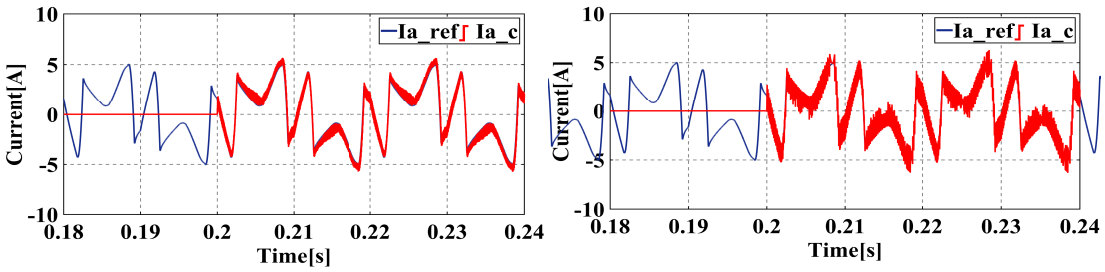

(a) *dq-PI* (b) adaptive HCC

Figure 6.7: Reference current and converter current comparison(case:2)

Figure 6.6 shows the supply three-phase voltage at PCC and the current drawn by the non-linear load. It can be seen that the load draws highly distorted harmonic and unbalanced current. This has resulted in the distortion of the voltage at the PCC.

Figure 6.7 shows that the converter is able to follow the reference current effectively with both *dq-PI* control (Figure 6.7(a)) and adaptive HCC control (Figure 6.7(b)).

From Figure 6.8, we can see that as soon as the SAF starts supplying compensating currents at 0.2 sec, the distorted source current become sinusoidal. As a result the THD in the source current reduces from 14.34% to 1.02% for *dq-PI* control. For adaptive HCC control (Figure 6.9), the THD in the source current is 1.69%.

Table 6.3 shows the percentage of different harmonic contents in the source current before and after the connection of SAF relative to the fundamental 50 Hz component. And again the SAF minimizes the harmonics with in the limits defined in IEEE-519.

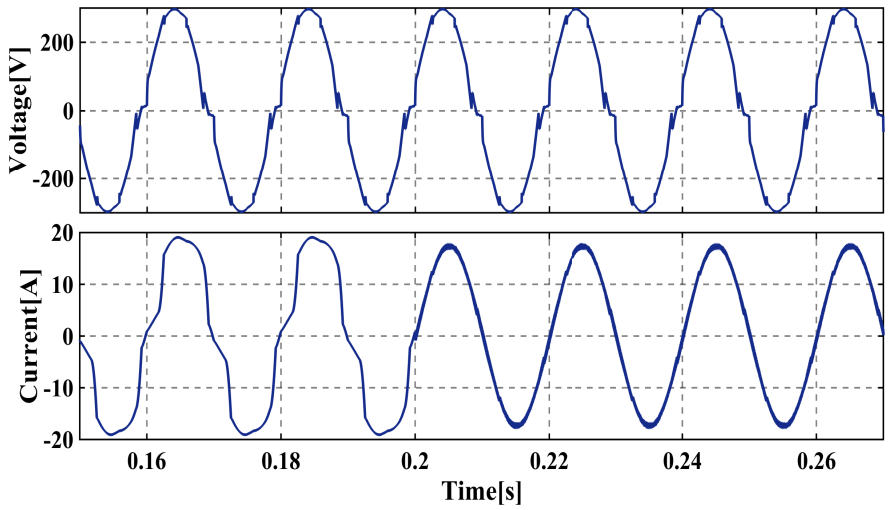

Figure 6.8: Phase-a current and voltage for *dq-PI* control(Case:2)

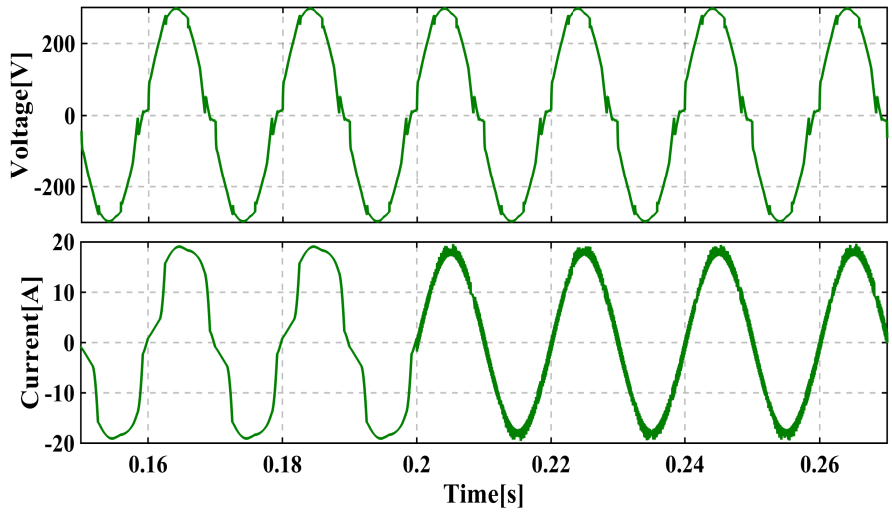

Figure 6.9: Phase-a current and voltage for HCC control(Case:2)

Table 6.3: Harmonics spectra of the source current (%)(case:2)

Harmonic Order	1	3	5	7	11	13	17	**THD**
Without Compensation	100	1.28	11.66	6.50	3.41	2.67	1.67	14.34
Compensation with dq-PI	100	0.26	0.50	0.30	0.39	0.24	0.27	1.02
Compensation with HCC	100	0.46	0.28	0.34	0.25	0.10	0.19	1.69

The SAF is also compensating the reactive power in the system. Figure 6.10 shows the instantaneous active and reactive power drawn from the source before and after the connection of SAF. After the connection of the SAF at 0.2 sec, the load draws no reactive power from the source, the converter supplies all the reactive power required in the system.

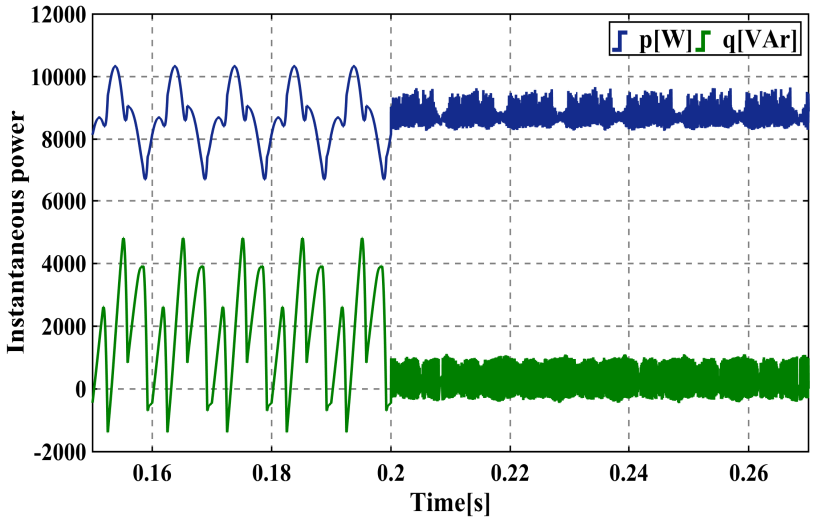

Figure 6.10: Instantaneous three-phase active and reactive power(case:2)

Since we are considering unbalanced three-phase system here, we can't achieve all the three basic control objectives described in chapter 3. The SAF only ensured sinusoidal source current and loads draw both average and oscillating active power from the source (Figure 6.10).

6.1.3 Case 3: Unbalanced Source with Balanced Load

In practical applications, the distribution supply voltages are not as ideal as in the cases considered above but have unbalances. In an unbalanced system, the voltages contain both positive and negative sequence components.

In this case, the system voltages are made strongly unbalanced by a 30% fundamental negative-sequence component. The phase angle of the fundamental positive-sequence component is set to zero and the other components are orthogonal to it. The system voltage is given by,

$$\begin{bmatrix} v_a \\ v_b \\ v_c \end{bmatrix} = \sqrt{2} \times 230 \left\{ \begin{bmatrix} \sin \omega t \\ \sin(\omega t - 120^\circ) \\ \sin(\omega t + 120^\circ) \end{bmatrix} + 0.3 \begin{bmatrix} \sin(\omega t + 90^\circ) \\ \sin(\omega t + 120^\circ + 90^\circ) \\ \sin(\omega t - 120^\circ + 90^\circ) \end{bmatrix} \right\} \tag{6.2}$$

The main system parameters that are used in this simulation are summarized in Table 6.4.

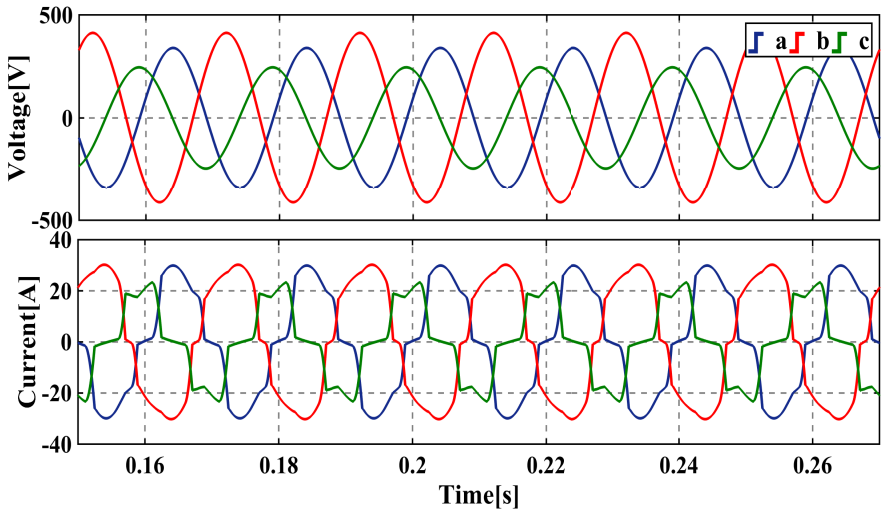

Figure 6.11: Three-phase source voltage and load current(case:3)

Table 6.4: Main parameters of the simulated system (case:3)

Parameter	Description
Source impedance	$R_s = 10\ [\mu\Omega], L_s = 1\ [\mu H]$
Converter filter	$R_f = 100\ [\mu\Omega], L_f = 4\ [mH]$
Load	One three-phase $R-L$ load, $P = 1.5\ [kW], Q = 250\ [VAr]$
	Two three-phase diode rectifier connected with commutation inductance, $L_d = 3\ [mH]$ and $R_{load} = 50\ [\Omega], L_{load} = 50\ [mH]$

Figure 6.11 shows the supply three-phase voltage and the current drawn by the loads. Since the supply voltage is unbalanced, it requires fundamental positive sequence voltage detector to extract the fundamental positive sequence voltage form the main supply voltage in order to implement sinusoidal current control strategy. The extracted three-phase fundamental positive-sequence voltage is shown in Figure 6.12.

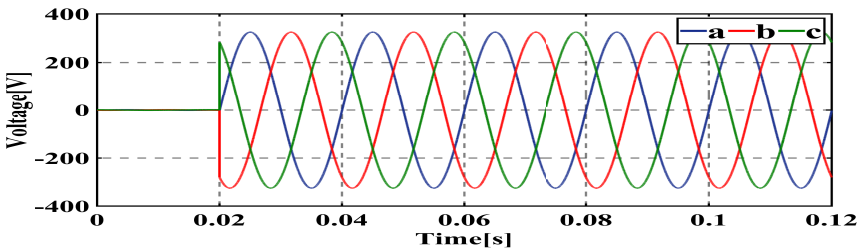

Figure 6.12: Three-phase voltage from the positive-sequence detector(case:3)

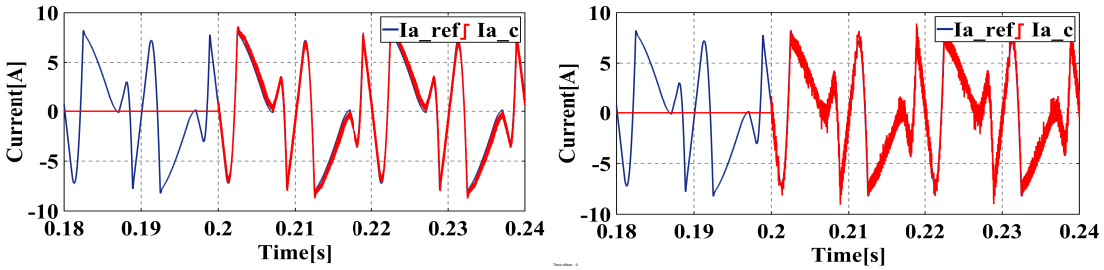

(a) *dq-PI* (b) adaptive HCC

Figure 6.13: Reference current and converter current comparison(case:3)

The controller uses these fundamental positive-sequence voltages and the load currents to calculate the reference currents. The reference currents and the compensating converter currents with *dq-PI* control and adaptive HCC control are shown in Figure 6.13. We can see that the converter is following the reference current even in unbalanced supply voltage conditions.

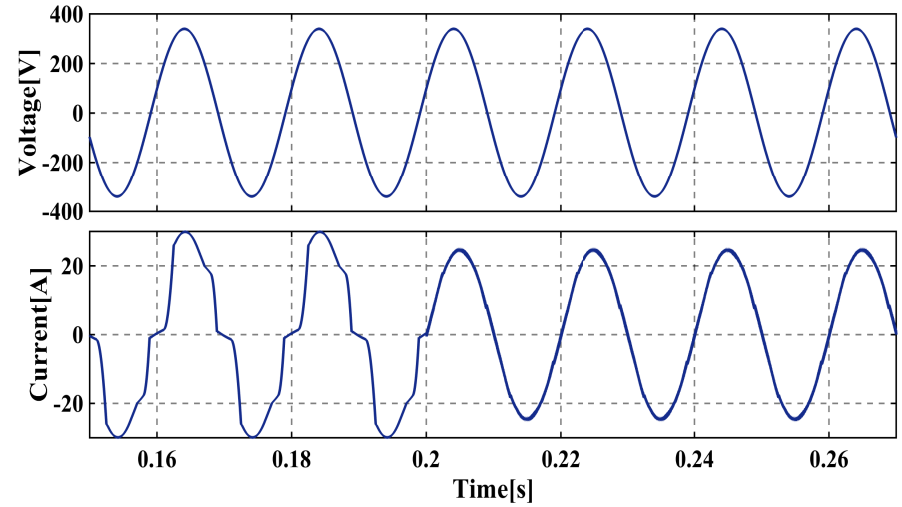

Figure 6.14: Phase-a current and voltage for dq-PI control(Case:3)

From Figure 6.14 and Figure 6.15, we see that as soon as the SAF starts supplying compensating currents at 0.2 sec, the distorted source current become sinusoidal. The THDs in the source current in this case are 1.63% and 1.52% for *dq-PI* control and adaptive HCC control respectively.

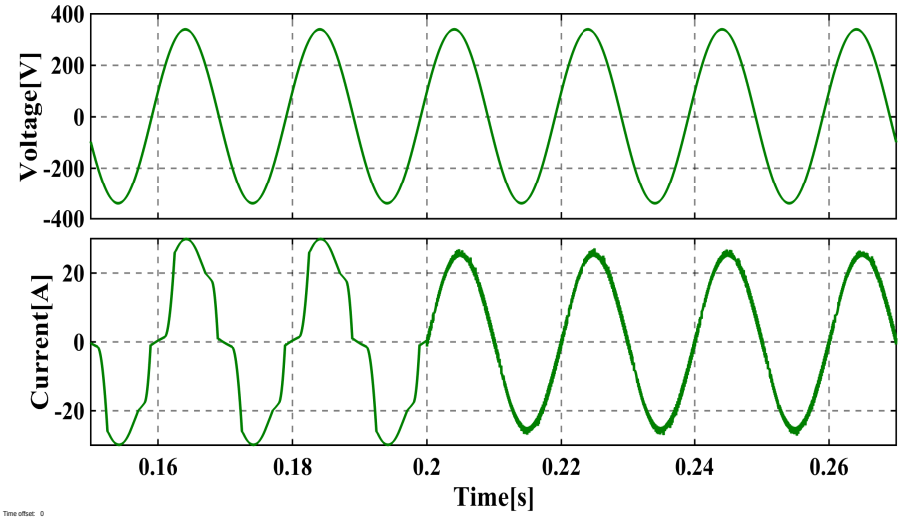

Figure 6.15: Phase-a current and voltage for HCC control(Case:3)

Table 6.5 shows the detailed harmonic contents in the source current before and after the connection of SAF relative to the fundamental 50 Hz component. Both the individual harmonics and the THDs are minimized well with in the limit.

Table 6.5: Harmonics spectra of the source current (%)(case:3)

Harmonic Order	1	3	5	7	11	13	17	**THD**
Without Compensation	100	12.12	12.82	8.01	4.26	2.02	1.54	20.12
Compensation with dq-PI	100	1.08	0.69	0.55	0.51	0.22	0.26	1.63
Compensation with HCC	100	0.96	0.37	0.31	0.03	0.17	0.08	1.52

From Figure 6.14 and Figure 6.15, we can also see that phase-a voltage is in-phase with the phase-a source current.This shows the SAF resulted in a unity power factor operation; thus the system draws no reactive power from the source. The converter supplies all the required reactive power in the system. This is also visible from Figure 6.16 which shows the instantaneous power drawn by the load from the source. The figure shows zero average reactive power being drawn.

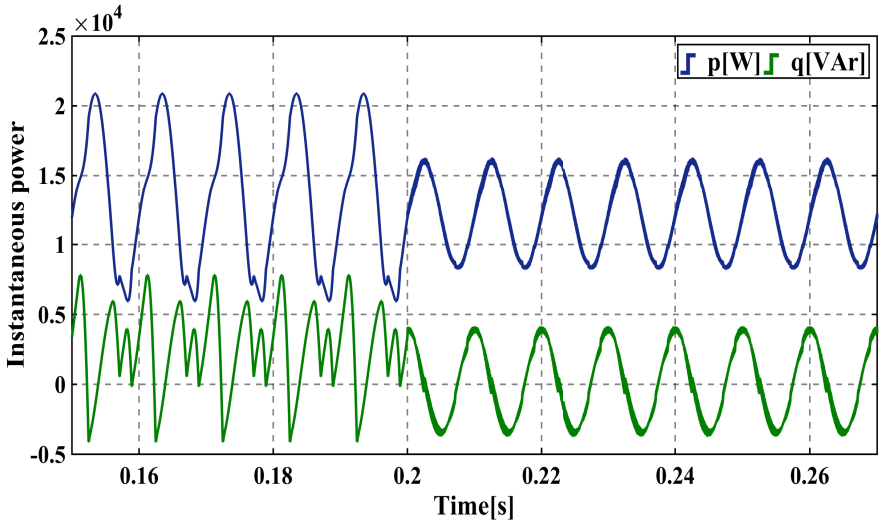

Figure 6.16: Instantaneous three-phase active and reactive power(case:3)

6.1.4 Case 4: Unbalanced Source with Unbalanced Load

The supply voltage in this simulation is the same as the case considered above (case:3, Equation 6.2) and the loads connected are the same as given in case:2 (Table 6.2). We need fundamental positive-sequence detector before the reference currents are calculated.

As shown in Figure 6.17, the supply voltages are highly unbalanced and the currents drawn by the connected loads are highly distorted and unbalanced.

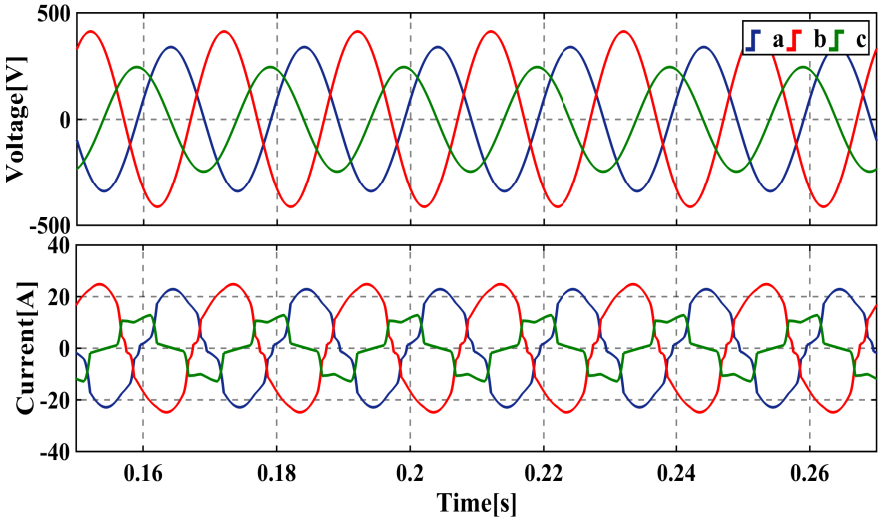

Figure 6.17: Three-phase source voltage and load current(case:4)

Even in the case of high unbalance and distortion in the load current, Figure 6.18 shows that the converter is able to follow the reference current effectively with both *dq-PI* control (Figure 6.18(a)) and adaptive HCC control (Figure 6.18(b)). But a close look at these figures shows that considerable amount of noises start to show up as compared with all the above cases considered. This is also evident from the fact that the THD in the source current is significantly larger than the previous cases.

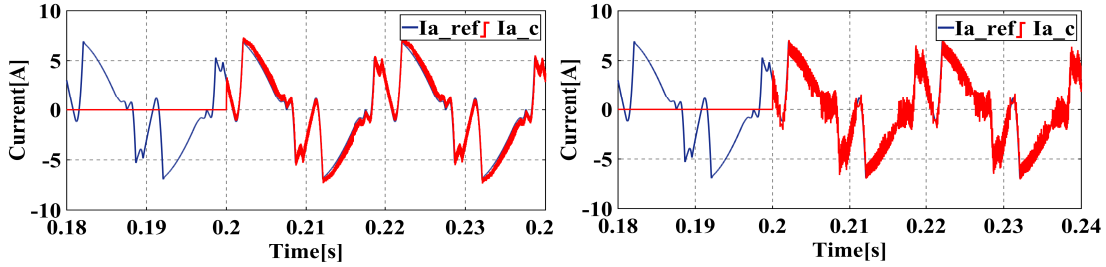

(a) *dq-PI* (b) adaptive HCC

Figure 6.18: Reference current and converter current comparison(case:4)

From Figure 6.19 and Figure 6.20, after the start of the active filter, the source current become in phase with the phase voltage, which means that the active filter compensated well the reactive power of the load. A close look at these currents reveals that some spikes are present in them. These are cause by a very high di/dt in the highly unbalanced and distorted currents, which cannot be fully compensate by the filter. These spikes affect the performance of the shunt active filter.

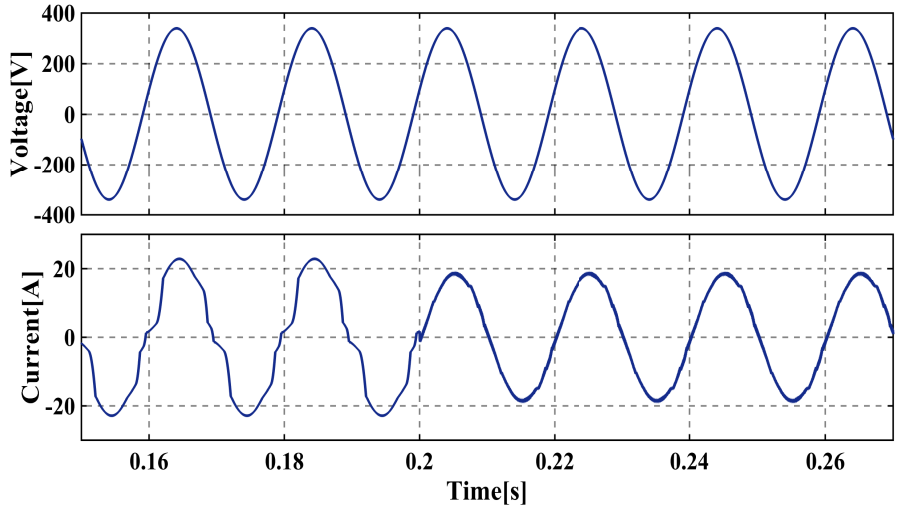

Figure 6.19: Phase-a current and voltage for dq-PI control(Case:4)

The THDs in the source current in this case are 2.22% and 2.38% for *dq-PI* control and adaptive HCC control respectively. Table 6.6 shows the detailed harmonic contents in the source current before and after the connection of SAF relative to the fundamental 50 Hz component. The individual harmonics are relatively larger than their corresponding values in the previous case but still they are well with in the limit.

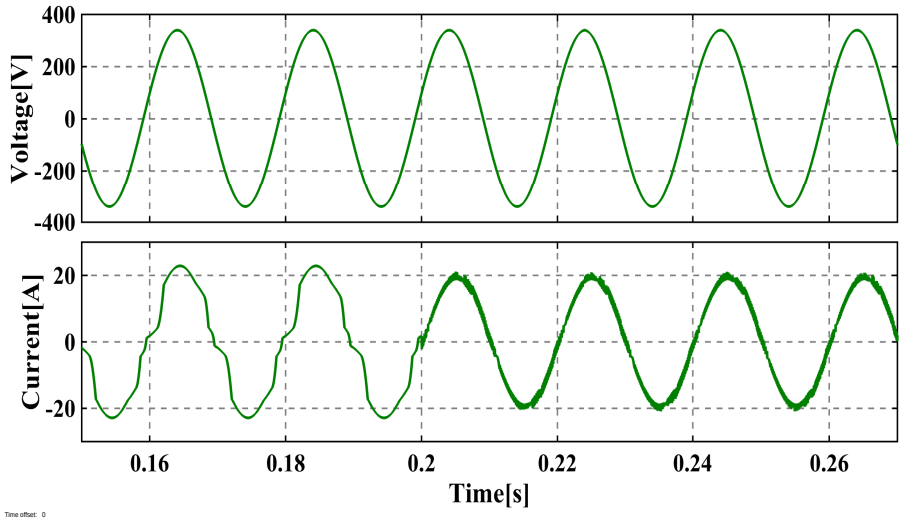

Figure 6.20: Phase-a current and voltage for HCC control(Case:4)

Table 6.6: Harmonics spectra of the source current (%)(case:4)

Harmonic Order	1	3	5	7	11	13	17	**THD**
Without Compensation	100	5.06	8.17	6.33	2.49	1.65	1.71	12.24
Compensation with dq-PI	100	1.16	0.94	0.92	0.54	0.58	0.62	2.22
Compensation with HCC	100	0.98	1.26	0.75	0.16	0.41	0.34	2.38

6.1.5 Case 5: Distorted Source with Balanced Load

The distortion in the electrical distribution system network has increased significantly due to the non-linear nature of the power electronic loads that are connected at PCC. The power electronic loads are very rich source of harmonics, and cause distortion in the supply voltage. Under such circumstances, the supply voltage is composed of both fundamental and harmonics voltages.

For this case, the system voltage is made both unbalanced and distorted. A distortion of 15.5% third harmonic, 11.5% fifth harmonic and 7.7% seventh harmonic is introduced to the system voltage. The harmonic components are made purely from the negative-sequence component. The time function corresponding to this voltage is given by Equation 6.3.

$$\begin{bmatrix} v_a \\ v_b \\ v_c \end{bmatrix} = \sqrt{2} \times 230 \left\{ \begin{bmatrix} \sin(\omega t) \\ \sin(\omega t - 120^0) \\ \sin(\omega t + 120^0) \end{bmatrix} + 0.3 \begin{bmatrix} \sin(\omega t) \\ \sin(\omega t + 120^0) \\ \sin(\omega t - 120^0) \end{bmatrix} + 0.2 \begin{bmatrix} \sin(3\omega t) \\ \sin(3\omega t + 120^0) \\ \sin(3\omega t - 120^0) \end{bmatrix} + 0.15 \begin{bmatrix} \sin(5\omega t) \\ \sin(5\omega t + 120^0) \\ \sin(5\omega t - 120^0) \end{bmatrix} + 0.1 \begin{bmatrix} \sin(7\omega t) \\ \sin(7\omega t + 120^0) \\ \sin(7\omega t - 120^0) \end{bmatrix} \right\} \tag{6.3}$$

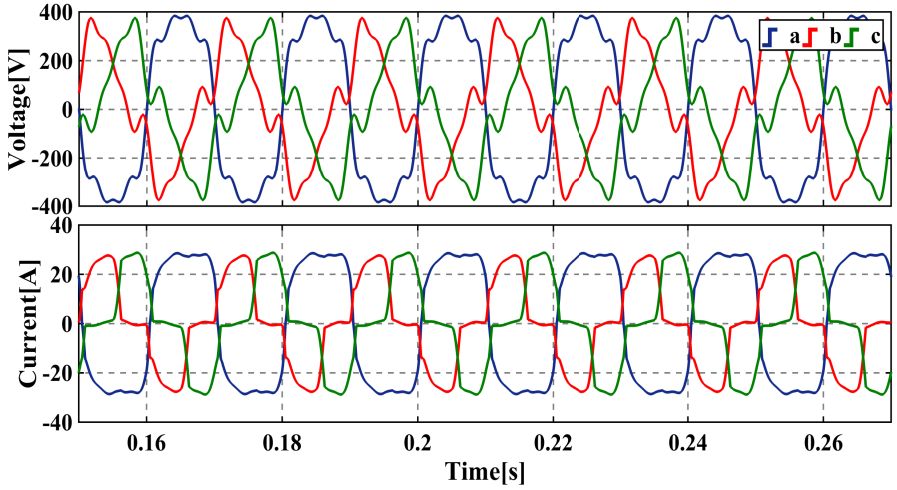

Figure 6.21: Three-phase source voltage and load current(case:5)

Figure 6.21 shows the supply three-phase voltage and the current drawn by the loads. The supply voltage is highly unbalanced and distorted, thus it requires positive sequence voltage detector to extract the fundamental positive sequence voltage from the main supply voltage in order to implement sinusoidal current control strategy. The extracted three-phase fundamental positive-sequence voltage is shown in Figure 6.22.

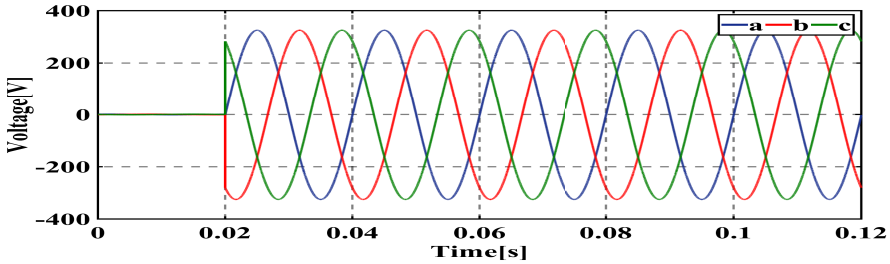

Figure 6.22: Three-phase voltage from the positive-sequence detector(case:5)

Figure 6.22 shows that the positive-sequence voltage detector is working well to extract the fundamental positive-sequence voltages from the distorted supply and these voltages will be used in the controller to calculate the reference currents.

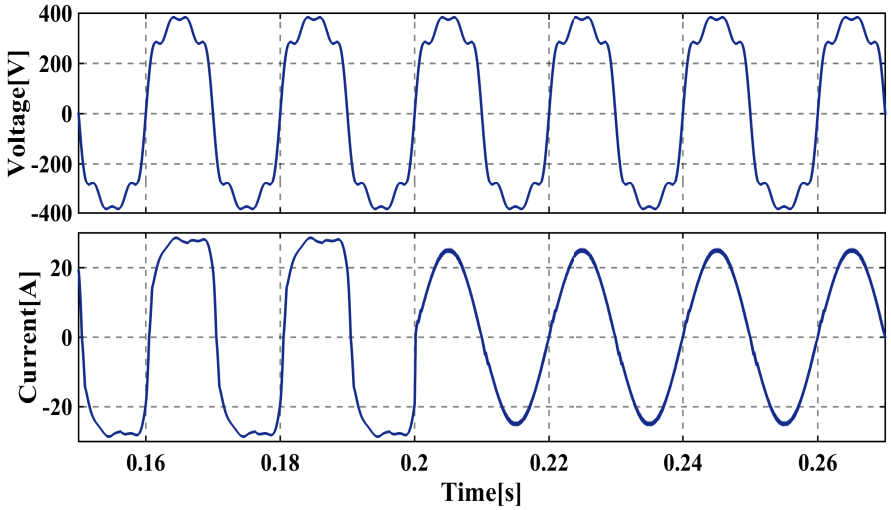

Figure 6.23: Phase-a current and voltage for dq-PI control(Case:5)

Figure 6.23 and Figure 6.24 show respectively the a-phase voltage and current for *dq-PI* control and adaptive HCC control. It can be seen that, by action of the shunt active filter, the power supply phase current becomes sinusoidal and in phase with the phase voltage. This means that reactive power is totally compensated by the SAF.

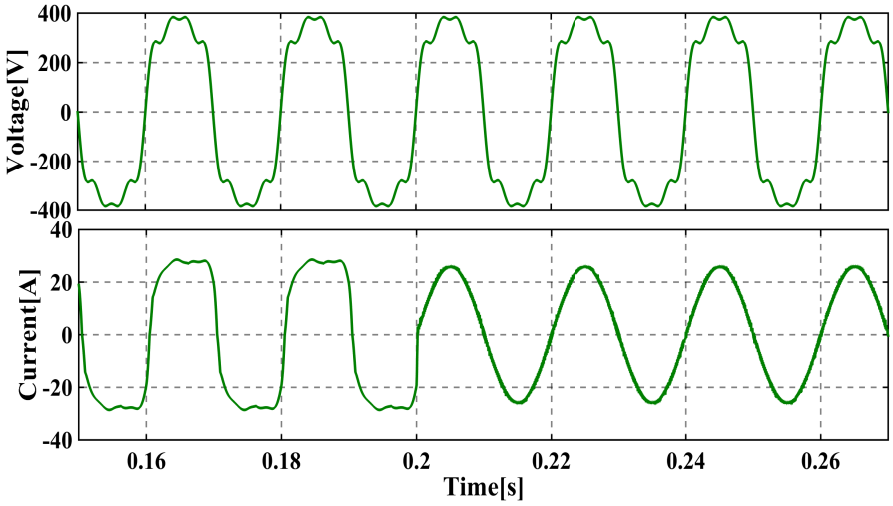

Figure 6.24: Phase-a current and voltage for HCC control(Case:5)

Table 6.7 shows that the THD in source current after active filtering reduced from 28.76% to 1.98% for *dq-PI* control and to 2.82% for adaptive HCC control. So the harmonics have been compensated to a level well below the defined harmonic standards. So, the *p-q* theory not only works well to eliminate the harmonics and compensate reactive power of ideal distribution power system but also for distorted and unbalanced systems.

Table 6.7: Harmonics spectra of the source current (%)(case:5)

Harmonic Order	1	3	5	7	9	11	13	**THD**
Without Compensation	100	25.27	11.16	6.49	3.09	2.29	1.79	28.76
Compensation with dq-PI	100	1.07	0.62	0.44	0.27	0.25	0.21	1.98
Compensation with HCC	100	0.41	0.16	0.42	0.11	0.20	0.13	2.82

6.1.6 Case 6: Distorted Source with Unbalanced Load

This is the most critical case since it assumes the worst conditions in both the supply voltage and the connected loads. The supply voltage is highly unbalanced and distorted as given in Equation 6.3 and the connected loads are unbalanced as given in Table 6.2.

Even in this condition, the active filter is able to calculate the reference currents from the load currents and voltages from positive-sequence detector. The converter is also able to generate the required currents to eliminate the harmonics and compensate reactive power in the system.

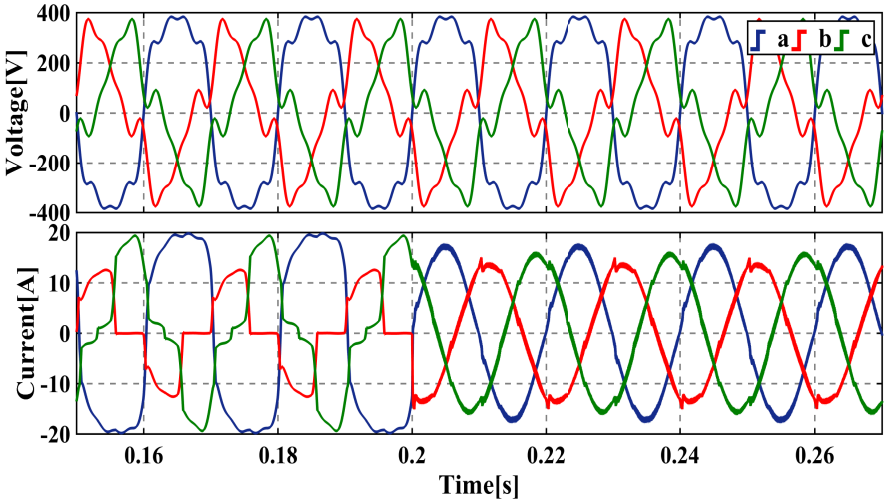

Figure 6.25: Three-phase source voltage and current with *dq-PI*(case:6)

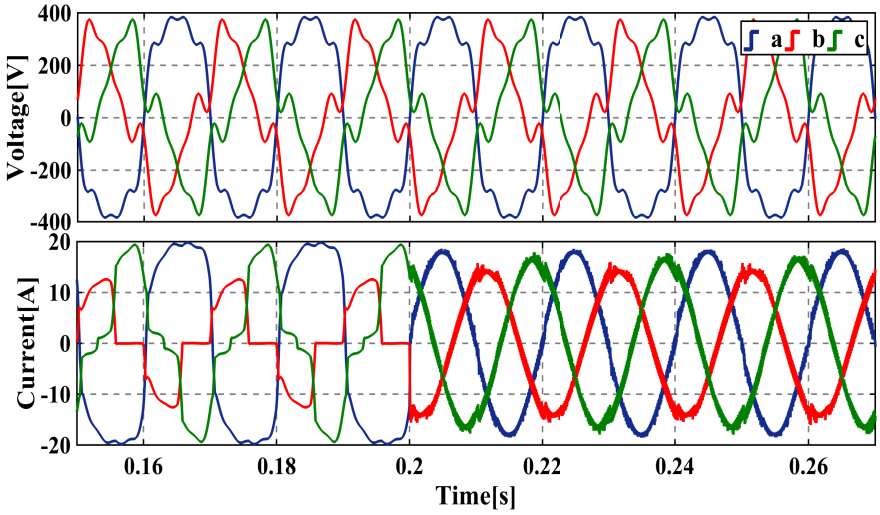

Figure 6.26: Three-phase source voltage and current with HCC(case:6)

Figure 6.25 and Figure 6.26 show three-phase source voltages and currents before and after the connection the SAF. From the figure, we can see that as soon as the active filter is connected at 0.2 sec, the source currents become sinusoidal but not balanced. In three-phase four-wire system, we will see that the source current will be both sinusoidal and balanced for the same conditions. The phase currents are in phase with their corresponding phase voltages, meaning that the reactive power in the system is being compensated.

The compensated source currents also contain spikes because of the high di/dt in the distorted load currents resulting in poor performance of the SAF. The THDs are understandably large for this case as shown in Table 6.8.

Table 6.8: Harmonics spectra of the source current (%)(case:6)

Harmonic Order	1	3	5	7	9	11	13	**THD**
Without Compensation	100	23.44	11.69	7.59	4.05	3.32	2.62	28.08
Compensation with dq-PI	100	1.04	0.89	0.43	0.69	0.87	0.43	2.24
Compensation with HCC	100	1.82	1.43	0.67	0.74	0.59	0.51	3.10

Simulation Summary

Table 6.9 presents the THDs in the source current in all the source and load condition studied above. And it can be seen that all are well with in the limits in IEEE-519 standard.

Table 6.9: THD summary for three-phase, three-wire systems

Case	dq-PI	Adaptive HCC
Balanced source-Balanced load	1.37	1.22
Balanced source-Unbalanced load	1.02	1.69
Unbalanced source-Balanced load	1,63	1.52
Unbalanced source-Unbalanced load	2.22	2.38
Distorted source-Balanced load	1.98	2.82
Distorted source-Unbalanced load	2.24	3.10

Figure 6.27 shows performance comparison in active shunt filtering between *dq-PI* and adaptive HCC control in three-phase, three-wire system. The loads are kept the same (balanced) in all the three conditions, while the source voltage is varied.

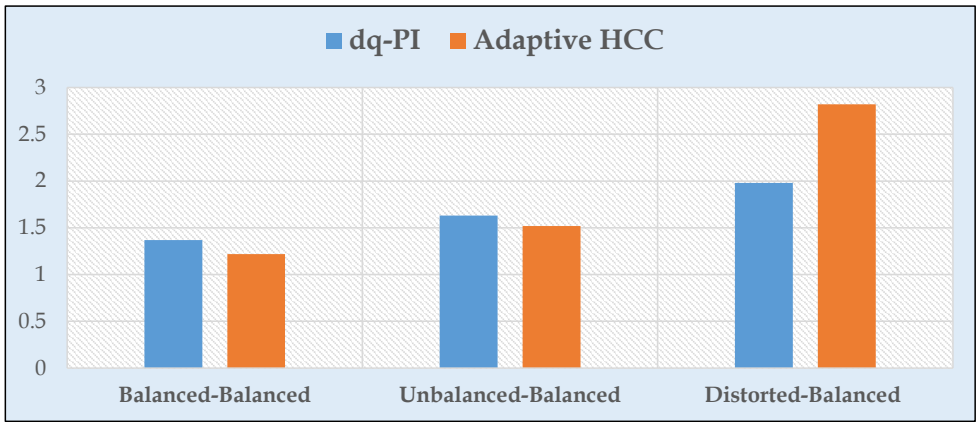

Figure 6.27: Comparison between *dq-PI* and Adaptive HCC in three-phase, three-wire system with balanced load

In both control techniques, the THD is seen to increase, when the supply voltage is varied from balanced type to distorted type. From this figure, we may be tempted to conclude that *dq-PI* control performs better than adaptive HCC, but as we will see in the next section, with all undesired current components being compensated, adaptive HCC results better control.

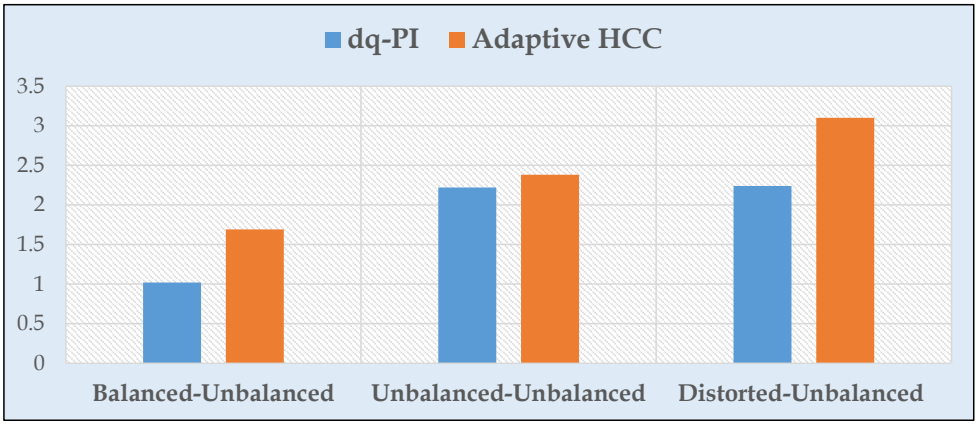

Figure 6.28: Comparison between *dq-PI* and Adaptive HCC in three-phase, three-wire system with unbalanced load

Same conclusion as above can also be made from Figure 6.28, which shows performance comparison between *dq-PI* and adaptive control in unbalanced load conditions.

6.2 Harmonic Elimination and Reactive Power Compensation in Three-Phase, Four-Wire System

In this section simulation results for harmonic elimination and reactive compensation in three-phase four-wire systems are presented and discussed. The "split-capacitor" converter topology is used in the design of the active filter. Additional feature of compensating the zero-sequence power is introduced in addition to the compensation characteristics discussed in Section 6.1. The oscillating portion of the real power, zero-sequence power and all of the imaginary power are compensated.

Two cases for both *dq-PI* control and adaptive HCC control are simulated depending on the type of supply voltage considered.

6.2.1 Case A: Balanced Source with Unbalanced Load

In this case, a balanced sinusoidal three-phase supply voltage is considered with a source impedance of $R_s = 10\ [\mu\Omega]$ and $L_s = 1\ [\mu H]$. One three-phase R-L diode

rectifier, one three phase linear R-L load and two single-phase diode rectifiers are connected at PCC. The Simulink model of the system is shown in Appendix B. The SAF is connected at 0.2 sec and the total simulation time is 0.4 sec. The supply voltage is given by the expression in Equation 6.1. The main system parameters that are used in this simulation are given in Table 6.10.

Table 6.10: Main parameters of the simulated system (case:A)

Parameter	Description
Source impedance	$R_s = 10\ [\mu\Omega], L_s = 1\ [\mu H]$
Converter filter	$R_f = 100\ [\mu\Omega], L_f = 4\ [mH], L_n = 2\ [mH]$
Load	One three-phase $R-L$ load, $P = 1.5\ [kW], Q = 250\ [VAr]$ One three-phase diode rectifier, with commutation inductance,$L_d = 3\ [mH]$ One single-phase diode rectifier connected between the a-phase and the neutral with commutation inductance, $L_d = 3\ [mH]$ One single-phase diode rectifier connected between the b-phase and the neutral with commutation inductance, $L_d = 3\ [mH]$

One simulation for each *dq-PI* and adaptive HCC control with the same parameters was performed for comparison between them. Both control techniques resulted in quite similar output for this case, but as we will see in the next case study, adaptive HCC showed much better performance in filtering of harmonics and reactive power compensation.

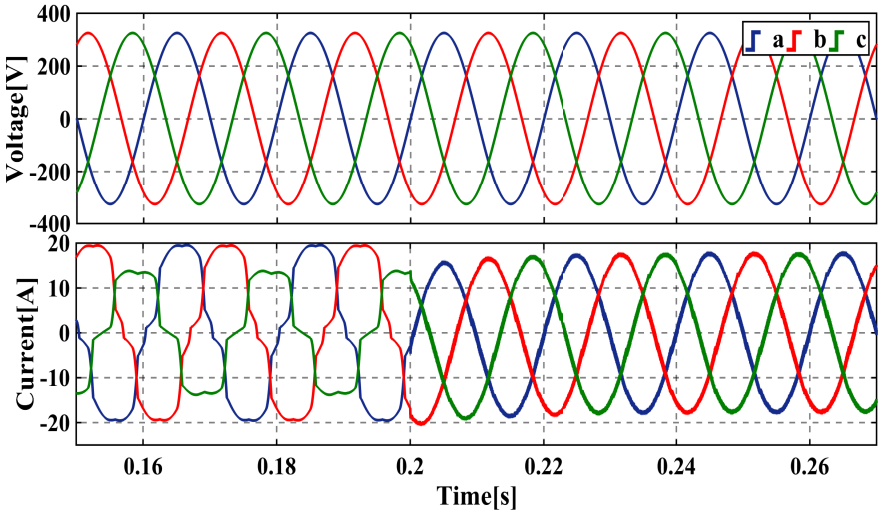

Figure 6.29: Three-phase source voltage and current with *dq-PI*(case:A)

Figure 6.29 and Figure 6.30 show three-phase source voltages and currents. Before the connection of the active filter, the source currents are not only strongly distorted, but also unbalanced. After the start of the active filter, the source currents become sinusoidal and balanced in both control techniques. But, we can still see a slightly better dynamics and performance from adaptive HCC control.

Figure 6.31 shows the dynamic performance of the shunt active filter with adaptive HCC control. It shows the source voltage, source current, load current and the converter current in phase-a. After the start of the SAF, the converter starts to supply the compensating current which forces the distorted source current to be sinusoidal and in phase with the source voltage, which means that the active filter compensated well the reactive power of the load and also minimized the harmonics in the source current. Similar results are obtained using *dq-PI* control (Appendix C).

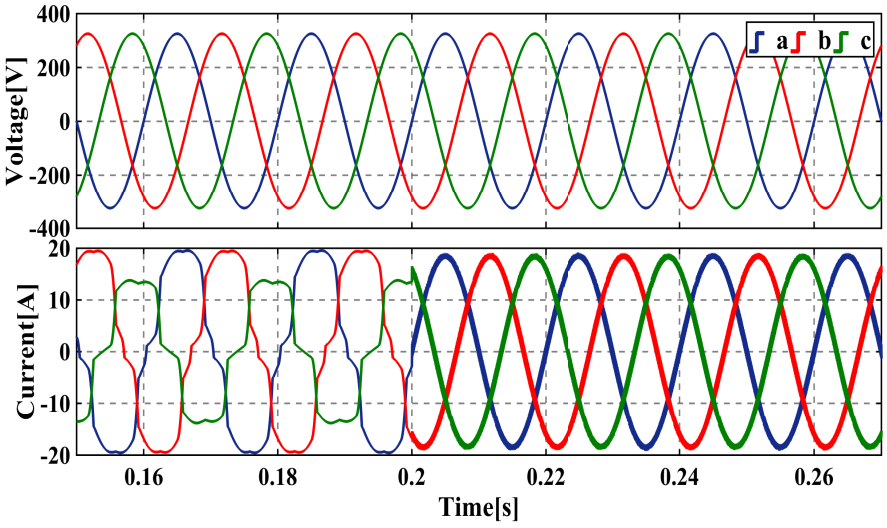

Figure 6.30: Three-phase source voltage and current with HCC(case:A)

Table 6.11 shows the percentage of different harmonic contents in the source current before and after the connection of SAF relative to the fundamental 50 Hz component. These new improved percentages of harmonics are well within the allowed limits defined in IEEE-519.

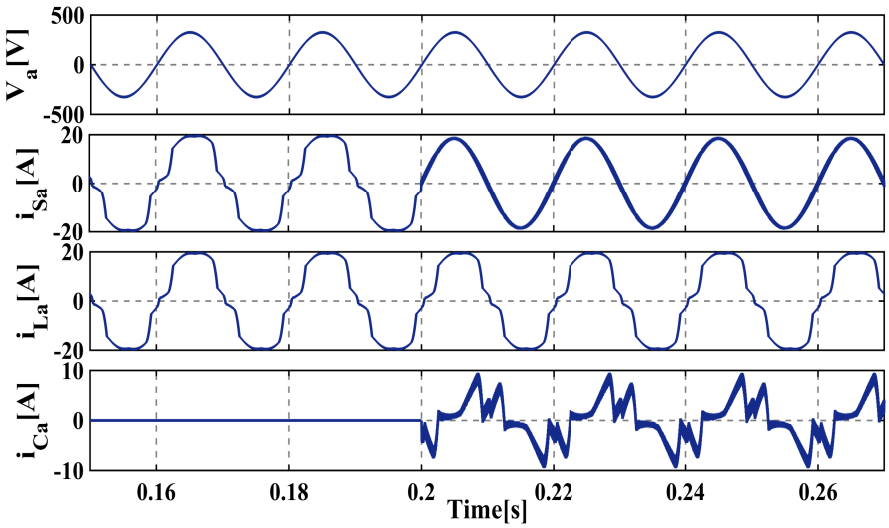

Figure 6.31: Dynamic behaviour of the SAF for a-phase with HCC(case:A)

Three-phase, Four-wire shunt active filters are specifically designed to compensate neutral currents (zero-sequence current components) in addition to realizing a sinusoidal source current and compensating the reactive power of the load.

Table 6.11: Harmonics spectra of the source current (%)(case:A)

Harmonic Order	1	3	5	7	11	13	17	**THD**
Without Compensation	100	2.30	9.96	5.44	3.91	2.96	1.75	12.90
Compensation with dq-PI	100	0.13	0.33	0.15	0.51	0.30	0.27	1.22
Compensation with HCC	100	0.16	0.03	0.01	0.03	0-01	0.02	0.24

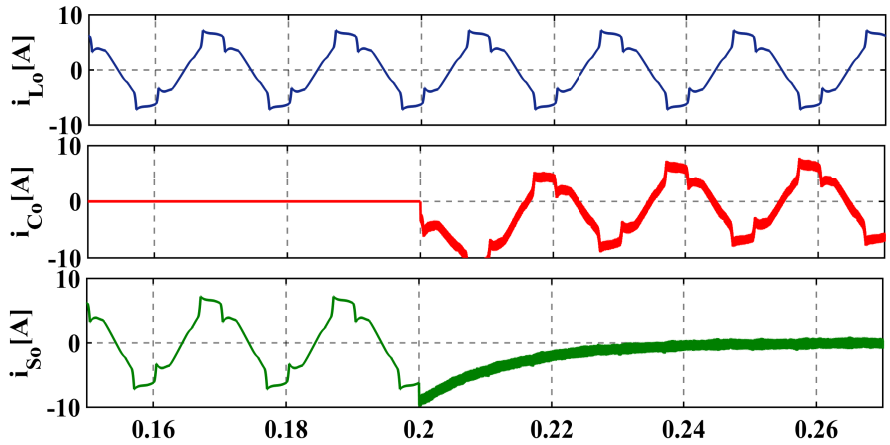

Figure 6.32: Neutral current compensation with *dq-PI* control(case:A)

Figure 6.32 and Figure 6.33 show that there is a neutral source current flowing in the

system before the connection of the filter. After the start of the filter, the converter supply the same magnitude in opposite direction neutral current as the load neutral current. Thus, there will be no neutral current flowing in the system after the filter is connected.

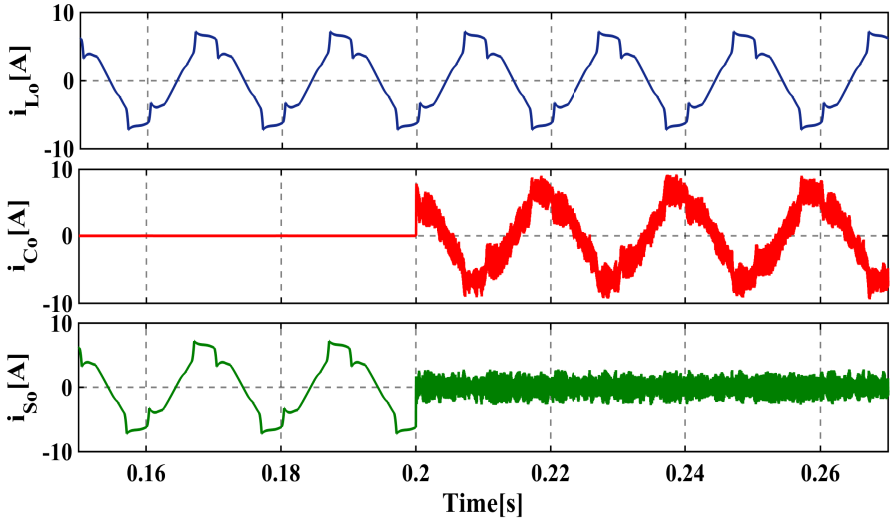

Figure 6.33: Neutral current compensation with HCC control(case:A)

6.2.2 Case B: Distorted Source with Unbalanced Load

For this case, the system voltage is made both unbalanced and distorted. The time function corresponding to this voltage is the same as given in Equation 6.3. Other than the supply voltage, the loads condition are the same as Case A considered above (Table 6.10).

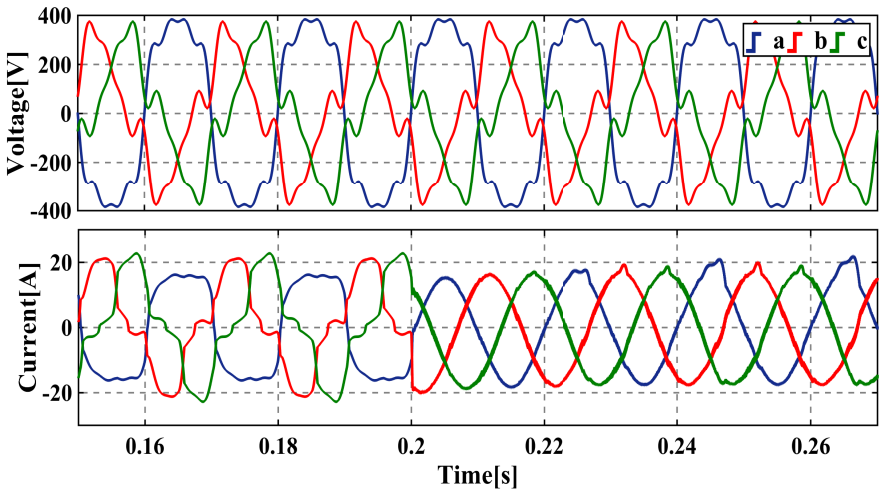

Figure 6.34: Three-phase source voltage and current with *dq-PI*(case:B)

Figure 6.34 and Figure 6.35 show three-phase source voltages and currents. Before the connection of the active filter, the source currents are strongly distorted and unbalanced. After the start of the active filter, adaptive HCC control is able to control the VSC to force sinusoidal and balanced source currents (Figure 6.35).

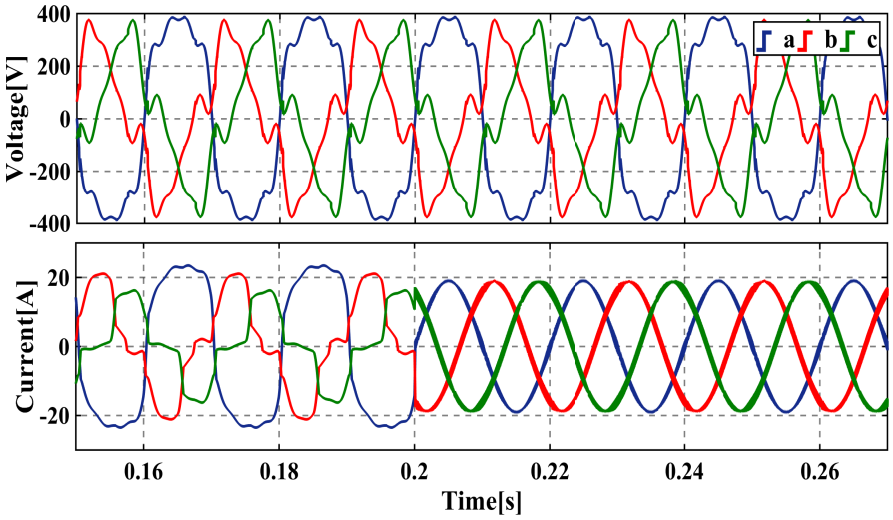

Figure 6.35: Three-phase source voltage and current with HCC(case:B)

The *dq-PI* control however is not able to effectively force the source currents to the design requirements (Figure 6.34). Actually, as it is visible form the wave from, the source currents are no more sinusoidal just after two power cycles and significantly large spikes begin to appear making the active filter not working as per design. This can also be seen from the large THD in the source currents. This and other simulation cases studied earlier show that, in highly distorted and unbalanced system, the *dq-PI* control performance deteriorates.

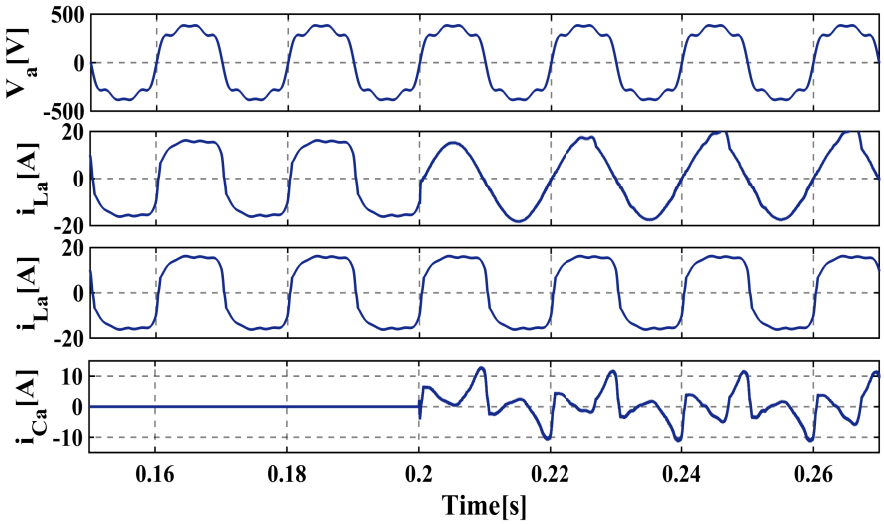

Figure 6.36: Dynamic behaviour of the SAF for a-phase with *dq-PI*(case:B)

The poor performance of *dq-PI* control is also visible from Figure 6.36. Although the source current is in phase with the phase voltage fulfilling reactive power compensation, the current is not sinusoidal with high harmonics content in it.

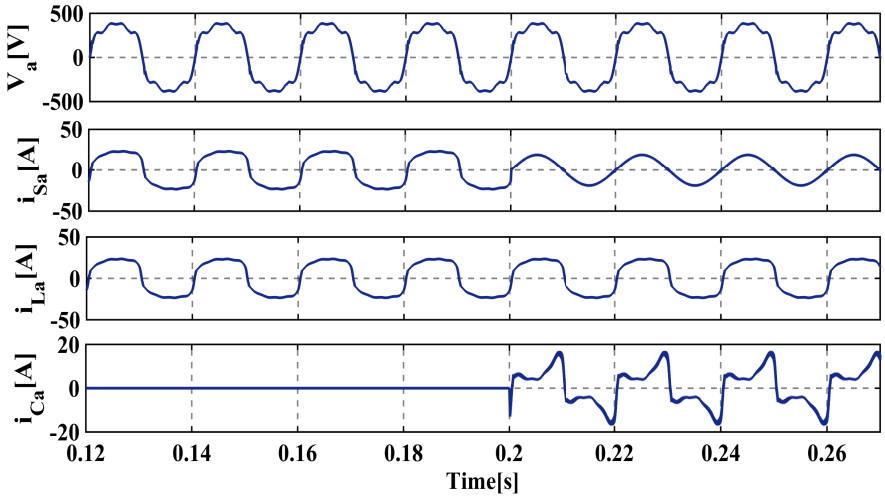

Figure 6.37: Dynamic behaviour of the SAF for a-phase with HCC(case:B)

Figure 6.37 shows the dynamic performance of the shunt active filter with adaptive HCC control. After the start of the SAF, the converter starts to supply the compensating current which forces the distorted source current to be sinusoidal and in phase with the source voltage, which means that the active filter compensated well the reactive power of the load and also minimized the harmonics in the source current.

Table 6.12: Harmonics spectra of the source current (%)(case:B)

Harmonic Order	1	3	5	7	9	11	15	**THD**
Without Compensation	100	21.54	10.92	6.96	3.37	2.73	2.14	28.17
Compensation with dq-PI	100	5.41	2.53	1.05	2.38	1.02	0.27	7.23
Compensation with HCC	100	0.43	0.09	0.06	0.04	0.02	0.03	0.51

Table 6.12 shows the percentage of different harmonic contents in the source current before and after the connection of SAF relative to the fundamental 50 Hz component. The harmonics are well minimized with adaptive HCC control but with *dq-PI* control, harmonic limits defined in IEEE-519 are violated and this type of control technique should be avoided in highly distorted systems.

Figure 6.38 shows the waveform for compensating the neutral current with *dq-PI* control. It shows that the source neutral current is zero after the SAF is connected at 0.2 sec. Similar result is also obtained with adaptive HCC control (Appendix C).

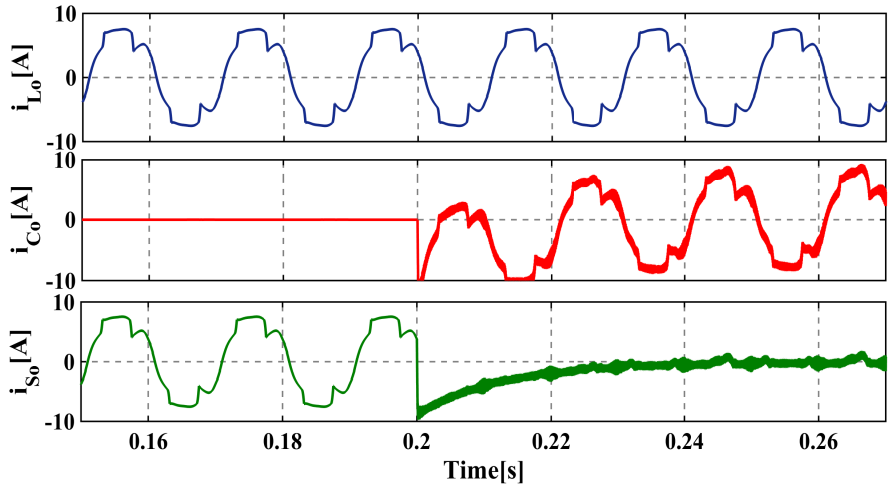

Figure 6.38: Neutral current compensation with *dq-PI*(case:B)

Simulation Summary

Figure 6.39 shows performance comparison between *dq-PI* and adaptive HCC control in three-phase, four-wire systems. It shows that adaptive HCC control gives a much better result when all undesirable current components are compensated.

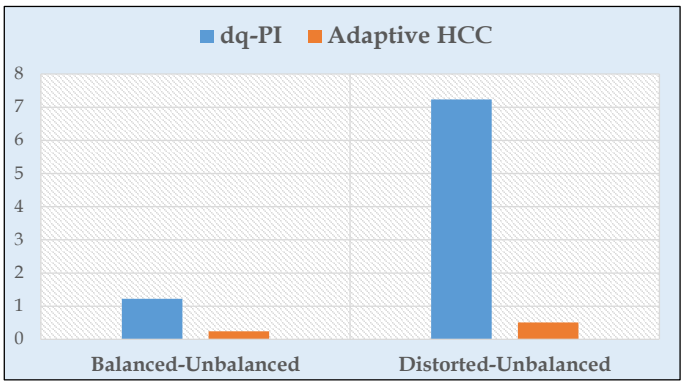

Figure 6.39: Comparison between *dq-PI* and Adaptive HCC in three-phase, four-wire system

Figure 6.39 can be compared with Figure 6.28 on page 79 for three-phase, three-wire system. From these two figures, we can conclude that adaptive HCC control is the better option when the system under study is highly distorted and unbalanced and *dq-PI* control performance deteriorates on highly non-linear and distorted systems.

Figure 6.40 shows the performance of adaptive HCC control in three-phase, three-wire (3P3W) and three-phase, four-wire (3P4W) system under the same unbalanced

load condition. It can be seen from the figure that, adaptive HCC performs much better in systems where all undesirable current components are taken into consideration (3P4W) in the design of active filters.

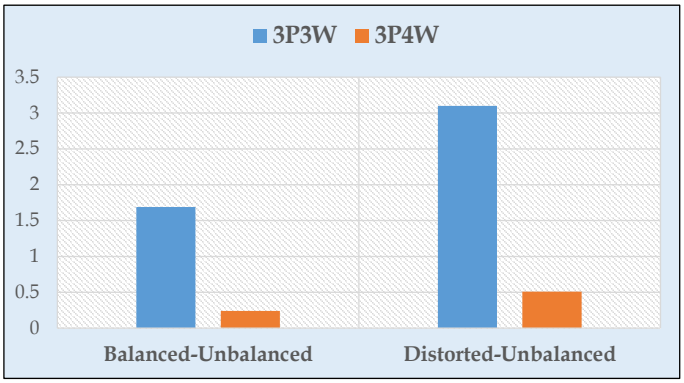

Figure 6.40: Adaptive HCC in three-phase, three-wire and three-phase, four-wire system

Chapter 7

Conclusion and Future Work

7.1 Conclusion

Telecom sites at different locations in the city have power converters and batteries that are installed with a primary purpose of supplying power to different telecom dc loads. In this study, the potential of these battery-converter combinations are studied in relation to aiding the grid in power quality improvement. They are used in shunt active filter configuration to mitigate source current harmonics and compensate reactive power in the system.

Two categories of shunt active filters are considered: three-phase, three-wire SAF and three-phase, four-wire SAF. The instantaneous power theory (p-q Theory) is used to design the controllers in these filters. And two types of control techniques (dq-PI control and adaptive HCC control) are used to modulate the converters to supply the required compensating currents from the active filter. The performance of these filters is investigated under different system conditions.

From the different simulations, it can be concluded that, active filter controller based on p-q theory, is able to calculate almost instantaneously the required compensating currents even under highly unbalanced and distorted system conditions. The performance of the shunt active filter is only limited by the type of modulation technique used.

In almost every case studied, the source current after the connection of the shunt active filter, becomes sinusoidal, 'free' from harmonics and in phase with voltage of the main supply. Thus ensuring a unity power factor operation, which also mean total compensation of the reactive power of the load. The THDs in the source current are reduced to a level well below the standard defined in IEEE-519.

Although both modulation techniques (*dq-PI* control and adaptive HCC control), are able to give relatively similar results in most of the conditions in three-phase, three-wire systems, it can be noted from the simulations that the performance of the SAF using *dq-PI* control deteriorates when non-linearity increases in the system and when three-phase, four-wire systems are considered. Thus, a choice between the two will be a compromise between fast response, easy control, switching losses and the required level of THD.

From this study, it is shown that we can use the power converters at different telecom sites to aid the grid in power quality improvement with harmonics and reactive power. It is also possible to add other functionality to this system. But it requires further research on the cost effectiveness of this arrangement.

7.2 Future Work

This study focused on understanding of smart grid, the challenges and opportunities from smart grid and analysis of different grid quality issues. The roles of energy storage and power converters in telecom sites for aiding power quality issues are studied through literature and simulations. Only harmonics and reactive power compensation was the focus of this study, but this can be expanded to include:

- Other issues like, import/export of active power as an additional feature,
- Investigation of different control strategies other than *p-q* theory and other modulating techniques,
- The system can be expanded to include renewable energy resources, like solar and wind power in addition to the batteries and also different telecom sites can be integrated together,
- The work presented here can be implemented and verified by experimental results.

Bibliography

[1] João L Afonso, MJ Freitas, and Júlio S Martins. pq theory power components calculations. In *Industrial Electronics, 2003. ISIE'03. 2003 IEEE International Symposium on*, volume 1, pages 385–390. IEEE, 2003.

[2] M.S. Todorovic, O.E. Djuric, I. Matinovic, and D. Licina. Renewable energy sources and energy efficiency for building's greening: From traditional village houses via high-rise residential building's bps and res powered co- and tri-generation towards net zebuildings and cities. In *Exploitation of Renewable Energy Sources (EXPRES), 2011 IEEE 3rd International Symposium on*, pages 29–37, March 2011.

[3] C.P. Vineetha and C.A. Babu. Smart grid challenges, issues and solutions. In *Intelligent Green Building and Smart Grid (IGBSG), 2014 International Conference on*, pages 1–4, April 2014.

[4] Grzegorz Benysek. *Improvement in the quality of delivery of electrical energy using power electronics systems*. Springer Science & Business Media, 2007.

[5] Ryszard Michal Strzelecki. *Power electronics in smart electrical energy networks*. Springer Science & Business Media, 2008.

[6] L Kannberg. Gridwise-transforming the energy system. In *Pacific Northwest National Laboratory, Conference Presentation*, 2003.

[7] Clark W Gellings. *The smart grid: enabling energy efficiency and demand response*. The Fairmont Press, Inc., 2009.

[8] ETP SmartGrids. Smartgrids strategic deployment document for europe's electricity networks of the future. *European Technology Platform SmartGrids*, 2010.

[9] A. Mohamed, S. Vanteddu, and O. Mohammed. Protection of bi-directional ac-dc/dc-ac converter in hybrid ac/dc microgrids. In *Southeastcon, 2012 Proceedings of IEEE*, pages 1–6, March 2012.

[10] F.B. Beidou, W.G. Morsi, C.P. Diduch, and L. Chang. Smart grid: Challenges, research directions and possible solutions. In *Power Electronics for Distributed*

Generation Systems (PEDG), 2010 2nd IEEE International Symposium on, pages 670–673, June 2010.

[11] Colin Bayliss, Colin R Bayliss, and Brian Hardy. *Transmission and distribution electrical engineering*. Elsevier, 2012.

[12] Sean Elphick, Vic Smith, Vic Gosbell, and Robert Barr. The australian long term power quality survey project update. In *Harmonics and Quality of Power (ICHQP), 2010 14th International Conference on*, pages 1–7. IEEE, 2010.

[13] N Karthikeyan, S Sasitharan, K Srinivas Bhaskar, Mahesh K Mishra, B Kumar, et al. Power quality survey in a technological institute. In *Power Systems, 2009. ICPS'09. International Conference on*, pages 1–6. IEEE, 2009.

[14] J. Arrillaga and N. R. Watson. *Power System Harmonics.* Wiley, 2003.

[15] Ned Mohan, Tore M Undeland, and William P Robbins. *Power electronics : converters, applications, and design*. Hoboken, N.J. : J. Wiley, 3rd ed edition, 2003.

[16] Angelo B Baggini et al. *Handbook of power quality*, volume 520. Wiley Online Library, 2008.

[17] HMS Chandana Herath and S McHardy. Power quality trends in energy australia distribution network. In *Harmonics and Quality of Power, 2008. ICHQP 2008. 13th International Conference on*, pages 1–6. IEEE, 2008.

[18] GM Shafiullah, Amanullah MT Oo, ABM Shawkat Ali, and Peter Wolfs. Potential challenges of integrating large-scale wind energy into the power grid–a review. *Renewable and Sustainable Energy Reviews*, 20:306–321, 2013.

[19] Prasenjit Basak, S Chowdhury, S Halder nee Dey, and SP Chowdhury. A literature review on integration of distributed energy resources in the perspective of control, protection and stability of microgrid. *Renewable and Sustainable Energy Reviews*, 16(8):5545–5556, 2012.

[20] Robert Passey, Ted Spooner, Iain MacGill, Muriel Watt, and Katerina Syngellakis. The potential impacts of grid-connected distributed generation and how to address them: A review of technical and non-technical factors. *Energy Policy*, 39(10):6280–6290, 2011.

[21] M.C. Such and C. Hill. Battery energy storage and wind energy integrated into the smart grid. In *Innovative Smart Grid Technologies (ISGT), 2012 IEEE PES*, pages 1–4, Jan 2012.

[22] Dinghuan Zhu and Gabriela Hug-Glanzmann. Robust control design for integration of energy storage into frequency regulation. In *Innovative Smart Grid Technologies (ISGT Europe), 2012 3rd IEEE PES International Conference and Exhibition on*, pages 1–8. IEEE, 2012.

[23] Sebastian Dierkes, Florian Bennewitz, Moritz Maercks, Lukas Verheggen, and Albert Moser. Impact of distributed reactive power control of renewable energy sources in smart grids on voltage stability of the power system. In *Electric Power Quality and Supply Reliability Conference (PQ), 2014*, pages 119–126. IEEE, 2014.

[24] BE Kushare, AA Ghatol, and MS Aphale. Survey of interharmonics in indian power system network. In *Power Engineering Conference, 2007. IPEC 2007. International*, pages 1230–1235. IEEE, 2007.

[25] Norbert Edomah. Effects of voltage sags, swell and other disturbances on electrical equipment and their economic implications. In *Electricity Distribution-Part 1, 2009. CIRED 2009. 20th International Conference and Exhibition on*, pages 1–4. IET, 2009.

[26] R Muralekrishnen and P Sivakumar. Improving the power quality performance for distributed power generation. In *Computing, Electronics and Electrical Technologies (ICCEET), 2012 International Conference on*, pages 203–211. IEEE, 2012.

[27] Hugo Morais, Tiago Sousa, Pedro Faria, and Zita Vale. Reactive power management strategies in future smart grids. In *Power and Energy Society General Meeting (PES), 2013 IEEE*, pages 1–5. IEEE, 2013.

[28] JJ Jamian, MW Mustafa, H Mokhlis, and MA Baharudin. Smart grid communication concept for frequency control in distribution system. In *Power Engineering and Optimization Conference (PEOCO), 2011 5th International*, pages 238–242. IEEE, 2011.

[29] M Shareghi, BT Phung, MS Naderi, TR Blackburn, and E Ambikairajah. Effects of current and voltage harmonics on distribution transformer losses. In *International Conf. on Condition Monitoring and Diagnosis (CMD)*, pages 633–636, 2012.

[30] A Elmoudi, M Lehtonen, and Hasse Nordman. Effect of harmonics on transformers loss of life. In *Electrical Insulation, 2006. Conference Record of the 2006 IEEE International Symposium on*, pages 408–411. IEEE, 2006.

[31] Hirofumi Akagi, Edson Hirokazu Watanabe, and Mauricio Aredes. *Instantaneous power theory and applications to power conditioning*, volume 31. John Wiley & Sons, 2007.

[32] CI Budeanu. The different options and conceptions regarding active power in nonsinusoidal systems. *Instytut Romain de l'Energie*, 4, 1927.

[33] S Fryze. Wirk-, blind-und scheinleistung in elektrischen stromkreisen mit nichtsinusförmigem verlauf von strom und spannung. *Elektrotechnische Zeitschrift, June*, (25), 1932.

[34] Nouredine Hadjsaid and Jean-Claude Sabonnadière. *Power Systems and Restructuring*. John Wiley & Sons, 2013.

[35] Edith Clarke. *Circuit analysis of AC power systems*, volume 1. Wiley, 1943.

[36] G.T. Heydt, S.P. Hoffman, A. Risal, R.I. Sasaki, and M.J. Kemper. The impact of energy saving technologies on electric distribution system power quality. In *Industrial Electronics, 1994. Symposium Proceedings, ISIE '94., 1994 IEEE International Symposium on*, pages 176–181, May 1994.

[37] L. Cividino. Power factor, harmonic distortion; causes, effects and considerations. In *Telecommunications Energy Conference, 1992. INTELEC '92., 14th International*, pages 506–513, Oct 1992.

[38] Abdlfettah Boussaid, Ahmed Lokmane Nemmour, Lamri Louze, and Abdelmalek Khezzar. A novel strategy for shunt active filter control. *Electric Power Systems Research*, 123:154–163, 2015.

[39] Laszlo Gyugyi and E Cl Strycula. Active ac power filters. In *Proc. IEEE/IAS Annu. Meeting*, volume 19, pages 529–535, 1976.

[40] M. Routimo, M. Salo, and H. Tuusa. Comparison of voltage-source and current-source shunt active power filters. *Power Electronics, IEEE Transactions on*, 22(2):636–643, March 2007.

[41] Mauricio Aredes, Jurgen Hafner, and Klemens Heumann. Three-phase four-wire shunt active filter control strategies. *Power Electronics, IEEE Transactions on*, 12(2):311–318, 1997.

[42] Suresh Mikkili, Anup Kumar Panda, et al. Instantaneous active and reactive power and current strategies for current harmonics cancellation in 3-ph 4wire shaf with both pi and fuzzy controllers. *Energy and Power Engineering*, 3(03):285, 2011.

[43] M.I.M. Montero, E.R. Cadaval, and F.B. Gonzalez. Comparison of control strategies for shunt active power filters in three-phase four-wire systems. *Power Electronics, IEEE Transactions on*, 22(1):229–236, Jan 2007.

[44] H. Akagi, Yoshihira Kanazawa, and A. Nabae. Instantaneous reactive power compensators comprising switching devices without energy storage components. *Industry Applications, IEEE Transactions on*, IA-20(3):625–630, May 1984.

[45] Qing-Chang Zhong and Tomas Hornik. *Control of power inverters in renewable energy and smart grid integration*, volume 97. John Wiley & Sons, 2012.

[46] Digital control of grid connected converters for distributed power generation.

[47] Parikshith Channegowda and Vinod John. Filter optimization for grid interactive voltage source inverters. *Industrial Electronics, IEEE Transactions on*, 57(12):4106–4114, 2010.

[48] Behrooz Bahrani. *Advanced control strategies for voltage source converters in microgrids and traction networks*. PhD thesis, Citeseer, 2012.

[49] Ned Mohan. *Advanced Electric Drives: Analysis, Control, and Modeling Using MATLAB/Simulink*. John Wiley & Sons, 2014.

[50] Temesgen Mulugeta Haileselassie. Control of multi-terminal vsc-hvdc systems. 2008.

[51] Chandra Bajracharya, Marta Molinas, Jon Are Suul, Tore M Undeland, et al. Understanding of tuning techniques of converter controllers for vsc-hvdc. In *Nordic Workshop on Power and Industrial Electronics (NORPIE/2008), June 9-11, 2008, Espoo, Finland*. Helsinki University of Technology, 2008.

[52] Ángelo JJ Rezek, Carlos AD Coelho, José Manuel E Vicente, José Antonio Cortez, and Paulo Ricardo Laurentino. The modulus optimum (mo) method applied to voltage regulation systems: modeling, tuning and implementation. In *Proc. International Conference on Power System Transients, IPST*, volume 1, pages 24–28, 2001.

[53] David M Brod and Donald W Novotny. Current control of vsi-pwm inverters. *Industry Applications, IEEE Transactions on*, (3):562–570, 1985.

[54] Akira Nabae, Satoshi Ogasawara, and Hirofumi Akagi. A novel control scheme for current-controlled pwm inverters. *IEEE Transactions on Industry Applications*, 4(IA-22):697–701, 1986.

[55] Wang Huaisheng and Xia Huifeng. A novel double hysteresis current control method for active power filter. *Physics Procedia*, 24:572–579, 2012.

[56] S Lotfi and M Sajedi. Role of a shunt active filter in power quality improvement and power factor correction. *Journal of Basic and Applied Scientific Research*, 2(2):1015–1020, 2012.

[57] N Senthilnathan and T Manigandan. A novel control strategy for line harmonic reduction using three phase shunt active filter with balanced and unbalanced supply. *European Journal of Scientific Research*, 67(3):456–466, 2012.

[58] Bimalk K Bose. An adaptive hysteresis-band current control technique of a voltage-fed pwm inverter for machine drive system. *Industrial Electronics, IEEE Transactions on*, 37(5):402–408, 1990.

[59] Murat Kale and Engin Ozdemir. An adaptive hysteresis band current controller for shunt active power filter. *Electric Power Systems Research*, 73(2):113–119, 2005.

[60] Ferhat Ucar, Resul Coteli, and Besir Dandil. Three level inverter based shunt active power filter using multi-level hysteresis band current controller. 88(11):227–231, 2012.

[61] Tarjei Midtsund. *Control of Power Electronic Converters in Distributed Power Generation Systems*. PhD thesis, MSc Thesis, Norwegian University of Science and Technology Department of Energy and Environment, 2010.

Appendix

Appendix A: Harmonic limits and Three-phase, four-wire SAF

Current Harmonic Limits The revised IEEE-519, which contains recommended practices and requirements for harmonic control in electric power systems, specifies requirements on the user as well as on the utility.

I_{SC}/I_1	$h < 11$	$11 \leq h < 17$	$17 \leq h < 23$	$23 \leq h < 35$	$35 \leq h$	THD
< 20	4.0	2.0	1.5	0.6	0.3	5.0
$20 - 50$	7.0	3.5	2.5	1.0	0.5	8.0
$50 - 100$	10.0	4.5	4.0	1.5	0.7	12.0
$100 - 1000$	12.0	5.5	5.0	2.0	1.0	15.0
> 1000	15.0	7.0	6.0	2.5	1.4	20.0

Adaptive bandwidth calculator

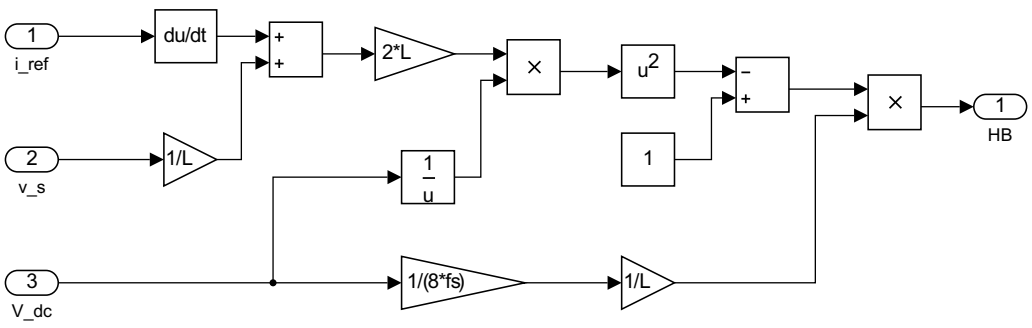

Three-phase, four-wire shunt active filter

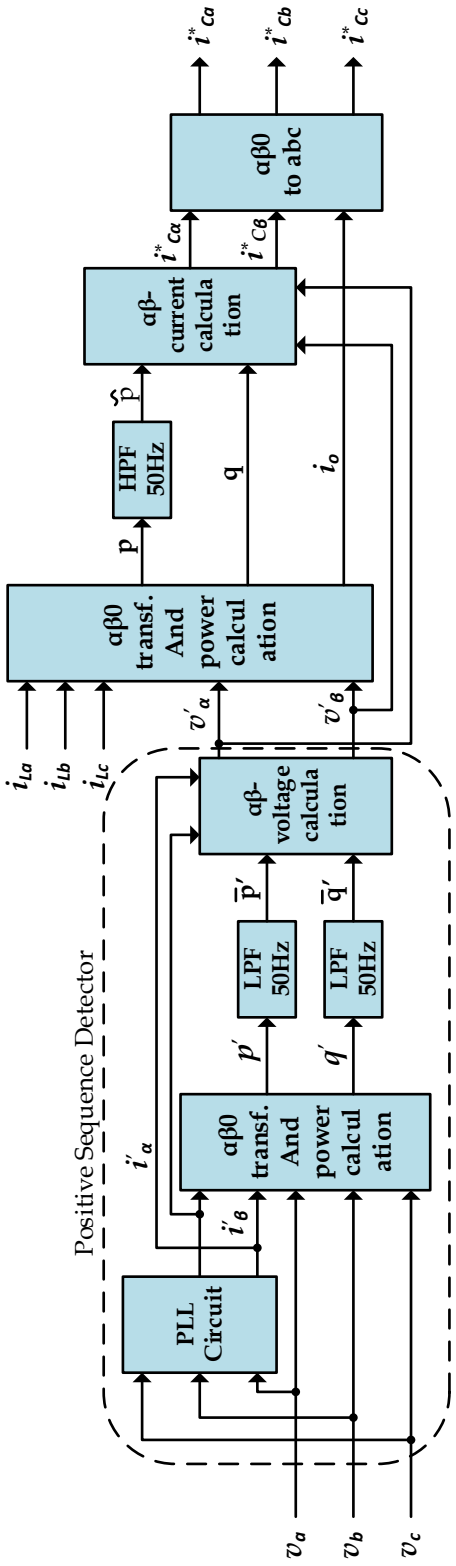

Appendix B: Simulation Models

Balanced source balanced load(case:1) simulation model

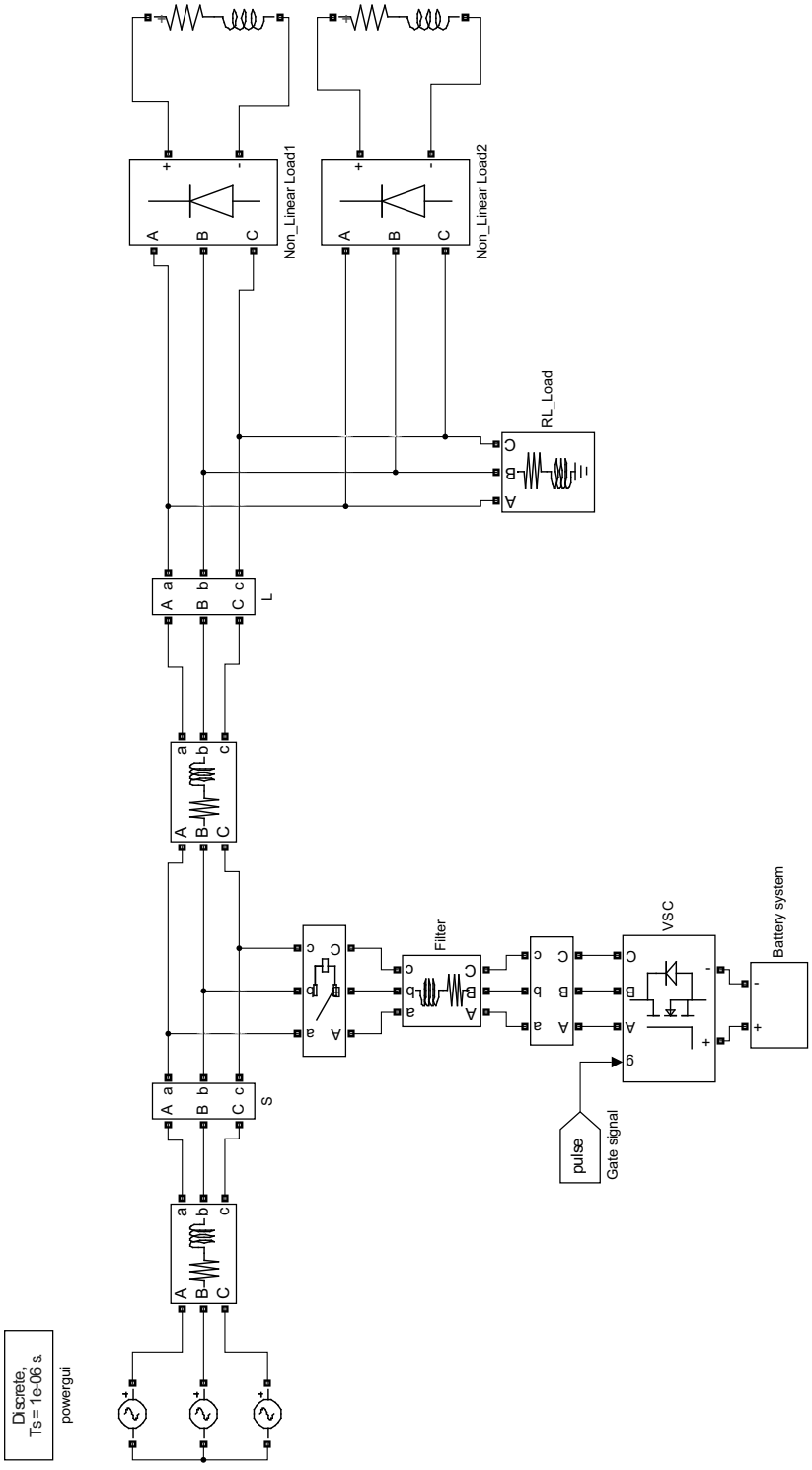

Three-phase, four-wire simulation model(case:A and Case:B)

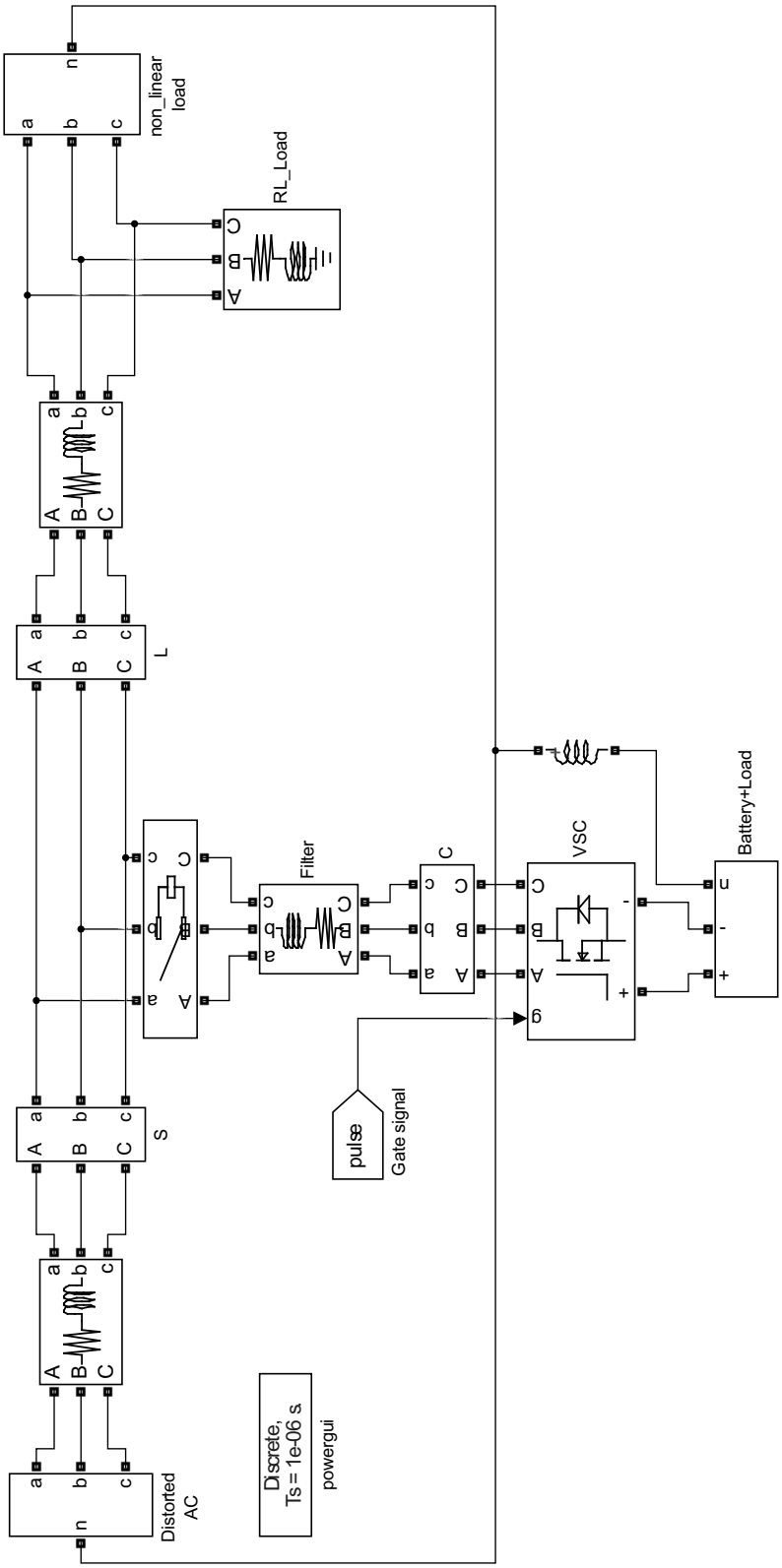

Appendix C: Simulation Results

Dynamic behaviour of the SAF for a-phase with *dq-PI*(case:A)

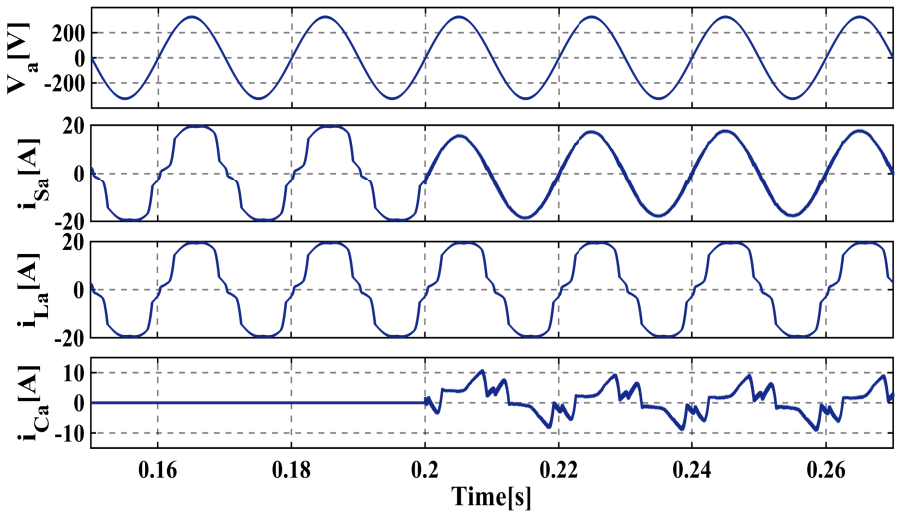

Neutral current compensation with adaptive HCC(case:B)